From Forest to Lake: Effect of Hydroelectric Reservoir Impoundment on the Net Ecosystem Exchange of CO_2

Marie-Eve Lemieux

Department of Geography
McGill University, Montréal

April 2010

A thesis submitted to McGill University in partial fulfillment of the requirements of the degree of Master of Science

Suggested short title :

The net effect on CO_2 of a young hydroelectric reservoir

Abstract

The purpose of this research was to determine the magnitude and direction of carbon exchange resulting from a boreal forest being flooded for hydroelectric purposes and to determine the net reservoir effect. In this study, carbon dioxide fluxes were measured from March 29th 2007 to November 30th 2008 in a mature black spruce forest and a flooded forest in Eastmain-1, James Bay, Quebec, Canada using eddy covariance towers. The unburned mature boreal forest was selected to act as a pre-flooded analogue site to the newly impounded hydroelectric reservoir. Flux tower measurement of the net ecosystem exchange (NEE) showed that the forest was a carbon sink during the growing seasons (DOY 102-304 in 2007 and 104 to 305 in 2008) with a similar cumulative NEE for both years, varying from -115.6 g C $m^{-2}d^{-1}$ in 2007 to -122.5 g C $m^{-2}d^{-1}$ in 2008. When compared to the pre-flooded site, flux measurement over the reservoir revealed that this flooded environment was a constant emitter of CO_2 throughout the study period. Two seasonal peaks of emissions were identified during the year defined as December 2007 to November 2008. The first occurred during the ice break up in the last week of May 2008 (DOY 143-152) with 1.78 ± 0.09 g C $m^{-2}d^{-1}$ and the second corresponded to the reservoir turnover at the end of August and September 2008 (DOY 229-274) with 1.27 ± 0.03 g C $m^{-2}d^{-1}$. Overall, the net reservoir effect was estimated to be 1.75± 0.07 g C $m^{-2}d^{-1}$ for the ice free period and of 289.2 ± 144.6 g C $m^{-2}yr^{-1}$ for the entire annual period.

Résumé

Le but premier de cette recherche était de déterminer l'ampleur et la direction des émissions de carbone provenant d'une foret boréale nouvellement inondée dans le but de la création d'un réservoir hydroélectrique. Ensuite, le bilan annuel net des émissions de ce nouveau réservoir a voulu être quantifié en utilisant des tours de carbone. Dans cette étude, les flux de carbone utilises proviennent de la période du 29 mars 2007 au 30 novembre 2008 au-dessus de deux sites distincts situes a Eastmain-1 dans la région de la Baie-James (Québec), soit une foret boréale vierge ainsi qu'une foret boréale nouvellement inondée. Ainsi, la foret vierge servait de site témoin. Les mesures de l'échange éco systémique net (EEN) obtenues a l'aide des tours de carbones ont démontrées que la foret boréale à la Baie-James était un puits de carbone lors de la période de croissance (jour 102-304 en 2007 et 104-305 en 2008) avec -115.6 g C $m^{-2}d^{-1}$ en 2007 et -122.5 g C $m^{-2}d^{-1}$ et 2008. Lorsque les flux de carbone du site témoin sont comparés à ceux de la foret nouvellement ennoyée, on s'aperçoit que le jeune réservoir était une source constante de carbone durant la période d'étude. De plus, deux pointes d'émissions ont été identifiées lors de la période d'étude de décembre 2007 à novembre 2008. La première pointe correspond à la rupture printanière de la glace sur le réservoir lors de la dernière semaine du mois de mai (jour 143-152) avec une émission moyenne de 1.78 ± 0.09 g C $m^{-2}d^{-1}$. Ensuite, la seconde pointe d'émission identifiée concorde avec le brassage automnal du réservoir, soit de la fin du mois d'aout à septembre (jour 229-274) avec une émission moyenne de 1.27 ± 0.03 g C $m^{-2}d^{-1}$. En somme, l'effet net du réservoir fut estimé à 1.75 ± 0.07 g C $m^{-2}d^{-1}$ pour la période exempte de glace sur le réservoir (juin à aout) et de 289.2 ± 144.6 g C $m^{-2}yr^{-1}$pour la totalité de l'année.

Acknowledgements

The last time I was on the top of the island tower, I remembered watching the sun twinkling on the reservoir's waves and my mind was thining about this whole project. Without this tower, which I was standing on top and enjoying the view, the project I am about to present would not have been possible. Similarly, without some key persons, its accomplishment would never have been the same.

First, Mom & Dad, you are to me the foundations of this tower. Thanks for your continuous support and for believing in me through my academic years.

Then, Ian, Nigel and Alain, you each represent a very important step of this tower. Ian, you helped me to reach the top without being too scared of the height of this challenge. You also taught me to take this project a step at the time.

Finally, Marc, to me you represent what is on the horizon. From day one of this project you were very much involved… you helped me to think outside the set boundaries and make me move forward. Together I am looking forward to explore what is beyond this island.

Contribution of Authors

"As an alternative to the tradition thesis format, the thesis can consist of a collection of papers of which the student is an author or co-author. These papers must have a cohesive, unitary character makig them a report of a single program of research."

This thesis consits of two manuscripts.

Forest Characterization

Marie-Eve Lemieux[1], Ian B. Strachan[2], Nigel Roulet[1], Alain Tremblay[3]

[1] Dept. of Geography, McGill University, Montreal, Quebec
[2] Dept. of Natural Resources Sciences, McGill University, Montreal, Quebec
[3] Hydro-Quebec, Montreal, Quebec

This manuscript is the original work of Marie-Eve Lemieux. Field sampling design, data collection and analyses were done by the thesis author. Drs. Strachan and Roulet provided expert advice and financial support. Dr. Tremblay provided logisitical support. Dr. Strachan contributed to the editing of this document. The candidate used Matlab scripts developed by Dr. O. Bergeron in Dr. Strachan's AER Lab.

Determination of direction and magnitude of net CO_2 fluxes for the post-flooded environment

Marie-Eve Lemieux[1], Ian B. Strachan[2], Nigel Roulet[1], Alain Tremblay[3]

[1] Dept. of Geography, McGill University, Montreal, Quebec
[2] Dept. of Natural Resources Sciences, McGill University, Montreal, Quebec
[3] Hydro-Quebec, Montreal, Quebec

This manuscript is the original work of Marie-Eve Lemieux. Field sampling design, data collection and analyses were done by the thesis author. Drs. Strachan and Roulet provided expert advice and financial support. Dr. Tremblay provided logisitical support. Dr. Strachan contributed to the editing of this document. The candidate used Matlab scripts developed by Dr. O. Bergeron in Dr. Strachan's AER Lab.

Table of Contents

List of Figures

List of Tables

Chapter 1 : Introduction

The 2007 Canadian Energy Outlook predicts increases in both population and energy demand of 0.7 % and 1.3%, respectively by 2010 (Natural Resources Canada, 2006). Canada's future total potential capacity for hydroelectric power generation is 3×10^5 GW with Quebec being the province holding most of this potential production (Figure 1.1; Statistics Canada, 2005). Hydroelectricity is considered a renewable source of energy since it depends on gravity and precipitation. However, through the creation of reservoirs, hydroelectricity is not without environmental problems. Some of the negative effects that have been identified and studied around the world include the displacement of aboriginal populations and burial sites (Fearnside, 2005), disruption of traditional hunting practices (Rosenberg *et al.*, 1995), fractioning of migration routes for large mammals (Cosson *et al.*, 1999; Vie, 1999; Mahoney and Schaefer, 2002) and methyl mercury release and bioaccumulation (Verdon *et al.*, 1991; Tremblay & Lucotte, 1997).

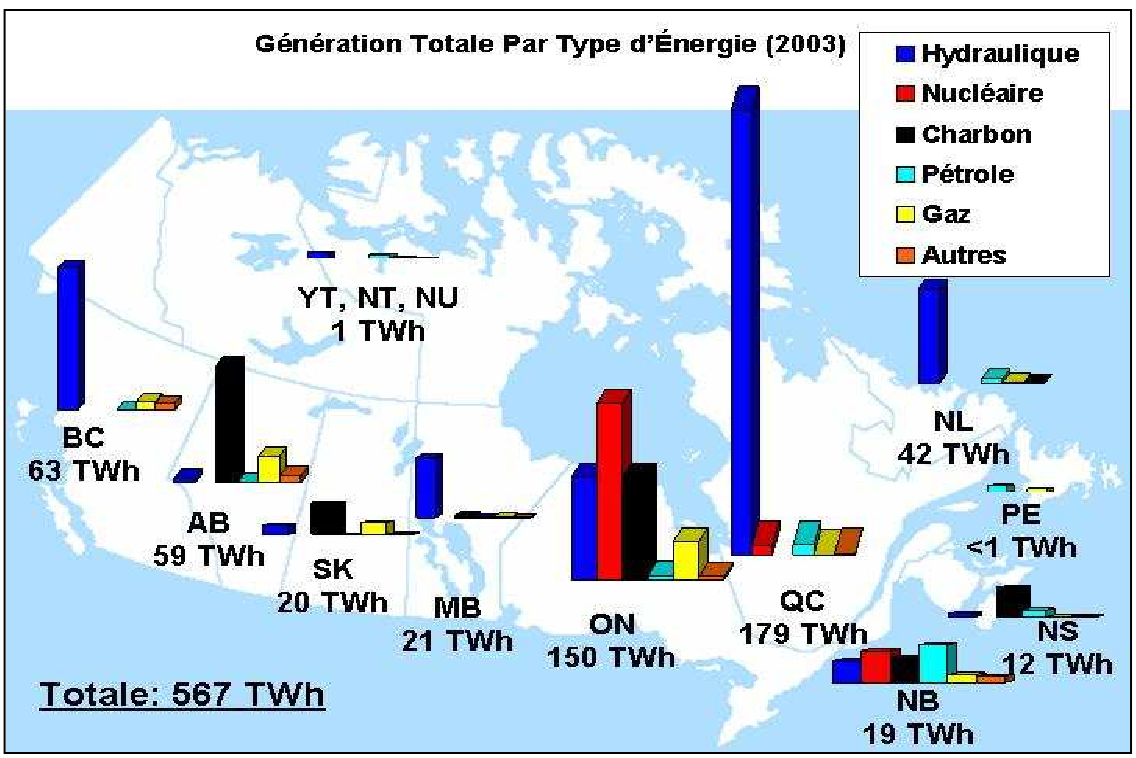

Figure 1.1 Type of energy generation per province. Source: Statistics Canada, 2005.

Despite the aforementioned problems, hydroelectricity is generally believed to be an environmentally-safe way to generate power. More recently however, it has been suggested that artificial hydroelectric reservoirs could constitute an anthropogenic source of GHG. This was confirmed when the first flux measurements on boreal reservoirs (Kelly *et al.,* 1994; Duchemin *et al.,* 1995) 10-years of age or older found emissions on an average of 0.4 ± 0.5 g CO_2-C m^{-2} d^{-1} and 6.6 ± 8.0 mg CH_4-C m^{-2} d^{-1} (Tremblay *et al.*, 2005). The World Commission on Dams report (Fearnside *et al.,* 1995) even went so far as to suggest that GHG emissions from tropical reservoirs may even be higher than those of a conventional oil-fired thermal generation plant.

While such studies have shown that emissions from tropical hydroelectric reservoirs can be higher than 2 g CO_2-C m^{-2} d^{-1} (Tremblay *et al.*, 2005), the few studies focusing on reservoirs in the northern latitudes have indicated that daily losses rarely exceed 0.5 g CO_2-C m^{-2} d^{-1} (Tremblay *et al.*, 2005). To date, most of this research has been conducted on older reservoirs with limited sampling. With more reservoirs being created to meet increasing electricity demand, it is imperative to document the CO_2 fluxes from a newly impounded reservoir. Despite the variability in the reported magnitude of reservoir carbon fluxes, it has certainly been established that the creation of reservoirs does affect the biosphere-atmosphere exchange on a local scale (Delmas, 2003) through the release of biogenic gases such as methane (CH_4) and carbon dioxide (CO_2). Changes in GHG exchange resulting from the creation of a reservoir are primarily induced from the suppression of the net primary production (NPP) of the vegetation following flooding, but also from the heterotrophic respiration coming from the large stock of carbon (C) stored in the flooded vegetation and soils. In turn, the atmosphere responds to the changes in the exchange of energy and water vapour from the surface. Although few measurements exist, younger reservoirs are believed to produce higher emissions than older reservoirs presumably due to fresher organic matter and nutrients. However, it is believed that fluxes stabilize to a level comparable to natural boreal lakes as decomposition decreases over time (Tremblay *et al.*, 2005). Nonetheless, the extent of these impacts is still largely unknown. Therefore, there is great interest in examining if changes, such as those induced by the flooding of a forest, could significantly affect the atmospheric concentrations of GHG.

1.1 The Net GHG Emissions Project

To date, despite a general knowledge that reservoir creation releases GHG, no serious study has attempted to quantify these emissions in a boreal environment through a comparison of the carbon exchange within pre- and post-flooded environments. On November 5th, 2005, in Eastmain, Northern James Bay, Hydro-Quebec created a 604 km^2 reservoir which reached its maximal impoundment capacity on May 29th, 2006. A multidisciplinary research project was established which aimed to quantify CH_4 and CO_2 emissions from the pre- and post-flooded environments using aquatic, terrestrial and atmospheric analysis. For the first time, the problem was addressed by treating the creation of a hydroelectric reservoir from a land cover change perspective. The overarching research question addressed by the entire project is: "***What is the net carbon exchange that results from the creation of a hydroelectric reservoir within the northern boreal forest region*****?**"

Through continuous carbon flux data obtained from micrometeorological techniques, this research aims to answer the following question: "*What is the* ***magnitude and direction of carbon exchange that results from a boreal forest being flooded for hydroelectric purposes***"?

1.2 Research Hypothesis and Research Objectives

The general hypothesis that frames this research is that the flooding of a boreal ecosystem for the creation of a hydroelectric reservoir changes the ecosystem from a net sink to a net source of carbon. The purpose of this research will be to bring together adequate understanding of the problem to produce a credible estimate of the effect that the creation of a Canadian Boreal reservoir has on the net emission of GHG, especially CO_2. The specific research questions and objectives are therefore to:

1. Determine and compare the eco-physiological characteristics of a boreal black spruce forest pre-flooded analogue site with similar areas in northern Quebec;
    a) To determine the temporal and spatial dynamics of the net CO_2 exchange in the first years following flooding;
    b) To characterize the forest as a representative Boreal black spruce forest – the dominant cover type in the region;

2. Determine the direction and magnitude of net CO_2 fluxes for the pre- and post-flooded environments;
    a) To use micrometeorological techniques to quantify the continuous CO_2 exchange in the flooded site and in a pre-flooded analogue site;
    b) To use static carbon chamber measurements to quantify the fluxes of the remaining vegetation on the post-flooded island site;

3. Identify the key environmental drivers of CO_2 over the flooded site;
    a) To identify and explain the flux differences between the pre- and post-flooded environments;
    b) To contribute to the larger project's modelling effort by providing relevant field information for model validation.

1.3 Thesis Format

This thesis consists of five chapters including this introductory chapter. **Chapter 2** provides a review of the research conducted to date on hydroelectric reservoir creation in northern environments with emphasis on CO_2 emissions. Two results chapters follow this review. The eco-physiological characteristics of the boreal black spruce forest are presented in **Chapter 3** where the analogue forest is compared with similar areas in northern Quebec (Objective 1). Biophysical variables and the net ecosystem exchange (NEE) of the Eastmain-1 (EM1) black spruce forest are presented for the study period. The direction and magnitude of net CO_2 fluxes derived from eddy covariance measurements from the post-flooded reservoir environment (Objective 2) are presented in **Chapter 4**. This chapter includes a comparison between the CO_2 fluxes from the flooded and pre-flooded analogue site and the key environmental drivers of CO_2 over the post-flooded forest are identified (Objective 3). This chapter also includes a discussion and summary of flux differences between the pre- and post flooded environments and potential reasons that these differences exist. The thesis culminates in **Chapter 5** where a summary of the research is presented.

Chapter 2: Literature Review

2.1 Dichotomy of Hydroelectric Reservoir Emissions

2.1.1 Beyond Science: Political and Corporate Interests

As world population increases and economies continue to grow, there will be increased demand for electricity. Consequently, there is also a growing acknowledgement of the greenhouse gas (GHG) emissions associated with electrical production and possibly on its impact on global climate but certainly on global policy.

The new administration in the United States is focusing its attention on America's foreign oil dependency within the context of climate change. The Obama-Biden New Energy for America Plan contains an emphasis on sustainable development, with a strong focus on renewable energy. Among the stated goals are to ensure that 10% of US electricity will come from renewable sources by 2012 and 25% by 2025 and to implement an economy-wide cap-and-trade program to reduce greenhouse gas emissions 80% by 2025 (U.S. Department of Energy, 2009).

Currently, 39.8% of US electricity comes from petroleum, 23.6% from natural gas, 22.8% from coal, 8.6% from nuclear and 6.8% from renewable energy (Energy Information Administration, 2008). As part of the New Energy for America Plan, wind power and solar energy could be considered, but hydroelectricity remains very efficient in terms of KWh per dollar invested. Thus, hydroelectric production could represent an interesting avenue for the United States.

It is popularly held that hydroelectric generation represents a source of clean energy production. However, early research indicated that reservoirs could emit more than a conventional oil-fired thermal generation plant (Fearnside, 1997; Rosa and dos Santos, 2000). This was particularly noticeable in tropical reservoirs of the southern hemisphere, especially at the Brazil Tucurui dam. This emission rate was supported by Duchemin *et al*. (2002) for reservoirs in the Northern hemisphere. Later, Dos Santos *et al.* (2006) appeared to reverse themselves by stating that although hydro-power is not a clean source of energy in terms of emissions to the atmosphere, it is still better than thermo-power plants. One of the main problems of such studies is their perceived lack of transparency since they were often conducted by hydro-electric companies themselves (Cullenward and Victor, 2006).

Nevertheless, the outcome of further research will be important for South American countries with hydro potential. The Brazilian government is planning new investment to satisfy growing demand for hydroelectricity (deOliveira, 2006; Cullenward and Victor, 2006). Since Brazil is considered a developing country by the United Nations, it currently faces no obligation to reduce its GHG under the Kyoto Protocol. However, the Conference of the Parties (COP/MOP) of the United Nations Framework Convention on Climate Change (UNFCCC) established the Protocol's Clean Development Mechanisms (CDM) which would allow both Brazil and Ecuador to seek financial compensation for projects that yield low emissions of GHG. These projects, which should stimulate sustainable development and emissions reduction, might involve a rural electrification through solar panels, energy-efficient boilers or the construction of hydroelectric dams. Currently, Brazil has applied for eighteen CDM hydroelectric facilities. Along with an existing biofuel programs, hydroelectricity appears to be Brazil's choice as these CDM projects are considered essential to enhance the national economy and meet the country's growing energy demand. As defined in Article 12 of the Kyoto Protocol: "*CDM allows a country with an emission-reduction or emission-limitation commitment to implement an emission-reduction project in developing countries".* Thus, developing countries, under the CDM would have the possibility of reducing their emissions and earning saleable certified emission reduction (CERs). However, if hydroelectricity is found, in tropical regions, to be a net producer of GHG, their hope of obtaining support from the CDM United Nations would become extremely reduced.

In contrast, the prevailing thinking is that hydroelectric generation in northern environments is not considered to be as great a source of GHG in comparison with tropical environments. Thus, in Canada, hydropower could offer the possibility of carbon revenue to any provincially owned corporation. Quebec has a tremendous potential for hydroelectricity and its provincial government, under Premier Jean Charest, has increased hydroelectric production and declared it to be a clean and sustainable way to produce energy. As a result, during the summer of 2009, Hydro-Quebec announced a 25 billion dollar investment to increase its total production. By doing so, the corporation is aiming to increase its exports to 38% by 2013, especially targeting the United States (Hydro-Québec, 2009). Although, like any other form of energy production, hydroelectricity is not absolutely harmless to the environment, but those projects agree with the Government's long term goal of making Quebec a world leader of green energy production. Thus, if studies indicate that boreal reservoirs are low net emitters of GHG, hydroelectric generation could represent a tremendous economic advantage to any Canadian province developing this source of energy.

The different CO_2 emissions obtained from measurements on hydroelectric reservoirs, with a particular focus on the boreal environment are summarized in Table 2.1. Large error bounds in the results are mainly due to the lack of standardized methods and clearly expose a need for a comprehensive and transparent GHG emissions assessment for such systems.

Location	Reservoir	Area (km^2)	Depth (m)	Age (yr)	Type of Flux	CO_2 (mg/m^2d)	References
Canada							
Quebec	Laforge-1	1000	6.2	1-5	D & B	2300 (200-8500)	Duchemin *et al.,* 1995; Duchemin, 2000
	Robert Bourassa	2500	NA	12-19	D & B	1500 (160-12 000)	Kelly *et al.,* 1994; Duchemin *et al.,* 1995; Duchemin, 2000
	Eastmain-Opinaca	1000	NA	12-13	D	3450 (2200-4300)	Kelly et *et al.,* 1994; Duchemin *et al.,* 1995; Duchemin, 2000
	Cabonga	400	NA	68-70	D & B	1400 (320-4800)	Duchemin *et al.,* 1995; Duchemin, 2000
	Boreal lakes (3)	8	4.7		D	333 ± 224	Soumis *et al.,* 2007
		1.6	1.6				
		17.5	3.6				
	Temperate lakes (3)	60.2	8.6		D	691 ± 1385	
		38.1	9.7				
		1764	15.5				
	Boreal rivers	NA	NA		D	802 ± 157	
	Boreal reservoir (LA1 & LaGrande) (whole)	1000 & 2835	6.2 & 22	1978 & 1996	D	779 ± 282	
	Boreal reservoir (coves)					632 ± 139	
	Boreal reservoir (thalweg)					877 ± 321	
	LG2	2835	22	1978	D	80-1800	Roehm *et al.,* 2006
	LG3	NA	NA	NA	D	400-1500	
	D24	NA	3	1978	D	15 471	Duchemin *et al.,* 2006
	LA40 (experimental)	1	<3	1-5	D	4898	
	LG2	2835	22	1978	D	20916	
	D24	NA	3	1978	B	1.0-0.140	
	LaGrande Region			1978	D & B	$2.8X10^5$	
British Columbia	Reveistoke	120	NA	8	D	2200 (1560-3000)	Schellhase *et al.,* 1997
	Kinsbasket	430	NA	19	D	530 (460-600)	
	Arrow	520	NA	22	D	1300 (570-1770)	
	Whatshan	15	NA	40	D	670 (540-790)	
Ontario	ELARP	0.2	NA	1993	D & B	2000 (1100-3700)	Kelly *et al.,* 1997
	FLUDEX	0.5-0.7 ha	1-2	1999	NA	1500-3000	Bodaly *et al.,* 2004;
Europe							
Finland	Lokka	216-417	2.3-5.0	1967	D	21-133	Huttunen *et al.,* 2002
	Porttipahta	34-214	4.4-6.3	1970	D	36-95	

	Lake Ekojarvi	NA	NA	NA	D	318 g c m2 /a	Arvola *et al.,* 2002

Table 2.1 Summary of the average CO_2 emissions of northern hydroelectric reservoirs. D: Diffusive Fluxes; B: Bubbling or Ebullition; NA: Data not available

2.2 Carbon Exchange in Boreal Ecosystems

The global boreal forest biome comprises 11% of the Earth's vegetative surface (Bonan and Shugart, 1989; Dixon *et al.,* 1994), or 12.2x10^6 km^2 (Black *et al*., 2005) extending in a broad belt around Eurasia and North America, between 50 and 60 degrees north latitude (Figure 2.1). Its soil and biomass hold 43% and 13% of the Earth's carbon, respectively (Schlesinger, 1997; Schulze *et al*., 1999). More than 36% of North American is covered by boreal forest (Black *et al.*, 2005) with black spruce (*Picea mariana*) being the most dominant species of this ecosystem (Connell *et al.,* 2003).

In Quebec, the majority of hydroelectric production and future potential is located within ecosystems characterized as black spruce boreal forest. This forested biome is characterized by a long, harsh and dry winter and moderately warm and moist summers (Golden *et al*., 1998). Several studies have suggested that the boreal forest plays a crucial role in regulating the climate of the northern hemisphere and in the global carbon cycle (Keeling *et al*., 1996). Thus, with the growing political and scientific concern over climate change at the international level, boreal forests have been extensively examined in order to determine their exact role in future climate change scenarios.

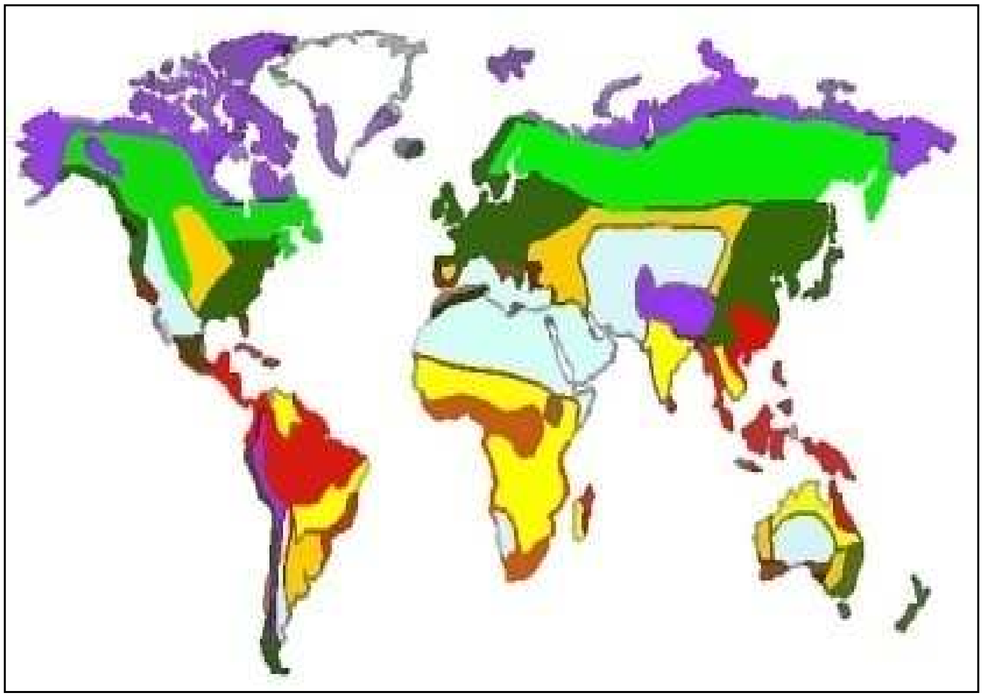

Figure 2.1 Global Biome Map indicating the regions classified as Boreal Forest (light green) (*from* World Biome, 1995).

On May 14th, 2008, both the Quebec Natural Resources Minister Claude Bechard, and the Quebec Minister of Sustainable Development, Environment and Parks, Mrs. Line Beauchamp, announced a 1% increase of the total protected area in Quebec (1800 natural sites representing 4.8% of Quebec's total territory or 80 000 km^2) (Ministere des Ressources Naturelles et de la Faune, 2008) which would not only maintain biodiversity, but also serve for natural carbon sequestration in the global balance. Out of those 18, 222 km^2 supplemental protected areas, 4,765 km^2 are located in Northern Quebec where the boreal forest dominates (Ministere des Ressources Naturelles et Faune, 2008). On September 26th 2008, Primier Charest presented the Province's Northern Development Plan. Now that politicians have demonstrated an increased interest in the carbon cycle and in northern environments, it is critical that scientific knowledge on the role played by the boreal forest in terms of carbon exchange is available.

2.2.1 Factors Affecting Carbon Fluxes

Factors affecting carbon exchange in boreal forest have been well documented by a variety of studies (e.g. Keeling *et al*., 1996; Bergeron *et al*., 2007; Bond-Lamberty *et al.*, 2007; Piao *et al.*, 2008). Drought, soil moisture or drainage, snow cover, air temperature and disturbance such as insects or fires, are factors that influence the carbon exchange. In boreal ecosystems, the net ecosystem exchange (NEE) is mainly driven by seasonality, including variations in precipitation and temperature.

The source-sink nature of boreal forests and the controls on the net carbon exchange have been the subject of much recent study. Bergeron *et al.* (2007) investigated the carbon budget variation of mature black spruce across Canada. They found that gross ecosystem production (GEP) and respiration (R) were related to the annual air temperature and to the starting date of the growing season. They indicated that the eastern old black spruce forest near Chibougamau, QC was carbon neutral on an annual basis and affected by the snow pack in winter and low light levels. Black spruce dominated forest at this latitude also expressed the lowest total annual net ecosystem production (NEP) when compared to other Canadian boreal forests. This may be due to a combination of effects: warmer soil insulated under a thicker snow pack may induce an increase in winter carbon loss for instance. The comparatively lower light levels during the short summer months would restrain NEP and GEP.

Net CO_2 exchange measurements were also obtained over a mature black spruce forest in central Saskatchewan (1999-2006) by Krishnan *et al.* (2006). They report that the growing season varied between 186 to 232 days and began when the daily mean temperature reached 4°C and 0°C for the air and the soil surface, respectively. This forest was revealed to be a weak annual sink for CO_2 with annual NEP ranging from 27 to 80 g C m^{-2} y^{-1} (56 ± 21 g C m^{-2} y^{-1}). In the Southern boreal forest of Saskatchewan, moisture appears to be the limiting factor in the C cycle.

Bond-Lamberty *et al*. (2007) investigated the effect of fires on the carbon balance in the boreal forest from 1948 to 2005. They found no direct evidence that the boreal environment has been affected by global climate change, but that eco-physiological changes such as the variation in the carbon balance and the vegetation dominance are a consequence of frequent fire disturbances.

More recently, Piao *et al.* (2008) reported that spring and autumn warming could enhance carbon sequestration and extend the period of net carbon uptake in the future. However, they found that despite an increase in both the photosynthetic activity and the respiration, respiration dominates. They found that during the spring, warming would stimulate photosynthesis more than respiration; however, if autumn warming occurred at a greater rate than in the spring, the capacity for northern ecosystems to sequester carbon would suffer.

It has also been suggested that the boreal forest response to temperature and rainfall was dependent upon its age. Measurements of CO_2 exchange were conducted by Andrew *et al*. (2008) over six Canadians boreal forests ranging from 4 to 155 years of age. They found that depending on the stand's age, a warmer than average spring would differently impact switchover; respectively for older and younger stands it can vary from 37 to 25 days. Alternatively, a warm and dry year resulted in a reduction of CO_2 uptake by the younger, but not the older stands. Overall, their study pointed out that the source of inter-annual CO_2 exchange variation is the result of the ability of older, evergreen stand to respond to warmer springs.

Finally, Amiro *et al.* (2006) concluded that uncertainties related to carbon and energy flux estimates in the boreal environment remain and called for more work to be done in order to adequately scale up results to the Boreal biome in general. Nevertheless, these studies allow the Eastmain-1 forest to be placed in the context of other northern boreal forests.

2.2.2 Biophysical Variables

Leaf Area index (LAI) is strongly related to key vegetation processes such as water vapor and CO_2 exchange. It is commonly interpreted as a measure of the projected leaf area per unit of ground area (Strachan *et al.*, 2005). Since LAI can be linked to plant biomass and therefore carbon uptake, obtaining this information is essential in conducting any assessment of C exchange.

LAI can be measured directly through harvesting or indirectly using optical techniques. For the latter, the passage of radiation through a canopy is influenced by the canopy's structure. Thus, by measuring the penetration of radiation and applying a model that describes the attenuation of radiation, one can predict the canopy structure that influenced the radiation measurement. The appropriate technique of measurement must be used for the appropriate spatial and temporal scale. Direct measurements are better for smaller spatial scales and can be used to follow the growing season while indirect techniques provide a much better spatial representation and can more easily cover a larger spatial area. Any direct techniques are rather time consuming, resource intensive and cause disturbance to the site through plant removal.

2.2.3 Optical Instrument Theory – LAI-2000 & TRAC

The most common definition of LAI stipulates that it is one half of the total green leaf area per unit ground surface area (Chen *et al.,* 1997). The LAI-2000 (Li-Cor, Lincoln, Nebraska) is in indirect measurement device for LAI that involves the measurement of transmitted blue light (400-490nm) beneath the primary canopy in five concentric rings and zenith angles (0-12°, 15-28°, 31-43°, 45-58°, 61-74°). This instrument provides a rapid estimate of the effective LAI (Le) based on a calculation of the canopy gap fraction but assumes a random distribution of foliage elements, thus underestimating the LAI when the foliage is clumped, as in a coniferous forest.

TRAC (Tracing Radiation and Architecture of Canopies, 3rd Wave Engineering) is an optical instrument for measuring LAI and the fraction of photosynthetically active radiation absorbed by the plant canopy (FPAR). It measures both the canopy gap size distribution and gap fraction. Gap size is the physical dimension of a gap in the canopy and gap fraction is the percentage of gaps in the canopy at a given solar zenith angle. It is important to take gap size into consideration because forest canopies are composed of distinct elements such as tree crowns, branches, shoots and needles. These structures determine the spatial distribution of needles. Gap fraction can be obtained from radiation transmittance. TRAC uses the solar beam as a probe and therefore repeated measures over half a day are required to compute the gap fraction. However, Chen and Cihlar (2002) showed that when TRAC is used near the solar zenith angle of 57.3° this adequately represented the average canopy distribution and provided estimates of LAI.

Conifer needles are organized into different hierarchies of clumping. Therefore, a correction factor (Ω) must be applied to the effective LAI of black spruce forest (Chen *et al*., 1997). Using the canopy gap size data from TRAC provides relevant information of the canopy architecture and can be used to quantify the effect of foliage clumping (Chen and Cihlar, 1995; Chen, 1996; Chen *et al*., 1997; Kucharik *et al*., 1997; Leblanc 2002). *Le* is obtained from gap fraction measurements and can be obtained from the LAI-2000. It can then be used as a basis to calculate LAI using (Chen *et al*., 1997):

$$\mathbf{LAI} = \frac{(1-\alpha)\mathbf{Le}}{\mathbf{\Omega}} \tag{1}$$

where α is the woody-to-total plant area ratio with typical values ranging from 0.12-0.17 (Chen *et al*., 1996; Gower *et al*., 1999) and (1−α) removes the contribution of the non-leafy material. Nonetheless, measuring the amount of needle area within the shoots remains challenging with optical instruments. Hence, the Ω value has to be separated into two components (Chen and Cihlar, 1995):

$$\Omega = \frac{\Omega_e}{\gamma_e} \tag{2}$$

where γ_e is the needle-to-shoot area ratio quantifying the effect of foliage clumping within a shoot (higher the clumping, higher the needle-to-shoot ratio) and Ω_e includes the effect of foliage clumping at scales larger than a shoot (it decreases with higher clumping). Thus the final LAI equation becomes (Chen *et al*., 1997):

$$\mathbf{LAI} = \frac{(1-\propto)\mathbf{Le}\,\gamma\mathbf{E_e}}{\Omega_e} \qquad (3)$$

Hemispherical LAI obtained from researchers (Woods Hole Research Center, 2007) working in the BOREAS study reported an overall value for black spruce of 1.3 (ranging from 0.4-2.3). However, Bergeron *et al.* (2007) reported a higher LAI value of 3.7 in Chibougamau, QC.

2.3 Carbon Exchange in Flooded Environments

2.3.1 Biological Factors Contributing to GHG Emissions

Flooding an area constitutes a major land use change; it stops photosynthesis (Aberg *et al.,* 2004) and engenders new chemical reactions, therefore understanding the mechanism by which a reservoir is emitting GHG is crucial. Several sources of GHG from reservoirs have been identified (DeRosa *et al.,* 2002; Bodaly *et al.,* 2004) and can be divided into three main categories: (1) pre-existing conditions, such as the amount and type of organic carbon deposits in the flooded land, the input of allochtonous organic carbon and the mineralization of dissolved organic matter (DOC), referred to as photochemical reaction; (2) environmental drivers, such as water temperature, wind speed and ice melt; and, (3) to a lesser extent, some physical aspects, including age and depth of the reservoir could be included.

Different forms and sources of organic carbon can be identified in aquatic environments including the flooded biomass; DOC; particulate organic matter brought in from the catchment area (Bodaly *et al.,* 2004); plants that grow on the surface; and, fluxes from the flooded shorelines (Cullenward & Victor, 2006). Along with organic carbon in aquatic systems, comes another important factor contributing to GHG emissions from hydropower production - bacterial decomposition, both aerobic and anaerobic, of organic matter (DeRosa *et al.*, 2002). CH_4 and CO_2 result from anoxic organic sediments, which are decomposed by methanogenic bacteria. At first, organic carbon decomposes quickly, depleting oxygen and elevating concentrations of MeHg, CO_2, CH_4, DOC and other dissolved nutrients (Bodaly *et al*., 2004). The Experimental Lake Area (ELA) experiment showed that most of the decomposition byproducts in a medium-carbon reservoir were exported in the first years, and the levels dropped in the following years (Bodaly *et al.,* 2004). These results also agree with Tremblay *et al.* (2004) who found that the maximum emissions of a boreal reservoir are reached in the first three to five years after impoundment and are followed by a decline of emissions. When measurements are done on older reservoirs, emissions seem to stabilize to a slightly higher level than natural lakes (Figure 2.2).

Environmental drivers of carbon exchange include air and water temperatures and wind speed (Coyne and Kelly, 1974). Degassing from the turbines could also be included since it seems to be a seasonally defined phenomenon (Rosa *et al.,* 2002; Roehm *et al*., 2006). The highest rate of degassing occurs in winter and spring because lower temperature affects CO_2 solubility (Roehm *et al*., 2006). Ice melt is another important component to take into consideration. It has been demonstrated that 67% of CH_4 emissions and 46% of CO_2 emissions occur during the first day after the ice melts (Rosa *et al.,* 2002).

To date, it is believed that emissions from an older reservoir resemble that of a natural lake in a boreal environment (Figure 2.2 and Table 2.2).

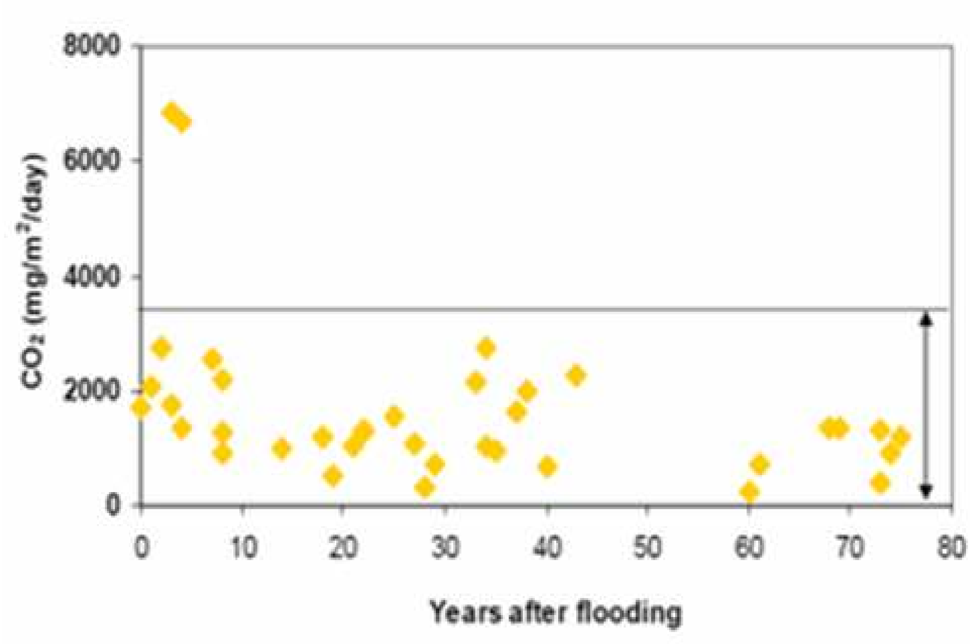

Figure 2.2 Carbon dioxide emission (mg m^{-2} yr) as a function of the boreal reservoir age. (*from* Tremblay *et al*., 2002).

Inherent in all of these measurements is a significantly large error term. This can be explained in part through the lack of standardization in the measurement techniques, principally the static floating chambers used for diffusive gas fluxes. Emissions are likely also to vary with the depth of the reservoir and the type of flooded environment (peatland, forest, river) leading to heterogeneity in measurement results.

Table 2.2 Summary of the Average CO_2 Emissions of Hydroelectric Reservoirs in Canadian Northern Environment (*from* Tremblay *et al.,* 2004)

Location	Old reservoir (>10 yrs)	Natural lakes	Young reservoir
		mg CO_2/m^2/day	
Quebec	1600 ± 1500	735 ± 1125	4400 ± 4000
Manitoba	3350 ± 2725	1365 ± 2375	NA
British Columbia	250 ± 800	500 ± 650	NA

2.4 Measurement of Diffusive Gas Fluxes

GHG in the form of CO_2 emitted to the atmosphere from reservoirs comes primarily from diffusive flow with bubbling estimated to account for only 1% (Rosa *et al.*, 2002). Thin Boundary Layer (TBL) with or without tracers, floating chambers and eddy covariance are the different techniques used to measure gas fluxes from aquatic systems.

2.4.1 Thin Boundary Layer Techniques

TBL does not involve direct flux measurement over the water. It rather calculates a flux using semi-empirical equations (Liss & Slater, 1974; Canuel *et al.,* 1997; Duchemin *et al.,* 1999) and environmental variables such as the concentration of the dissolved gas in the water, wind speed and water temperature. The technique is less well defined for low (<5 ms^{-1}) and high (> 10 ms^{-1}) wind speeds (Duchemin *et al.,* 1999). In practice, water is collected in a bottle that is sealed underwater at a depth of 15 to 30 cm. Samples of the dissolved gas are then sent to the laboratory for analysis. This method is efficient in terms of the number of sample collected per day as it takes less than five minutes at each location. However, samples must be handled appropriately and quickly analyzed, which might not be easy in a remote field location. Finally, results obtained from this method have been suggested to be lower than the theoretical dissolved CO_2 concentration (Lambert & Frechette, 2002).

2.4.2 Aquatic and Terrestrial Static Carbon Chamber

Carbon chambers were first used in 1920 by Bornemann, and the technique has been reviewed by several authors (Livingston & Hutchinson, 1995; Holland *et al*., 1999; Livingston & Hutchinson, 2002). The manual chamber technique has been extensively used to measure net ecosystem exchange (NEE) in aquatic systems (Delgiorgio and William, 2005; Prairie *et al.,* 2002) as well as in terrestrial ecosystems such as wetlands (Frolking *et al*., 1998; Waddington and Roulet, 2000) and forested areas (Goulden and Crill, 1997). Chambers can be automated such as systems used in the Fluxnet sites (Burrows *et al*., 2005; Bubier *et al*., 2003). The main criticisms associated with this method are the small temporal and spatial extent of the sample; the creation of an artificial microclimate through the disturbance of the natural flow of air; the promotion of artificial turbulence in aquatic sampling; the perturbation of local pressure; and the alteration of the heat and water balance in the soil (Livingston & Hutchinson, 1995; Baldocchi, 1993). Perturbation of natural conditions is inevitable and can modify the flux that was intended to be measured. Physical and biological factors such as soil and air temperature, humidity, photosynthesis, soil respiration can be affected by the chamber deployment. Also, the design of the chamber itself might constitute a relative source of error, either through the chamber air mixing regime or leaks. Manual chambers require time and physical labor, logistics, transportation and power. Nighttime and winter measurements are more logistically difficult. While conducting carbon chamber measurements, factors such as temperature, PAR (photosynthetic active radiation), must be measured and water table and plant diversity when conducted on terrestrial environment.

2.4.3 Eddy Covariance

Eddy covariance (EC) is a micrometeorological technique that is routinely used to measure net ecosystem exchange (NEE) of CO_2, water vapor, and sensible heat fluxes. NEE is the net carbon exchange resulting from photosynthetic uptake of CO_2 by the vegetation and the respiration of CO_2 from soil and plant material. A typical eddy covariance system consists of an ultrasonic anemometer and a high frequency gas analyzer, along with meteorological instruments and a fast-response data logger. This technique calculates a vertical turbulent flux (*Fc*), which is defined as a covariance between the vertical wind speed (*w*) and CO_2 concentration (s) as:

$$\mathbf{Fc} = \overline{\mathbf{w}'\mathbf{s}'} \tag{4}$$

EC is the most direct flux measurement technique. The main advantage of using this micrometeorological technique is that it allows an undisturbed measurement of the exchange of a scalar such as CO_2 between the atmosphere and a large spatial area of the surface continuously through time (Baldocchi *et al.,* 1998). The spatial area is referred to as the upwind footprint and is highly dependent upon atmospheric stability (Leclerc *et al*., 1989) and surface roughness. In order to obtain the best measurements, the tower must be installed over a wide, flat and homogeneous surface (Baldocchi, 2003). Poor mixing conditions in the atmosphere, rain and extreme weather events, power and instrument failures all represent some limitations to data collection with this technique.

Nonetheless, the eddy covariance technique is now widely used to measure NEE of CO_2, since it provides continuous flux information integrated at the ecosystem scale (Baldocchi, 2003). Already, long-term measurements in boreal forests have been conducted over several forests around the Northern Hemisphere (Blanken *et al.,* 1997; Jarvis *et al.,* 1997; Goulden *et al.,* 1998; Lindroth *et al.,* 1998; Markkanen *et al.,* 2001; Bergeron *et al.,* 2007). Frequently, these studies also looked at the source area in order to correlate tower measurements to the physical characteristics of the site.

2.4.3.1 Aquatic Measurements Using Micrometeorology

While the boreal forest has been the site of several long-term studies using tower flux techniques, relatively few studies have been conducted over large bodies of water for an extended period of time. The flux tower was first used above the open ocean by James and Smith in 1977. Most of the studies that followed agreed on a flux value of 0.05 mg C $m^{-2}s^{-1}$ above the ocean. However, in 1986, Liss *et al*. conducted two independent studies over the ocean which were quite controversial. The flux estimates were found to be substantially larger (100x) than those determined from isotopic and tracer methods. In 2000, Blanken *et al*. conducted a study investigating the evaporation from Great Slave Lake, Northwest Territories, using micrometeorological measurements with an upwind area extending between 5 and 8 km across the lake for two summers. They found that values for the latent heat flux were primarily negative (directed toward the surface) but became and remained positive soon after the ice break up. However, the study did not assess CO_2 fluxes. Eugster *et al.* (2003) investigated the CO_2 exchange between air and water in an Arctic Alaskan and a mid-latitude Swiss lake, comparing both the floating chamber and the eddy covariance (EC). They found that the fluxes obtained from floating chambers were larger than those from the EC by a factor of 2. More recently, Guerin *et al.* (2007) conducted a similar study in French Guyana for a three-day period over a reservoir. They indicated that the comparison between the two

Table 2.3 Comparison of different CO_2 fluxes measured over large bodies of water.

Methods	**Fluxes** (mg C m^{-2} d^{-1})	**Location**	**Duration**	**References**
Eddy covariance	114 ± 33	Boreal Lake, Alaska	1-3 days	Eugster *et al*., 2003
Boundary Layer Model	131 ± 2			
Surface renewal model	153 ± 3			
Floating chamber	365 ± 61			
Eddy covariance	4005 ± 3213	Tropical	24 hours	Guerin *et al*., 2007

Floating chamber	5941 ± 3961	Reservoir, French Guyana		

methods should be taken with caution since it is based on a small dataset (24 hours). The fluxes obtained by the EC over water are summarized in Table 2. 3 To our knowledge, the present study presents the first long term dataset of CO_2 measurement over water using the eddy flux tower.

2.5 The Challenge of Gap filling

2.5.1 Pre-Flooded site (forest)

Gaps in the eddy covariance data are inevitable and can result from power failure, inadequate meteorological conditions (poor atmospheric mixing) or extreme weather events and instruments maintenance. According to Falge *et al.* (2001) the acquisition of 65% of possible data periods constitutes a good dataset. However, gaps in eddy covariance datasets can normally be filled, although there is no standard widely accepted method of gap filling (Falge *et al.,* 2001). Lafleur *et al*. (2003) separate gaps into shorter (< 2 hours) and longer periods (snow-covered and snow-free period). Any short gaps are gap filled by linear interpolation. However, for longer gaps, more manipulation is required. During the snow-covered period, gaps are filled by weekly averages, thus net ecosystem values are needed. For the snow-free period, most micrometeorologists use physiological relationships to fill the nighttime and daytime gaps separately. Over terrestrial ecosystems, nighttime gaps can be filled by a non-linear relationship between NEE (equivalent to the ecosystem respiration at night) and the soil temperature. Daytime gaps can be filled by a rectangular parabolic relationship between NEE and PAR, which can also be a separate relationship for each month of the study to account for the time and seasonal changes in plant biomass and microbial activity (Hollinger *et al.,* 1999; Lafleur *et al.,* 2001).

Wofsy *et al.* (2001) have identified a few other strategies for long term energy flux measurements. Those can be summarized as mean diurnal variations of previous periods (MDV) and LookUp tables (Falge *et al.,* 2000). MDV consists of replacing the missing observations by the mean for that time period (half-hourly averages) based on previous and subsequent days. For energy fluxes independent windows of 14 days size can be found and to reduce the errors, the averaged values can be introduced which would show a nonlinear dependence on environmental variables. However, unlike the LookUp tables, MDV does not account for the daily variations in weather conditions. LookUp tables need to be created for each site so that missing values of λE and H could be looked up based on environmental conditions associated with missing data. While gap filling over a forest environment is well documented, gap filling techniques are not well established over a large body of water. Through this research, gap filling the reservoir will be further explored.

2.5.2 Micrometeorological Processes of Carbon Fluxes Over a Flooded Environment

Anderson *et al*. (1999) in their study have provided new knowledge on how to estimate the lake-atmosphere CO_2 exchange. First, CO_2 measurements between the atmosphere and a large body of water should account for the gaseous transport between the two fluids (Denmead and Freney, 1992; MacIntyre *et al*., 1995). They explained how the atmospheric surface layer over a lake and the turbulent motions are the main actors for transporting gas between the free atmosphere and the vicinity of the lake surface. To comprehend the turbulent motions of a lake, it is easier to divide it into three distinct layers. First, there is a 1 mm thick layer, lying between the air and the surface. This is the viscous layer where molecular diffusion gas transport is primarily driven by molecular diffusion. Then, there is the air-water interface, just a few microns thick and referred to as the water film. It is very similar to the viscous sublayer, but usually contains sharp gradients in gas concentration and temperature. Deacon's (1977) boundary-layer theory explains that the thickest of this layer varies as a function of temperature and wind conditions. The third layer is the well-mixed bulk water column. Unlike the boundary-layer theory, the surface-renewal model (Danckwerts, 1951) mentions that the viscous sublayer is inhomogeneous and unstable due to thermal and density-driven convection. Nonetheless, both theories lead to a concentration difference (units of density) between the well-mixed bulk of water and the atmosphere. Therefore, the CO_2 flux (Fc) can be defined as:

$$F_{\downarrow}c = \mathbf{V}_{\downarrow}\mathbf{B} \ \left(C_{\downarrow}w/S - \mathrm{Ca}\right) \tag{5}$$

where Cw is the bulk water concentration, Ca is the well-mixed atmosphere concentration, S is the dimensionless solubility ranging between 0.7 and 0.8, depending on temperature ($S \alpha T^{-7.5}$) and the physical chemistry of gas-water interaction. Fc is then governed by the bulk transfer velocity (V_B).

When the boundary layer is considered homogeneous, V_B is closely approximated by Deacon's equation (1977, 1981):

$$V = \frac{\alpha\, S u_{*w}}{Sc_t^{\frac{1}{3}} Sc^{\beta}} \ for\ Sc > \mathbf{200} \tag{6}$$

where α and β are constants (0.082 and 2/3) and the friction velocity of the water's surface ($u*_w$) is equal to the friction velocity in air (u*) times the square root of the ratio of fluid density (air and water). Sc is the Schmidt dimensionless number which is used to define a fluid flow. Both Sc and Sc_t are functions of the surface water temperature. More recently, Eugster *et al.* (2003), after conducting a study on Alaskan and mid-latitudes Swiss lakes, found that CO_2 fluxes over a large body of water were enhanced by the vertical stratification of CO_2 in the water column and the penetrative convection.

Both Anderson's and Eugster's studies have provided precious information to help determining the processes behind the carbon exchange above the flooded site in Eastmain-1. Nonetheless, as mentioned earlier, not as many studies have been conducted over a large body of water and for a continuous period of time. Since the reservoir has only been recently flooded at the time of the study (November 2005) and that carbon fluxes are not yet equilibrated, this is adding complexity to the gap filling process.

PREFACE CHAPTER 3

There is a lack of research on net greenhouse gas emissions (GHG) related to the flooding of boreal ecosystems for hydroelectric reservoir creation. Towards the determination of the net GHG emissions from the reservoir, the CO_2 exchange in the pre-flooded boreal forest needed to be first established. In this chapter, the biophysical and ecophysiological characteristics of the black spruce forest in close proximity to the Eastmain-1 reservoir are explored as a pre-flooded analogue site. We use measurements of tree age, height and density, forest leaf area index, ground vegetation cover, and soil temperature and moisture regimes in comparison with other boreal forest to establish that the pre-flooded analogue site is a representative boreal black spruce forest. The temporal and spatial dynamics of the CO_2 exchange over two years obtained using eddy covariance are used to document the net ecosystem exchange of this forest ecosystem.

CHAPTER 3: Net Ecosystem Exchange of an Eastern Boreal Black Spruce Forest

ABSTRACT

The effects of environmental factors and the forest bio-physical characteristics on the net ecosystem exchange (NEE) were investigated for two growing seasons spanning the period of March 2007 to October 2008 for a boreal forest located in the James Bay, region of Quebec. The forest was comprised of black spruce (*Picea mariana*) with the floor cover dominated by *Sphagnum spp*., *Lichen spp*., *Rhododendron groenlandicum* and *Vaccinium myrtilloides*. Based on four 30 m X 30 m plots arranged near the flux tower, the average tree density was 0.5 trees m^2, and the average tree height and age were respectively, 8.9 ± 2.8 m and 84 ± 3 years. A value of 1.34 was obtained for the leaf area index based on optical techniques. A tower-based eddy covarience system provided continuous measurements of net ecosystem exchange. The forest was a net sink of carbon from May to October. Seasonal NEE and ecosystem respiration (ER) were at their highest in both summers of 2007 and 2008 with an average NEE of -0.8 g C $m^{-2}d^{-1}$ and -0.9 g C $m^{-2}d^{-1}$ and an average ER of 1.5 g C $m^{-2}d^{-1}$ and 2.2 g C $m^{-2}d^{-1}$ respectively. The cumulative NEE at the site was similar for both growing seasons, varying from a sink of -115.6 g C $m^{-2}d^{-1}$ in 2007 to -122.5 g C $m^{-2}d^{-1}$ in 2008.

3.1 INTRODUCTION

Factors affecting carbon (C) exchange in boreal forest have been well documented by a variety of studies (e.g. Keeling *et al*., 1996; Bergeron *et al*., 2007; Bond-Lamberty *et al.*, 2007; Piao *et al.*, 2008). Drought, soil moisture or drainage, snow cover, air temperature and disturbance such as insects or fires, all may influence the carbon exchange. In boreal ecosystems, the net ecosystem exchange (NEE) is mainly driven by seasonality, including variations in precipitation and temperature.

The source-sink nature of boreal forests and the controls on the net carbon exchange have been the subject of much recent study. Bergeron *et al.* (2007) investigated the carbon budget variation of mature black spruce forests across Canada. They found that gross ecosystem production (GEP) and ecosystem respiration (ER) were related to the annual air temperature and to the starting date of the growing season. They indicated that the eastern old black spruce forest near Chibougamau, Quebec, was carbon neutral on an annual basis and that the CO_2 fluxes were affected by the snow pack in winter and low light levels in summer. Black spruce dominated forest at this latitude also expressed the lowest total annual net ecosystem production (NEP) when compared to other Canadian boreal forests (Krishnan et *al.*, 2006; Bergeron et *al*., 2007). This may be due to a combination of effects. Warmer soil insulated under a thicker snow pack may induce an increase in winter carbon loss and the comparatively lower light levels during the short summer months would restrain NEP and GEP.

Net CO_2 exchange measurements were also obtained over a mature black spruce forest in central Saskatchewan (1999-2006) by Krishnan *et al.* (2006). They report that the growing season varied between 186 to 232 days and began when the daily mean temperature reached 4°C and 0°C for the air and the soil surface, respectively. This forest was revealed to be a weak annual sink for CO_2 with annual NEP ranging from 27 to 80 g C m^{-2} y^{-1} (56 ± 21 g C m^{-2} y^{-1}). In this Southern boreal forest of Saskatchewan, moisture appears to be the limiting factor in the C cycle.

More recently, Piao *et al.* (2008) reported that spring and autumn warming could enhance carbon sequestration and extend the period of net carbon uptake in the future. However, they found that despite an increase in both the photosynthetic activity and the respiration, respiration dominates. They reported that during the spring, warming would stimulate photosynthesis more than respiration, however, if autumn warming occurred at a greater rate than in the spring, the capacity for northern ecosystems to sequester carbon would suffer.

It has been suggested that the boreal forest response to temperature and rainfall was dependent upon its age (Andrew et *al*., 2008). In that study, measurements of CO_2 exchange were conducted over six Canadians boreal forests ranging from 4 to 155 years of age. They found that a warmer than average spring would differently impact switchover time with a variation for older and younger stands from 37 to 25 days, respectively . Alternatively, a warm and dry year resulted in a reduction of CO_2 uptake by the younger, but not the older stands. Overall, their study pointed out that the source of interannual CO_2 exchange variation is the result of the ability of older, evergreen stand to respond to warmer springs.

Amiro *et al.* (2006) concluded that uncertainties related to carbon and energy flux estimates in the boreal environment remain and called for more work to be done in order to adequately scale up results to the Boreal biome in general. For instance, Bond-Lamberty *et al*. (2007) investigated the effect of fires on the carbon balance in the boreal forest from 1948 to 2005. They found no direct evidence that the boreal environment has been affected by global climate change, but that eco-physiological changes such as the variation in the carbon balance and the vegetation dominance are a consequence of frequent fire disturbances. Nevertheless, these studies allow the Eastmain-1 forest to be placed in the context of other northern boreal forests.

Among human disturbances, energy production certainly plays a major role, either through the burning or removal of biomass or the flooding of the forest both for the creation of hydroelectric reservoirs. Flooding has been studied principally in terms of the gross GHG emissions produced. Since the pre-existing boreal forest is likely a net sink for carbon, the problem is better addressed by treating the creation of a hydroelectric reservoir as a land cover change issue and instead examining the net emissions of GHG. It is therefore critical to examine the NEE of this boreal forested environment.

The focus of this chapter is directed toward the black spruce forest and not on the other components of the boreal ecosystem. Forests represent 65% of the newly flooded area with the remaining area split between waterways (lakes/rivers; 21%) and wetlands (14%). These other cover types are being studied by research partners and are beyond the scope of the current study. In this study, we first use measurements of forest biophysical parameters to compare this forest with other black spruce stands reported in the literature. We then report the results of two years (2007-2008) of eddy covariance flux measurements of the forest eco-physiological characteristics and net ecosystem exchange (NEE) in order to establish the net source-sink nature of this system.

3.2 MATERIALS AND METHODS

3.2.1 Site Description

The study was conducted in the Eastmain-1, James Bay region of Quebec in an unburned black spruce forest, hereafter, referred to as the pre-flooded site (Figure 3.1). A 23-m tall scaffold tower served as the primary instrument platform (52°06'16" N, 076°11'48" W). Vegetation disturbance was minimized around the tower during its installation in the summer of 2006 with the exception of two large clearings to the east of the tower for helicopter access; these areas were subsequently excluded from flux measurements. The pre-flooded site was located 5 km from the main road and was accessible by all terrain vehicles (ATV), helicopter or snowmobile during the winter.

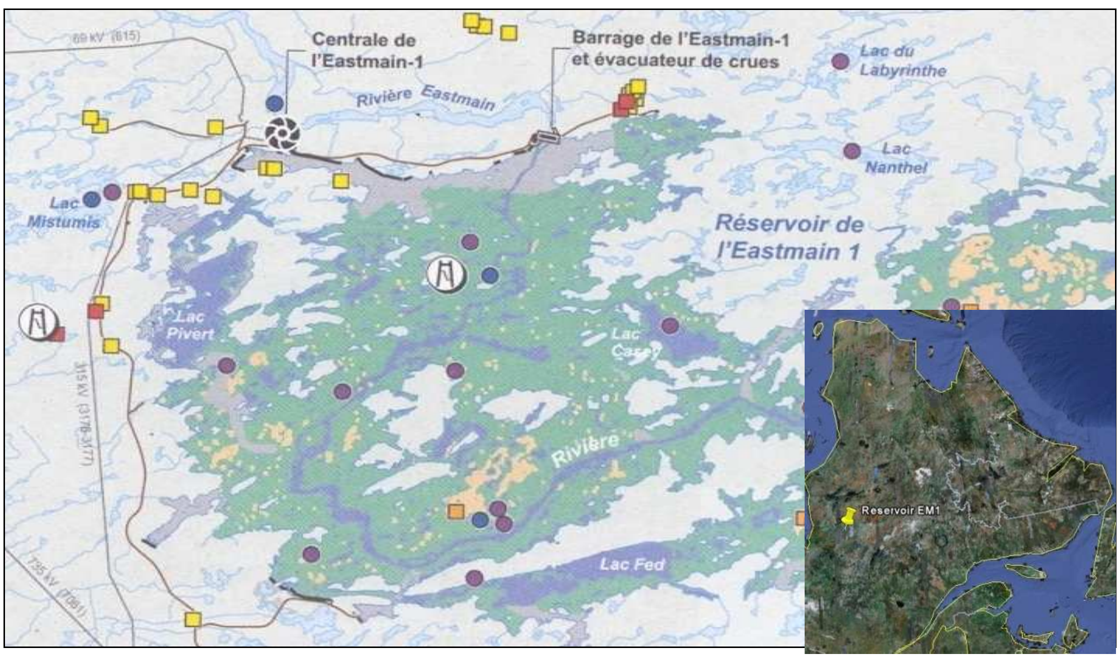

Figure 3.1 Location of the Eastmain 1 hydroelectric reservoir, Quebec. Location of eddy flux towers at the pre- and post- flooded sites are indicted by the tower symbols. Pre-flooded biomes (i.e. as of 2005) are indicated by: darker blue for the original Eastmain river bed; darker green for forest; and beige for wetlands. The inset image of the Province of Quebec was taken from Google Earth, 2009.

3.2.2 Forest Characterization

Biophysical variables were collected to characterise the forest in relation to previously studied black spruce stands. The field measurement scheme (Figure 3.2) was modified from a protocol used by Lucas *et al.* (2006) taking into account any disturbances that may have occurred while installing the tower, structural diversity, topography and soil diversity.

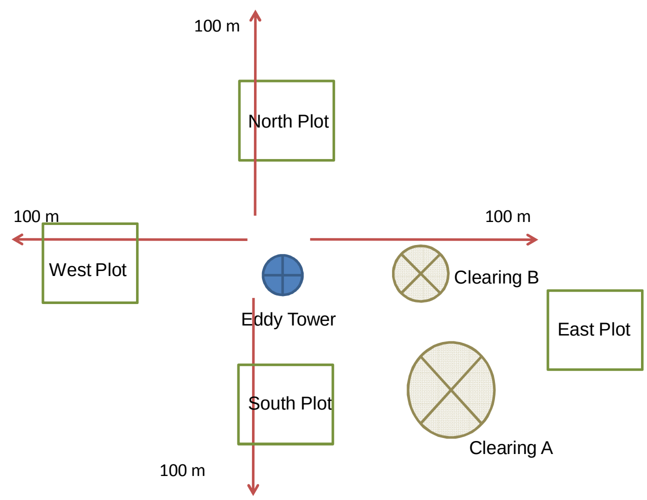

Figure 3.2 Field representation of the four plots installed in all four cardinal points. The red arrows represent the LAI-2000 and TRAC transects, each of 100m.

Four plots (each 30 m x 30 m) were located at a distance of 100 m from the tower and oriented in the cardinal directions (Figure 3.2). Within each plot, species composition, as well as diameter at breast height (DBH; 1.37m), crown width in North-South and East-West directions and tree height were measured for all trees. The crown width was determined using a measuring tape placed underneath the tree canopy going from one edge to the other of the branches, following a North-South and East-West pattern. Tree height was measured using a compass-clinometer. The distance between the observer and the tree trunk at the base was recorded as well as the angle obtained from the compass-clinometer. This information was then used to compute the tree height. A representative number of cores (ten per plot) were also taken to determine the average tree age. An allometric equation using DBH (Lambert *et al*., 2005) was used to calculate the forest biomass (kg).

Aboveground biomass in the understorey was measured in mid-August 2008 to assure that the ecosystem had reached its maximum state of productivity. In each plot, aboveground understorey vegetation was cut from six quadrats of 0.50 m X 0.50 m whose locations were randomly selected. All aboveground understory vegetation tissue was removed from each quadrat and stored in a cooler at 4°C before processing. All vegetation was identified, then divided by species into fruits, twigs, leaves, mosses, bryophytes and litter. Clippings were oven dried at 65°C until mass remained constant and weighed to 0.1 g to determine biomass.

3.2.3 Soil Moisture and Temperature Variability

Volumetric soil moisture and soil temperature were measured from ten points randomly selected within each plot. Soil moisture was an integrated reading of the top 20 cm using Time Domain Reflectrometry (TDR 100, Spectrum Technologies, Inc.). Soil temperature was measured at 10 cm, using a digital thermometer (Fisher Scientific, Digital Thermometer, Fisher Scientific). These same locations were regularly monitored during the consecutive summer campaigns, for a minimum of three times per campaign per location. A total of 350 (35 days X 10 spots) measurements per sampling location were obtained throughout the summer of 2008.

3.2.4 Leaf Area Index

Several direct and indirect methods exist to determine Leaf Area Index (LAI). Non-destructive instruments such as the LAI-2000 (Li-Cor, Lincoln Nebraska) and TRAC (Tracing Radiation and Architecture of Canopies, 3rd Wave Engineering, Ottawa, ON) utilize an inversion of non-interceptance (gap fraction) of radiation transmission to compute LAI. However, the LAI-2000, which measures the diffuse sky radiation at five zenith angles simultaneously, tends to underestimate LAI of coniferous species (Chen *et al*., 1997). The TRAC instrument (Chen *et al*., 1997) determines the canopy gap size distrubution in direct sunlight and can be used to quantify the conifer hierarchical clumping effect.

3.2.4.1 LAI-2000 Measurement Procedure

The LAI-2000 measures the transmitted diffuse blue light (400-490nm) beneath the primary canopy in five concentric rings and zenith angles (0-12°, 15-28°, 31-43°, 45-58°, 61-74°). This instrument provides a rapid estimate of the effective LAI (Le) based on the canopy gap fraction but assumes a random distribution of foliage elements, thus underestimating the LAI when the foliage is clumped, as in a coniferous forest.

Transects of 100-m length were laid out in the four cardinal directions (with the eddy covariance tower as the central point) to allow a description of the spatial hetergeneity and also to compare with the measured bio-physical information. All LAI-2000 measurements were taken under completely overcast sky, on August 11th and 17th. The August 11th sky conditions proved to be the most consistent and these values are reported here.

Data were acquired using a protocol adapted from Strachan and McCaughey (1996) and Gower *et al.* (1999). A first LAI-2000 measurement was recorded in a large (50 m x 50 m) clearing near the tower, corresponding to the "above-canopy" brightness (A reading). The operator then walked each transect and took a series of measurements beneath the canopy (B reading), every 10 m at pre-marked locations. After completing a transect, another "above-canopy" measurement was taken from the same forest clearing (second A reading) facing the same direction. This measurement allowed any changes in sky brightness which could have occurred between the measurements to be accounted for within the LAI-2000 software (Strachan and McCaughey, 1996). A series of measurements were repeated within each plot in a cross-like shape for a total of 1200 meters. This combined protocol follows the FluxNet Canada recommendation for a minimum of 300 meters for LAI measurements in the tower footprint (FluxNet Canada, 2003).

The overstory within the area surrounding the tower was heavily dominated by black spruce (*Picea mariana*) with only a few jack pine (*Pinus banksiana*) and larch (*Larix laricina*). To correct the LAI-2000 measurements for clumping, values for the coniferous needle-to-shoot area ratio (dimensionless) and the element width (mm) were assigned values from the literature of 1.30-1.40 and 30 mm, respectively (Chen *et al*., 1997). Both the high and low values of needle-to-shoot area ratio were used. All file processing was done using the FV2000 software (LAI-2000 File Viewer, 1.09, Li-COR, 2007).

3.2.4.2 TRAC Measurement Procedure

TRAC which was first developed by Chen and Chilar (1997), is an optical instrument for measuring LAI and the fraction of photosynthetically active radiation absorbed by the plant canopy (FPAR). It consists of three quantum (400-700 nm) sensors (LI-COR, Lincoln, Nebraska) and a storage module. It measures both the canopy gap size distribution and gap fraction. Gap size is the physical dimension of a gap in the canopy and gap fraction is the percentage of gaps in the canopy at a given solar zenith angle. It is important to take gap size into consideration because forest canopies are composed of distinct elements such as tree crowns, branches, shoots and needles. These structures determine the spatial distribution of needles.

TRAC is also used to determine a coefficient that represents the hierarchical clumping present in conifer stands (Ω). More precisely, it uses canopy sunflecks to determine a gap size distribution through the measurement of transmitted direct beam PAR at a frequency of 32 Hz. Unlike the LAI-2000, which samples at five zenith angles simultaneously, the TRAC instrument relies on the solar beam. Indeed, it uses the solar beam as a probe and therefore repeated measures over half a day are required to compute the gap fraction. However, Chen and Chilar (2002) showed that when TRAC is used near the solar zenith angle of 57.3° this also adequately represents the average canopy distribution and provides a good estimate of LAI.

One needs to keep in mind that conifer needles are organized into different hierarchies of clumping. Therefore, as mentioned above, a correction factor (Ω) must be applied to the effective LAI of black spruce forest (Chen *et al*., 1997). Using the canopy gap size data from TRAC provides relevant information of the canopy architecture and can be used to quantify the effect of foliage clumping (Chen and Cihlar, 1995; Chen, 1996; Chen *et al*., 1997; Kucharik *et al*., 1997; Leblanc 2002). *Le* is obtained from gap fraction measurements and can be obtained from the LAI-2000. It can then be used as a basis to calculate LAI using (Chen *et al*., 1997):

$$\mathrm{LAI} = \frac{(1-\alpha)Le}{\Omega} \qquad (1)$$

where α is the woody-to-total plant area ratio with typical values ranging from 0.12-0.17 (Chen *et al*., 1996; Gower *et al*., 1999) and and (1−α) removes the contribution of the non-leafy material. Nonetheless, measuring the amount of needle area within the shoots remains challenging with optical instruments. Hence, the Ω value has to be separated into two components (Chen and Cihlar, 1995):

$$\Omega = \frac{\Omega_e}{\gamma_e} \qquad (2)$$

where Ω_e is the clumping index at scales larger than shoots and γ_e is the needle-to-shoot area ratio. Equation (2) becomes (Chen and Chilar, 1997):

$$LAI = \frac{(1-\alpha)Le\ \gamma E_e}{\Omega_e} \quad (3)$$

where L_e is the effective LAI from LAI-2000 and α is the woody-to-total area ratio

TRAC measurements were taken in bright sunlight conditions on August 9th and 12th between 9h00 and 14h00 and on August 13th between 8h30 and 13h00. The TRAC operator walked the same transects previously described at a steady pace of approximately 0.3 ms^{-1} and ensured that the instrument remain leveled with no operator shadow interfering with the PAR sensors. After each transect, the operator moved to the next transect. It took on average one hour to complete all four transects around the tower (North, South, East, West) and the process was repeated for the half-day period. Thus, TRAC measurements were taken on each transect at least four separate times in the course of this half-day. Separate files were created for each run and files from each respective cardinal direction were merged and averaged together. Because measurements were achieved over a complete half day period, the obtained TRAC value provided the clumping index, but also corresponded to an estimate of the LAI value. TRAC data were processed using the TRACWIN software (3rd Wave Engineering, Ottawa, Ontario, Canada).

3.2.5 Flux Measurements

Eddy covariance (EC) was used to measure the net ecosystem exchange from the boreal black spruce forest. EC involves the direct measurement at high frequency of the vertical wind speed (*w*) and a corresponding scalar (*c*) such as CO_2 concentration (Baldocchi, 2003). The resulting turbulent flux is usually described as the covariance:

$$\mathrm{Fc} = \overline{w' \rho_C'} \quad (4)$$

where the prime is an instantaneous departure from the mean and the overbar represents a temporal averaging period (typically 30-minutes). The eddy covariance system consisted of a sonic anemometer (CSAT-3, Campbell Scientific, Logan, Utah), a fine-wire thermocouple and an open-path infrared gas analyser (IRGA; LI-7500, LI-COR, Lincoln, NA). All data were recorded using a fast response data logger (CR5000, Campbell Scientific, Logan, Utah) at 10 Hz, and 30-minute flux averages were computed on the go with the high frequency data retained. Eddy covariance measurements began on August 20^{th} , 2006, but data will be presented using the complete growing seasons of 2007 and 2008 starting on March 28^{th}, 2007 (DOY 87). Micrometeorological sign convention was respected to define vertical fluxes of carbon as positive when there was a net release to the atmosphere and negative when there was a net uptake by the surface.

3.2.6 Climate and ancillary measurements

Supporting meteorological instruments included a tipping bucket rain gauge (TE525M, Texas Electronics, Dallas, TX), a wind speed and direction sensor (05103-10, RM Young, Traverse City, MI), a net radiometer (CNR1, Kipp and Zonen, Delft, Netherlands) and a temperature and relative humidity sensor (HMP45A, Vasala, Finland). During the winter 2007-08, a snow depth sensor (SR50A Sonic Ranging Sensor, Campbell Scientific, Edmonton, Canada) was installed near the forest tower, at 1.7m above ground. Soil heat flux plates (HFT3, Campbell Scientific, Edmonton, Canada) and an averaging soil thermocouple (TCAV, Campbell Scientific, Edmonton, Canada) were installed at a depth of 8 cm to determine the integrated soil heat flux. All variables were sampled at two second intervals and output every 30 minutes to a CR23X datalogger (Campbell Scientific, Edmonton, Canada). The original electrical power system was modified during the summer of 2007 at both sites. Cabans were built to protect dataloggers from the harsh winter conditions, but also to store ten 6 V marine batteries. These were recharged by four 80 W solar panels (Shell) and two wind propellor generators. In ideal conditions, the total battery capacity of this system allowed for up to 21 days autonomy.

3.2.7 Data Handling and Processing

Initial cleaning of the flux data was done using an automated Matlab (v.7.0 Mathworks, Natick, MA) script adapted by McGill's Atmospheric and Environmental Research Lab from that used within the Fluxnet Canada Research Network to ensure the quality and continuity of the dataset. High frequency flux data were screened and rejected based on the presence of spikes (Vickers and Mahrt, 1997). Flux data were then corrected for density effects (Webb *et al.*, 1980). A three-axis rotation was applied such that the 30-minute mean transverse (*v*) and vertical (*w*) wind components were equal to zero (Tanner and Thurtell, 1969). To ensure that all data were within realistic ranges of values and that no instrument malfunction was affecting dependent variables, a visual monitoring procedure was used. Half-hourly flux data were also rejected for instrumental failures, tower maintenance, or during unfavorable weather events such as dew, rain, or heavy ice. Only a few points were missing for the environmental variables such as meteorological and soil data and these were linearly interpolated for gaps smaller than four half-hours. An automated quality control of flux and meteorological data was achieved using a Matlab visual cleaning tool developed in the AER Lab. Spikes and fluxes corresponding to periods with an insufficient number of samples (< 2/3) were discarded (Vickers and Mahrt, 1997). The difference between the block average and the linear detrended fluxes were verified to respect the established acceptable range, of respectively >1 and <0.5. Any data indicating winter uptake of CO_2 were rejected. When the atmosphere is stable such as calm nights, inadequate mixing of air occurs and the turbulent flux is ill defined (Lafleur *et al.*, 2001; McCaughey *et al*., 2006). To determine the periods when such stable conditions lead to unreliable fluxes, we used a threshold of friction velocity (u*). Flux data were divided into daytime and nighttime by defining daytime as incoming shortwave radiation > 10 W m^{-2}. Half-hourly values of u* were plotted against nighttime NEE. (Figure 3.3). A u* threshold of 0.3 ms^{-1} was determined as the value above which NEE is no longer correlated with u* and used to reject nighttime respiration data. This constitutes an accurate indication of a loss of ability to measure the flux in low mixing conditions (McCaughey *et al*., 2006). Less than 6% of the remaining nighttime fluxes were rejected based on the u* filtering protocol. Only flux data within the range of a (±) three fold monthly standard deviation range were kept. Less than 2% of the remaining flux data were rejected during this step. Finally, fluxes recorded when wind direction was from between 43.5° and 123.5° were conservatively rejected due to the upwind presence of the forest clearing created for helicopter access. For the study period (March 28th, 2007 to October 31st, 2008), 84% of the original data were retained.

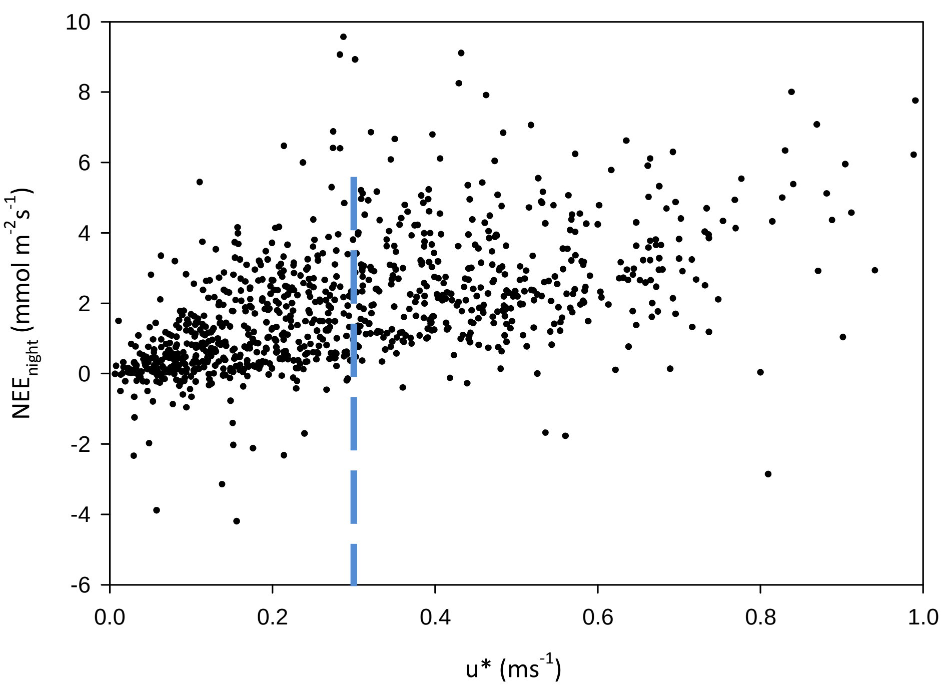

Figure 3.3 Scatter plot of 30-minute friction velocity (u*) and nighttime net ecosystem exchange (NEE) for the summer months of June to August 2008. The dashed line represents the u* threshold.

The storage flux (F_s) of CO_2 within the layer between the the forest floor and the sonic anemometer was accounted for by integrating the concentration difference between successive time intervals over this layer following Mongerstern *et al*. (2004):

$$F_s = h_m \rho_a \frac{\Delta S_c}{\Delta t} \qquad (5)$$

where h_m is the measurement height (23m), ρ_a is the mean dry air density in the layer, and ΔSc is the mean CO_2 mole mixing ratio, which was calculated as the difference between the following and the preceding half-hours. The storage was calculated prior to the gap filling, thus only when the tower instruments were working perfectly. Fs was then combined with the CO_2 turbulent flux measured from the EC tower (F_C) to calculate the half-hourly net ecosystem exchange (NEE) as:

$$NEE = Fc + Fs \qquad (6)$$

3.2.8 Gap Filling Strategy

In order to determine the annual and seasonal sums of NEE, gap filling is essential (Lafleur *et al*., 2003). NEE data were divided into growing and non-growing season and daytime and nighttime values. Each gap less than four half hours was filled by linear interpolation. We then used filling techniques for longer gaps based on the standard Fluxnet-Canada algorithm.

Longer NEE gaps outside of the growing season were filled using an NEE-soil temperature relationship. We plotted nighttime NEE against air and soil temperature at different depths. The best relationship, based on the resulting r^2 values, was determined to be NEE and soil temperature at 5 cm.

For daytime gaps longer than four 30-minute periods, during the growing season, we used a rectangular hyperbolic relationship between NEE and PAR (Frolking *et al.,* 1998):

$$\mathrm{NEE} = (\alpha * \mathrm{PPFD} * \mathrm{Pmax})/(((\mathrm{Pmax} + (\alpha * \mathrm{PPFD})\,)) - \mathrm{ER} \qquad (7)$$

where α is the initial slope of the curve, P_{max} is the maximum gross productivity, PPFD is the photosynthecially active radiation and ER is the dark respiration value. To then gap fill the growing season, we modeled the gross ecosystem production (GEP), which was initially calculated as GEP = ER – NEE, using Lafleur *et al.* (2001):

$$GEP = \frac{\alpha * PPFD * GPmax}{(Pmax + (\alpha * PPFD))} \quad (8)$$

GEP was set to 0 and NEE = ERGEP outside of the growing season. To determine GEP_{max} for the growing season, the best relationship between $GEP_{measured}$ and PAR, on a biweekly basis was determined. By plotting $GEP_{measured}$ and $GEP_{modeled}$ a weekly multiplier was determined and applied to GEP_{max}. Distinct relationships were applied for each study year.

3.3 RESULTS AND DISCUSSION

When compared to other well studied black spruce sites, such as those in Western Canada, the Eastmain forest is younger (Table 3.1), but holds more biomass than some older forests surveyed in the literature such as the Saskatchewan site. This could be explained by Eastmain's more Southern geographic location, thus potentially higher monthly average incoming solar radiation and air temperature. On this point, we also found that the onset of photosynthesis, as suggested by Suni *et al*. (2003) and Jarvis and Linder (2000) depends upon air temperature, soil temperature and soil water content.

Table 3.1 Comparison between the Eastmain forest and other representative Canadian black spruce forests.

Location	Manitoba	Saskatchewan	Quebec	Quebec EM-1
Lat. / Long	55.880°N / 98.481°W	53.987°N/ 105.118°W	49.692°N/ 74.342°W	52.104°N/ 76.196°W
Age	160	130	95	84
Height (m)	9.1	7.2	13.8	9.0
DBH (cm)	8.5	7.1	12.7	10.0
LAI	4.8	3.8	3.7	1.7

3.3.1 Meteorological and Seasonal patterns

At this latitude, the climate is characterized as being cold, wet and sub-arctic continental. Seasons range from mild, short summers to long, harsh winters. Mean annual air temperature was -0.7°C. Average temperature generally stayed close to –18.5°C in winter from December 21st 2007 to March 28th 2008 and occasionally dropped below –30°C, especially in February. Based on the average daily air tempererature, the first winter freeze in 2007 occurred around DOY 307.

Studies have demonstrated that the onset of photosynthesis can be determined by various relevant field observations such as air temperature (Suni *et al*. 2003), soil temperature and soil water content (Jarvis & Linder, 2000) or gross ecosystem production (GEP) (Bergeron *et al.*, 2007). We used soil and air temperature thresholds of 0°C and 5°C, respectively to determine the beginning and end of the growing season. Using this technique, we determined that the growing season extended from April 12th (DOY 102) to October 31st (DOY 304) in 2007 and from April 13th (DOY 104) to October 31st (DOY 305) in 2008 for a total of 202 and 201 days.

The average growing season Bowen ratio in 2007 and 2008 was 1.5 and 1.0, respectively, indicating that 2008 was wetter than 2007. 2008 received more precipitation than 2007, with respectively 496.7 mm and 400.5 mm of rainfall during the summers months. The first snow to stay on the ground occurred on DOY 297 in 2007 and on DOY 302 in 2008 (Environment Canada, 2009). The forest floor was entirely snow free on DOY 136 (2007).

Wind roses were created (WindRose Pro 2.3.11; Enviroware srl.) for each season and year of the study. 30-minute average wind speed values from the wind monitor were divided into five bins; <2, 2-3, 3-4, 5-7 and >7 ms^{-1}. South-westerly winds dominated during the spring, fall and winter of 2007. During the summer of 2007, winds were mainly from the West. In 2008, the range in wind direction during the Spring was wider than in 2007 and varied between South-West and South-East. Direction was between West and South-West in the summer of 2008 with windspeed averaging between 5 and

7 ms^{-1}. In the fall and winter of 2008, windspeed was at the strongest, i.e. higher than 7 ms^{-1} and dominantly from the West. In summary, prevailing winds were west and southwest, being predominantly south-southwesterly in the summer and westerly in the winter (Figure 3.4).

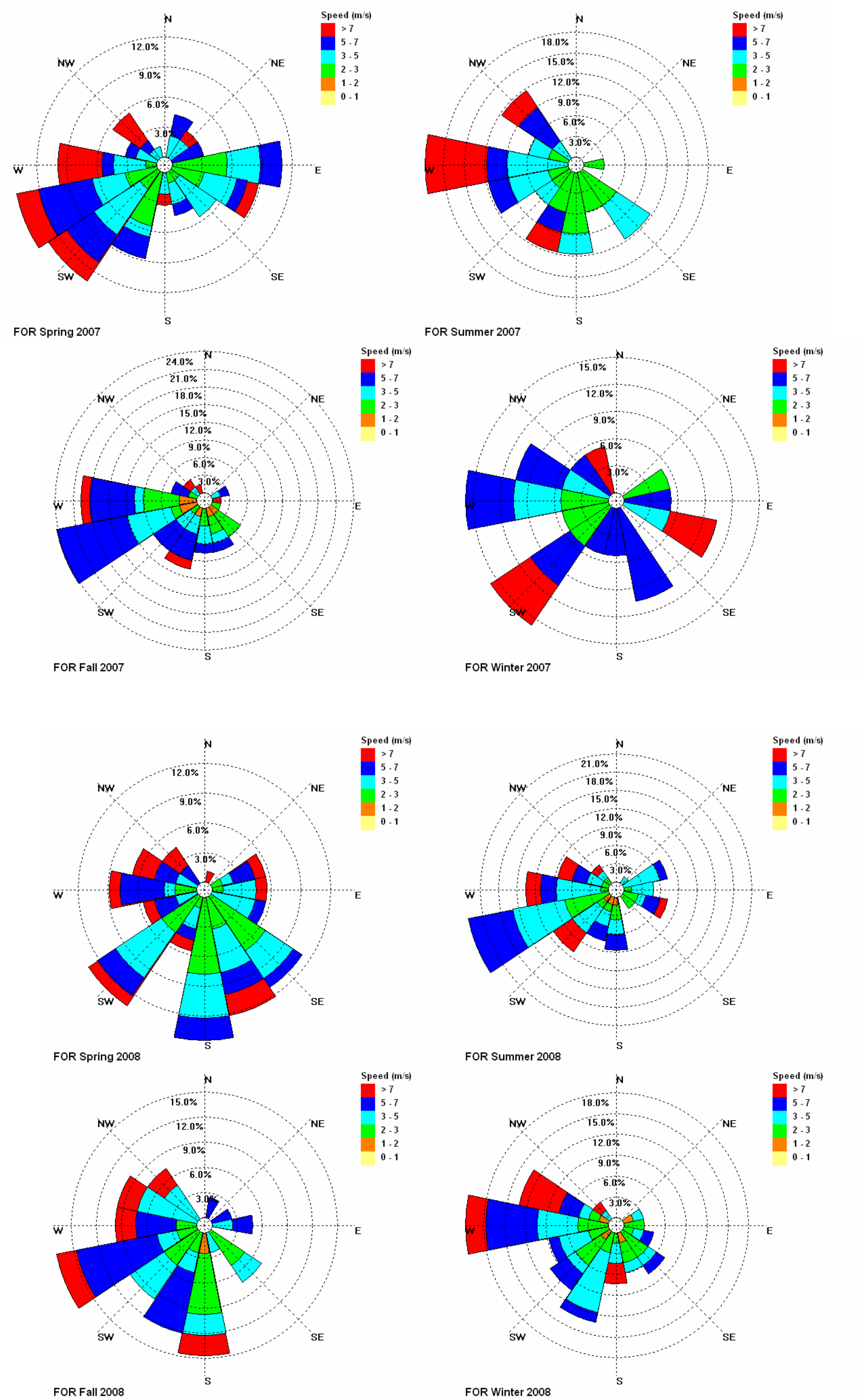

Figure 3.4 Top Figure: 2007 Seasonal wind rose at the forested site. Wind speed was divided into 5 bins; 1-2, 2-3, 3-4, 5-7 and >7 ms-1. Bottom figure: 2008.

3.3.2 Forest Characterization

The average tree height and age were found to be respectively 8.9 ± 2.8 meters and 84 ± 3 years (Figure 3.5 and Table 3.2). The number of trees per plot ranged from 164 to 752. DBH was 12.4 ± 5.7 cm and the crown width was 195.4 ± 132.3 cm in the North-South direction and 182.0 ± 107.9 cm in the East-West direction. Black spruce trees at Eastmain are on average shorter and smaller in diameter at breast height (DBH) than the Boreal forests reported by Lambert *et al*. (2005) for British Columbia, the Maritimes and Southern Quebec, and this difference is likely latitude-temperature driven.

Figure 3.5 Eddy covariance tower at the pre-flooded site. View from the East. Picture taken by Marie-Eve Lemieux, 2007.

Table 3.2 Summary of the forest characterization in each 30 x 30 m sampling plot. BS: black spruce; JP: jack pine.

	Forest type	n	Age AVG (yrs)	STD	Tree height (cm)			All DBH (cm)		DBH (>5cm)		Crown width (cm)				Avg Tree biomass (kg)	
					Mean	Range	STD	Mean	Range	Mean	Range	North-South		East-West		**All trees**	**DBH >5**
North	BS + Larch	288	79.5	24.5	874	306-2856	380	7.4	1.1-24.9	12.1	5-24.9	173	56-350	174	72-330	**27.8**	**55.3**
South	BS	164	85.9	10	655	0.9-2822	462	9.2	1-25.7	12.4	5.2-25.7	154	38-346	154	40-330	**36.1**	**53.9**
East	BS +JP	752	87.1	5.9	572	334-937	238	4.6	1.1-12.4	6.9	5-12.4	92	28-281	86	34-186	**5.8**	**11.8**
West	BS	598	83.8	7.3	636	281 -1293	380	5.9	1-21.2	8.7	5.0-21.2	132	49-305	130	44-310	**12.0**	**22.1**
TOTAL/Mean		**1820**	**84**	**12**	**891**	**248-1775**	**-**	**10**	**3 – 33**	**12**	**8 – 33**	**195**	**73 – 380**	**182**	**75 – 365**		

The forest floor was dominated by *Lichen spp*., *Pleurozium schreberi* and shrubs (*Rhododendron groenlandicum, Vaccinium myrtilloides, Kalmia polifolia and Kalmia angustifolia*), with an average height of 25 cm. *Pleurozium schreberi* distribution accounted for 10 to 80% of the total above ground biomass within each 1 m X 1 m plot assessed, which generally agrees with the figure of 65% from DeLuca *et al.* (2002) for the same environment. All relevant information concerning above ground biomass is summarized in Table 3.3. The more quantitative destructive sampling results also confirmed visual observations (Table 3.4).

Table 3.3 Percent cover of the different vegetation species in each sampling plot. TR: trace amount of the species.

	Species	**%**
North	Sphagnum *spp*.	90-100
	Rhododendron groenlandicum	25-75
	Chiogenes hispudula	TR-25
	Carex *spp*.	TR-25
	Pleurozium schreberi	10-80
South	Lichen *spp*.	25-80
	Vaccinium myrtilloides	10-50
	Rhododendron groenlandicum	TR-25
	Kalmia polifolia	TR-25
	Pleurozium schreberi	10-80
East	Sphagnum *spp*.	50-75
	Lichen *spp*.	TR-45
	Chameadaphnea calyculata	10-25
	Rhododendron groenlandicum	5-15
	Pleurozium schreberi	10-80
West	Vaccinium myrtilloides	50-75
	Rhododendron groenlandicum	35-55
	Vaccinium angustifolia	40
	Pleurozium schreberi	10-80

Table 3.4 Summary of above ground biomass from direct sampling.

	Bryophytes *(Pleurozium shreberi)*		Others		Foliage		Twigs		Litter	
	%	g / 1m^2	%	g / 1m^2	%	g / 1m^2	%	g / 1m^2	%	g / 1m^2
North	46.7	410.4	5.2	45.8	3.8	33.2	20.4	179.6	22.5	198.1
South	26.8	277.5	28.3	292.7	4.7	48.3	12.6	130.7	27.7	286.7
East	54.8	727.7	13.2	175.7	3.3	43.7	14.2	188.5	14.4	191.3
West	34.5	307.3	51.3	456.3	3.5	30.9	10.3	91.7	24.6	218.9

3.3.2.1 Soil Moisture and Temperature Variability

The average monthly volumetric soil moisture measured for July 2008 was 32.2% (± 4.6%) and for August 2008 was 35.2 (± 5.4%) and was generally lower in the South and East directions (Table 3.5). Average soil temperature increased by 0.6 – 0.9 °C from July to August in the West and North plot, but decreased during the same period in the South and East plot. Simultaneously, the soil moisture in the North, South and East plot increased with time, but decreased in the West plot.

Table 3.5 Average soil moisture and temperature in the four plots for the months of July and August 2008.

		Monthly Average	
Plots	**Month**	**Soil Temp. (°C)**	**Soil Moisture (%)**
North	Jul	10.0	33.1
	Aug	10.9	44.3
South	Jul	11.7	24.9
	Aug	11.5	25.7
East	July	12.3	24.9
	Aug	11.5	33.9
West	Jul	10.3	45.9
	Aug	10.9	36.8

These soil moisture data correspond well with the visual vegetation survey: dry sphagnum was found in the South plot and Jack pine, which grows in drier, more well drained areas, was only found in the drier East and South plots. Nonetheless, through visual observations and measurements, it was noticed that the soil surrounding the tower had abundant water through the study period summers.

3.3.2.2 Leaf Area Index

LAI-2000 provides a rapid estimate of the effective LAI (Le) based on the canopy gap fraction but assumes a random distribution of foliage elements, thus underestimating the LAI when the foliage is clumped, as in a coniferous forest. Different LAI values were obtained either from the raw LAI-2000 measurement or the corrected omega factor (Ω) and from the TRAC optical instrument (Table 3.6).

Table 3.6 Summary of LAI for each 100m transect around the tower. Le is from LAI-2000;and the needle-to-shoot average (γ) and woody-total area ratio (α)are used to compute the clumping factor Ω is from TRAC.

	Plot ID	Tree Density (m^{-2})	Effective LAI (*Le*)	Trac omega (Ω) Needle-to-shoot average (γ_s)	Trac omega (Ω) Woody-to-total area ratio (α)	Average LAI
	North	0.32	1.54	0.71	1.68	1.68
	South	0.18	1.33	0.70	1.10	1.10
	East	0.84	1.44	0.74	1.64	1.64
	West	0.80	0.95	0.73	0.93	0.93
Mean			**1.32**			**1.34**

While conducting LAI measurements, the low density of each plot was noticed. While looking at the tree density and the LAI value for each respective plot, it is to be noticed that the plot is merely a subset of the LAI transect exceeded. The East plot has the highest tree density and the second highest LAI-2000 and TRAC values. This agrees with the *in situ* observations. The LAI transects can contain natural variability in the density of the forest. For example, at least half of the West transect is very low density whereas the corresponding sampling plot was located in a medium density area. Finally, figures 3.6a to 3.6d below show the overstory LAI values for all four transects, in all three views orientation. Each plot was on average started between 30 and 60 meters away from the tower and was 30 meters long. This specific representation allows to identify gaps in the canopy, which corresponds to the visual observations noted on site. For instance, note on Figure 3.6a that the North transect expresses a low tree density in the middle and terminates with a dense tree canopy.

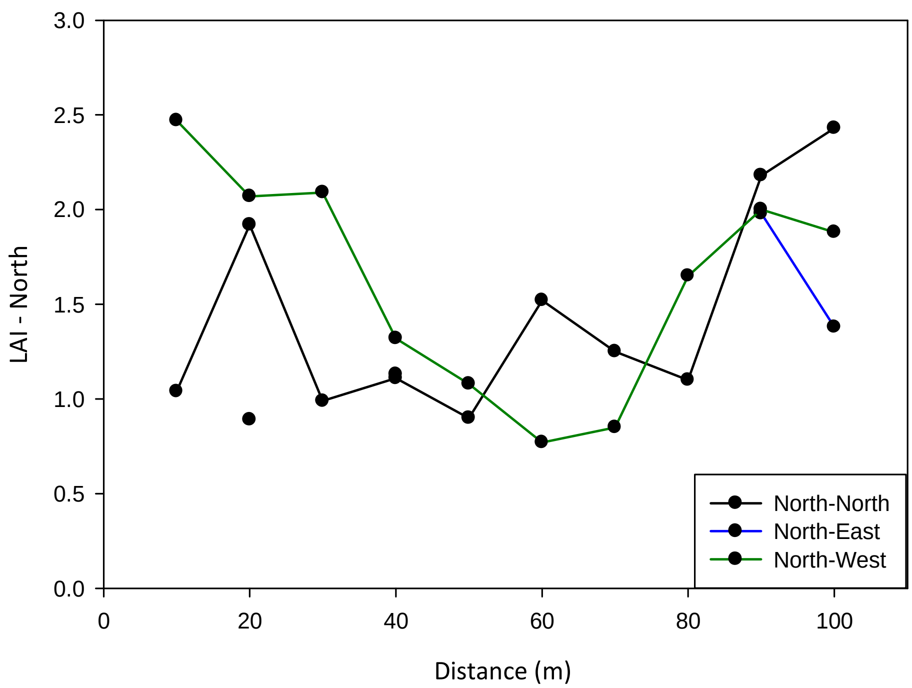

Figure 3.6a Canopy leaf area index by LAI-2000 values recorded at every 10 meters intervals along a 100 meters North transect for each three view orientation.

The mean corrected LAI value obtained from the TRAC measurements was 1.68 and figure 3.6a expresses a decrease of LAI (i.e. tree density) in the middle of the 100 m transect from the eddy tower. Larch (*Larix laricina*) tends to occur in the North-West plot where soil moisture was considerably higher. Trees in that plot also expressed a larger DBH. At this location, the forest soil was characterised by high aboveground biomass and abundance of thick mosses (90-100%). *In situ* observations revealed that the northern plot was certainly the most wet since, in many places, the water table was at ground level. The increase in soil moisture in August was the result of a two-weeks period of strong precipitation.

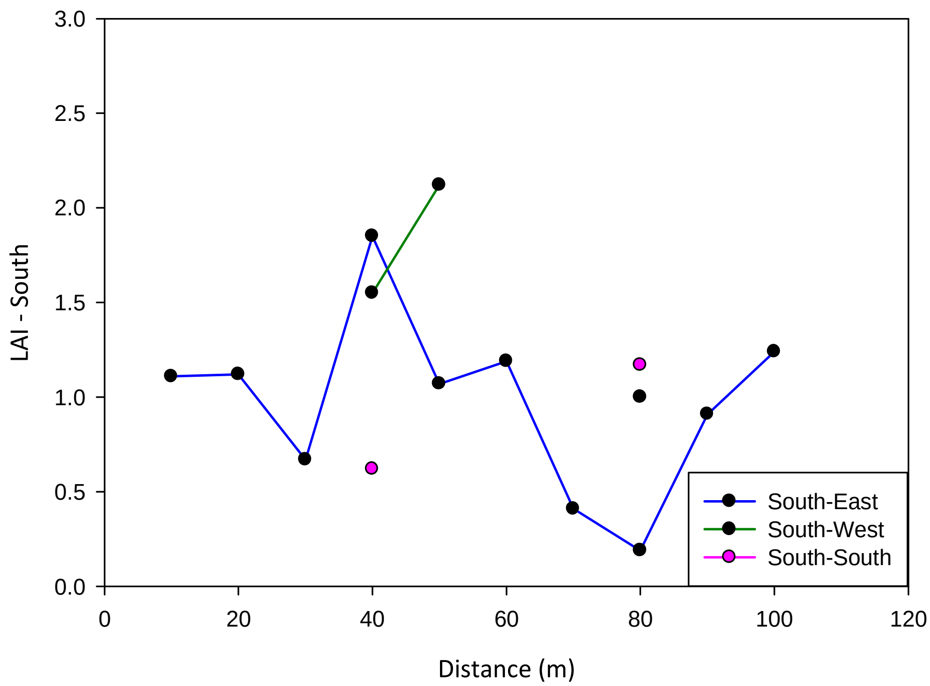

Figure 3.6b Canopy leaf area index by LAI-2000 values recorded at every 10 meters intervals along a 100 meters South transect for each three view orientation.

The South plot expresses the second lowest tree density with an effective LAI of 1.33 and a corrected TRAC value of 1.10. Throughout the summer of 2008 this Southern plot was also the driest. This can be explained by the low tree density, which allowed more sunlight to penetrate and warm the forest floor, but also corresponding to the highest position of the sun in the sky, so more incoming solar radiation. This is confirmed by the lowest soil moisture values obtained in July and August, hovering around 25%. After conducting the above ground sampling, it was found that lichen *spp.* was the dominant species (25-80%), immediately followed by *Vaccinium myrtilloides* (10-50%).

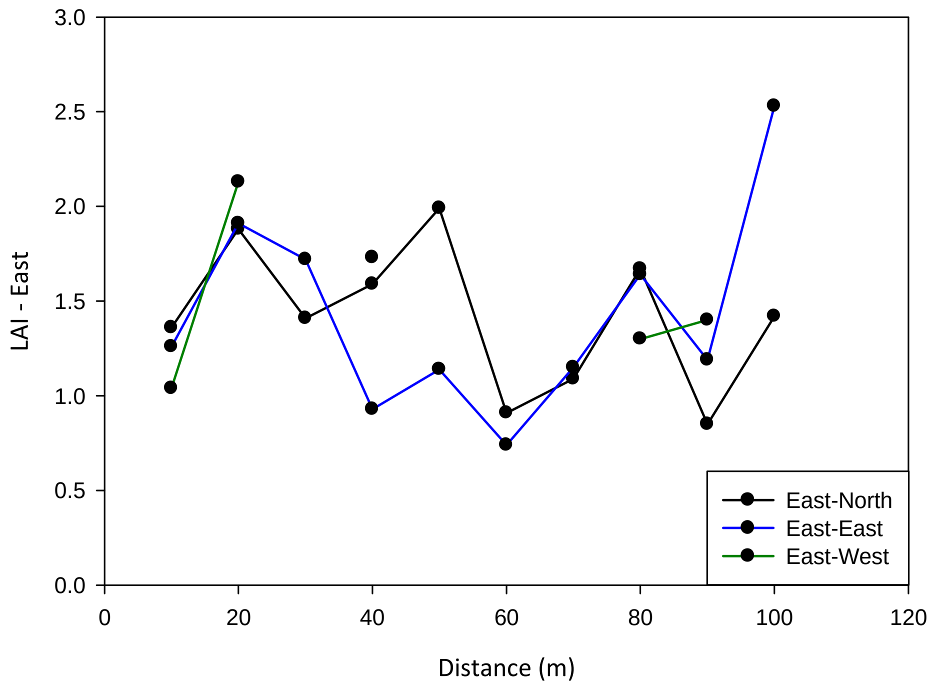

Figure 3.6c Canopy leaf area index by LAI-2000 values recorded at every 10 meters intervals along a 100 meters East transect for each three view orientation.

Figure 3.6c expresses a fairly constant trees density throughout the 100 meters east transect, in all three cardinal directions. This plot had the hightest tree density (752 trees), but the average tree height and DBH was also the lowest. This is probably due to the high clumping, which is also expressed by the high mean effective LAI of 1.44 and a corrected TRAC value of 1.64. The forest soil moisture was especially low in July 2008 on this transect. Although *Sphagnum spp*. was dominant (50-75%), many shrubs (*Chamedaphnee calyculata, Rhododendron groenlandicum*) were identified at this location. Finally, Jack pine (*Pinus banksiana*) which tends to occur in a well drained soil, were found especially in this Eastern plot with an average soil moisture of 28.5%.

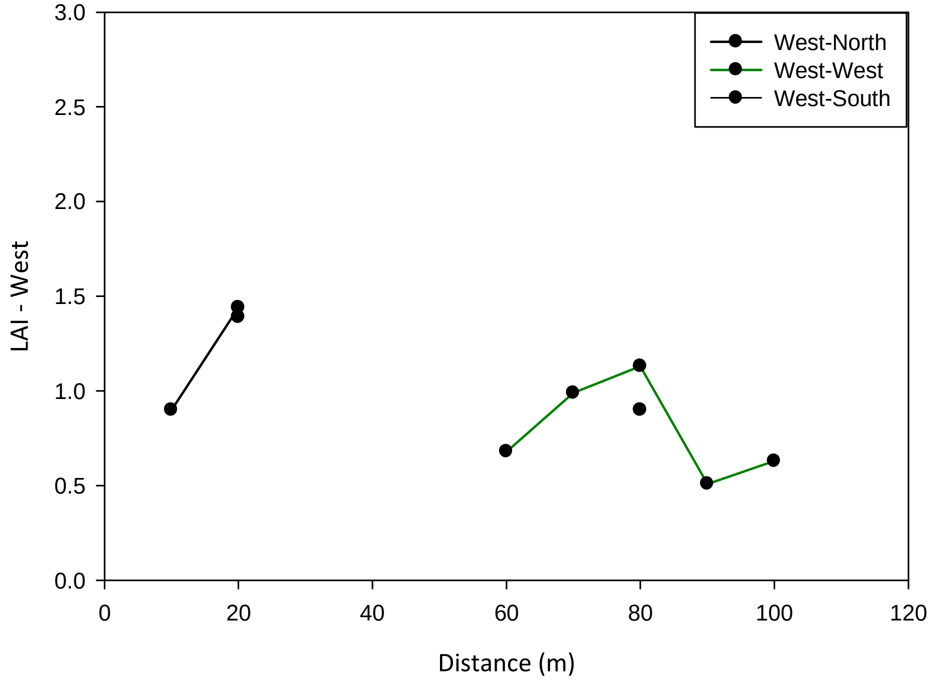

Figure 3.6d Canopy leaf area index by LAI-2000 values recorded at every 10 meters intervals along a 100 meters West transect for each three view orientation.

At the west transect, the effective LAI was noted to be 0.95 and the corrected TRAC value to be 0.93. Regardless of missing data (gaps in canopy), while looking at figure 3.6d and especially from field observations, it is confirmed that the west side of the tower was not the densest part of this forest. The western plot was actually similar to the northern plot, although slightly less moist and not as sphagnum dominated. It was actually dominated by V*accinium myrtilloides* and *angustifolia* (50-75% and 40%) and *Rhododendron groenlandicum* (35-55%).

3.3.3 FOREST NET ECOSYSTEM EXCHANGE

3.3.3.1 Diurnal and Monthly Patterns

For the study period, the storage flux (F_S) represented about 10% of the net ecosystem exchange (Table 3.7). Storage was positive before sunrise and after sunset with large additions to storage in the summer evenings and subsequent release in the morning (Figure 3.7).

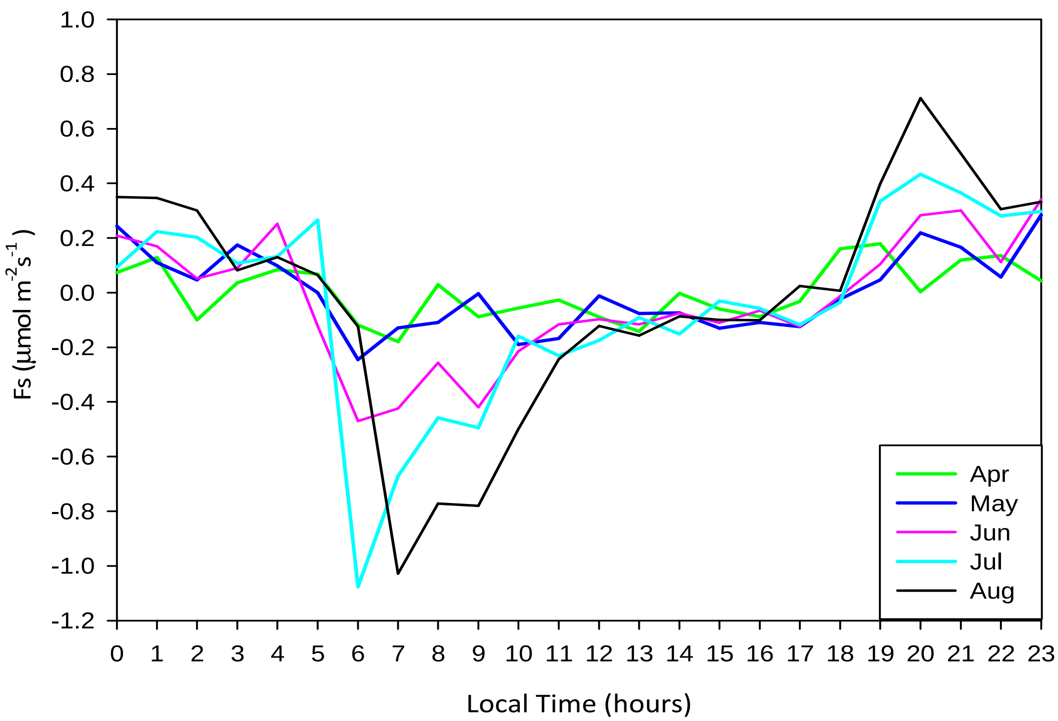

Figure 3.7 Hourly storage flux (□mol $m^{-2}s^{-1}$) for April- August, 2008.

Table 3.7 Monthly F_c, F_s, and F_{NEE} (□mol $m^{-2}s^{-1}$) averages (non gapfilled) at the EM1 forest for 2007 and 2008. Fluxes were computed for daytime and nighttime.

Months	AVG Fc	AVG Fs	AVG NEE	AVG Fc	AVG Fs	AVG NEE	AVG NEE
	(Daytime 2007) (μmol $m^{-2}s^{-1}$)			(Nighttime 2007) (μmol $m^{-2}s^{-1}$)			(24 hours 2007) (μmol m-2s-1)
Jan	N/A	N/A	N/A	N/A	N/A	N/A	N/A
Feb	N/A	N/A	N/A	N/A	N/A	N/A	N/A
Mar	-0.16	0.01	-0.15	0.12	0.01	0.13	-0.02
Apr	-0.35	-0.03	-0.38	0.22	0.04	0.26	-0.12
May	-0.83	-0.02	-0.85	0.46	0.06	0.52	-0.33
Jun	-1.97	-0.11	-2.09	1.18	0.18	1.36	-0.73
Jul	-1.84	-0.14	-1.98	1.13	0.20	1.33	-0.65
Aug	-2.24	-0.18	-2.42	1.58	0.20	1.78	-0.64
Sep	-1.40	-0.15	-1.55	1.67	0.07	1.74	0.19
Oct	-1.51	-0.06	-1.56	1.06	0.05	1.11	-0.45
Nov	-0.15	-0.07	-0.23	0.54	0.08	0.63	0.40
Dec	-0.13	-0.16	-0.29	0.45	0.06	0.51	0.22
Months	AVG Fc	AVG Fs	AVG NEE	AVG Fc	AVG Fs	AVG NEE	AVG NEE
	(Daytime 2008) (μmol $m^{-2}s^{-1}$)			(Nighttime 2008) (μmol $m^{-2}s^{-1}$)			(24 hours 2008) (μmol m-2s-1)
Jan	1.00	-0.38	0.62	1.71	0.047	1.76	2.38
Feb	0.28	0.01	0.29	1.15	-0.04	1.11	1.40
Mar	0.71	-0.21	0.49	0.85	0.03	0.88	1.370
Apr	-0.79	-0.05	-0.84	0.66	0.07	0.70	-0.14
May	-1.15	-0.09	-1.24	0.65	0.14	0.79	-0.44
Jun	-1.53	-0.13	-1.66	1.26	0.14	1.41	-0.25
Jul	-2.46	-0.14	-2.60	2.86	0.20	3.06	0.46
Aug	-2.95	-0.22	-3.17	2.77	0.33	3.10	-0.07
Sep	-2.61	-0.18	-2.79	1.89	0.12	2.01	-0.78
Oct	-2.29	-0.18	-2.47	0.93	0.02	0.95	-1.52
Nov	N/A	N/A	N/A	N/A	N/A	N/A	N/A
Dec	N/A	N/A	N/A	N/A	N/A	N/A	N/A

During, July and August, stronger convective heating after sunrise, lead to the large releases. The magnitude of the storage flux in August was similar to July, but the morning release occured an hour later following the trend of decreasing daylength and later sunrise. Storage was approximately zero during the daytime period in this open forest canopy.

For both years of the study, NEE showed a clear diurnal trend with daytime CO_2 uptake and nighttime CO_2 release (Figure 3.8). The daily CO_2 uptake was accentuated during the growing season, especially in June, July and August as the solar radiation and temperature increased. Diurnal patterns of CO_2 flux also revealed a clear increase in the ecosystem respiration from June to July 2008 with a monthly average daily NEE of -0.25 $\mu mol\ m^{-2}s^{-1}$ to 0.46 $\mu mol\ m^{-2}s^{-1}$, respectively. For 2007 the diurnal patterns of CO_2 flux revealed an increase in the uptake from May to June, with a monthly average of -0.33 $\mu mol\ m^{-2}s^{-1}$ and -0.73 $\mu mol\ m^{-2}s^{-1}$, respectively. However, less carbon uptake and a greater ecosystem respiration was observed from June to September 2008 in comparison with the same months for the previous year. 2008 was generally sunnier (greater incoming solar radiation) and warmer (higher average air temperaure) for those three months (Figure 3.9). Both of these would have lead to greater photosynthetic uptake in 2008, but also a greater soil respiration.

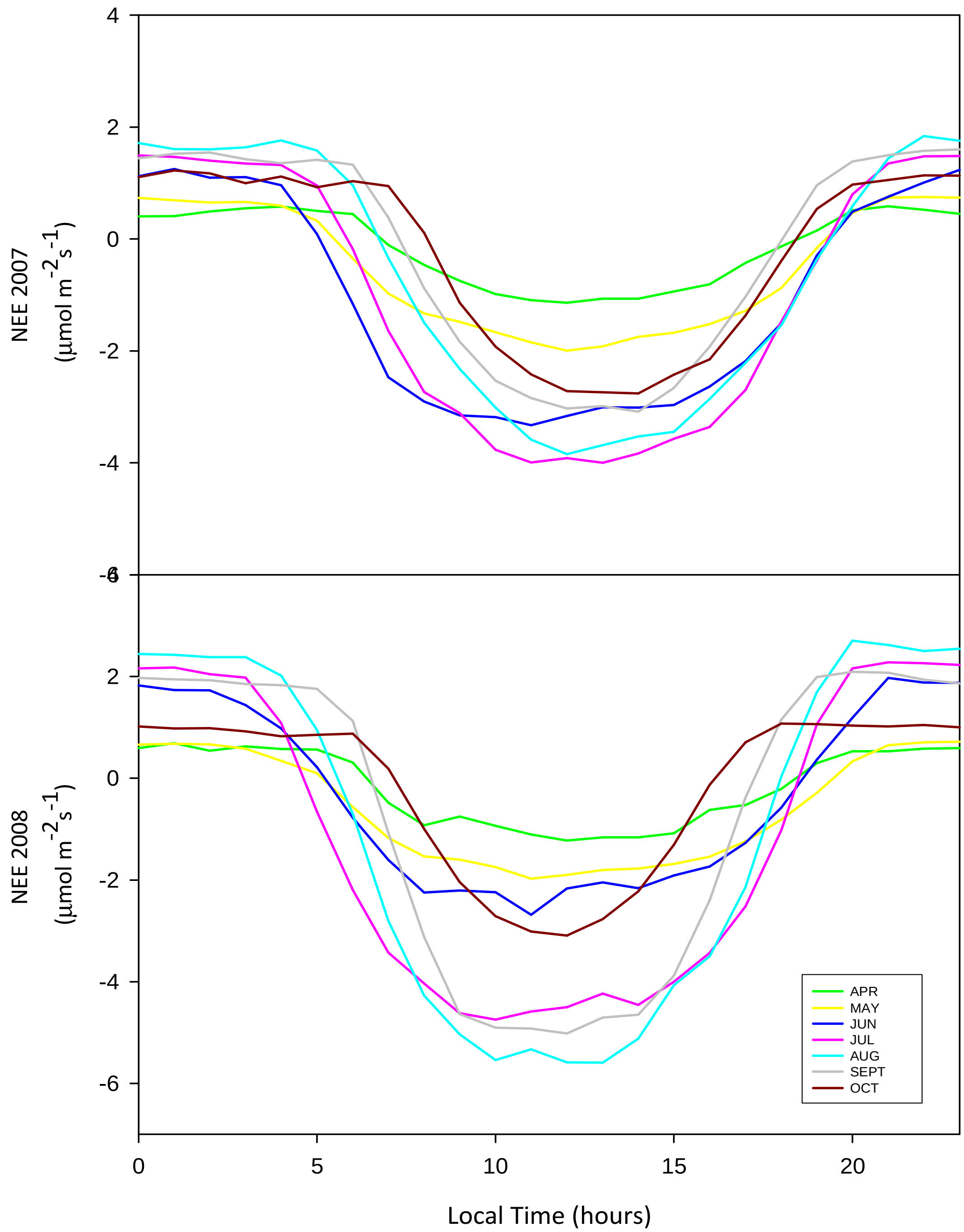

Figure 3.8 Diurnal ensemble 30-minute averages of gap filled NEE, including storage (□mol $m^{-2}s^{-1}$) at the EM1 forest for 2007 and 2008.

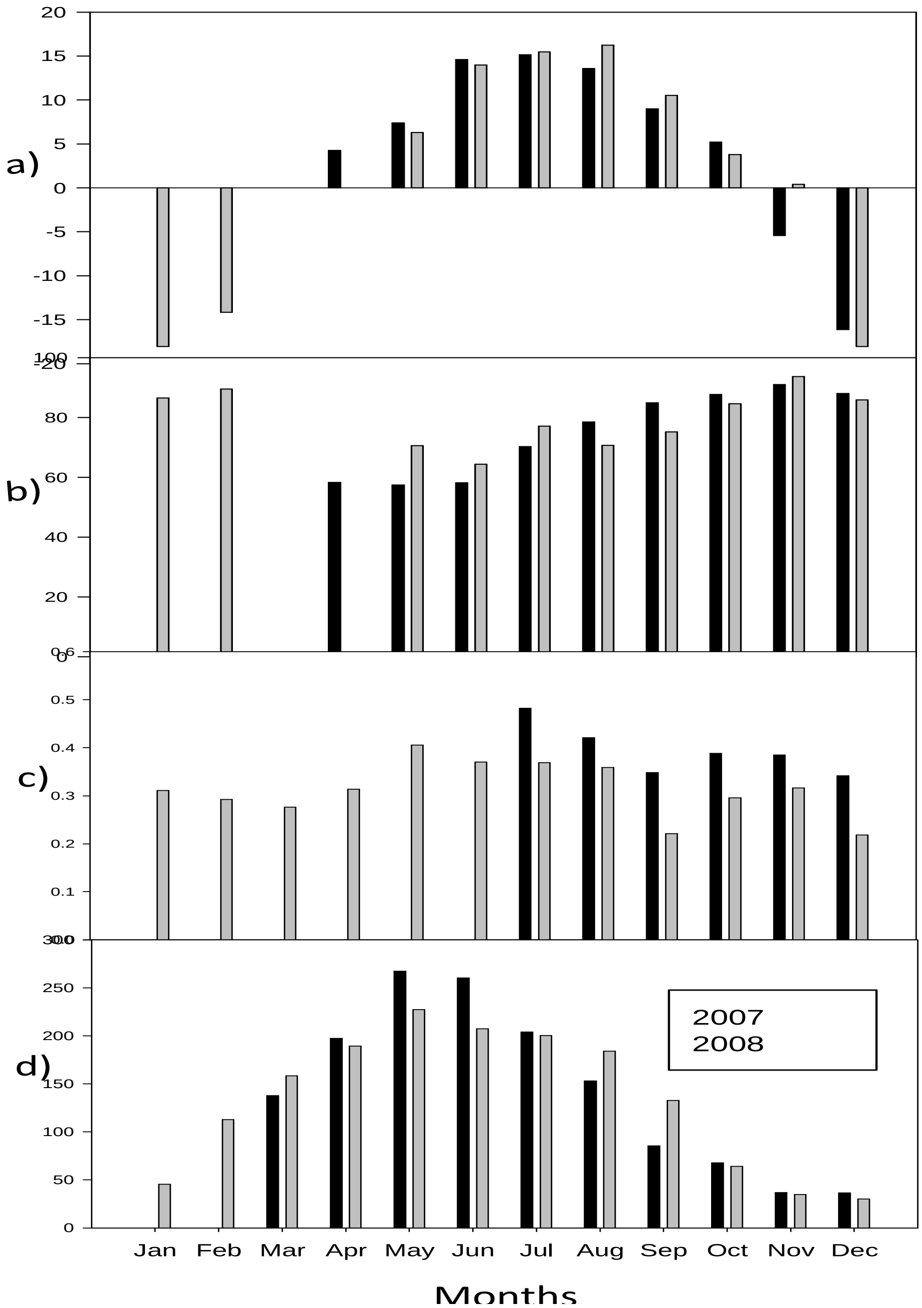

Figure 3.9 Monthly averages of (a) air temperature (°C), (b) relative humidity (%), (c) soil water content (m^3m^{-3}) and (d) incoming shortwave radiation (W m-2) at the Eastmain-1 forest from March 2007 to December 2008. The black bars represent 2007 and the gray bars represent 2008.

3.3.3.2 Annual Patterns

The growing season was defined as the period where both daily average air and soil temperatures were above 0°C and 5°C on consecutives days (Frolking *et al.,* 2006). The forest switched to a net carbon sink on DOY 102 in 2007 and on DOY 104 in 2008. Although the growing season length was about 202 days in each year, the net carbon uptake was slightly larger in 2008. The average carbon uptake from the Eastmain-1 forest was -0.6 μmol $m^{-2}s^{-1}$ for both growing seasons 2007 and 2008. Cold season loss was consistently about 50% of the growing season uptake. Although there is not much difference between the fluxes of both years, Spring 2007 had a greater amount of precipitation, thus more cloudiness and less light for photosynthesis. Air temperature was higher in the latter part of the 2008 growing season. During two periods of 2007 (DOY 159-170 and DOY 202-224), NEE switched to a weaker carbon sink (Figure 3.10 and 3.11). In these periods, air temperature went from an average of 10°C in the preceeding seven days to 21°C and from 12°C to 16°C. This increase in temperature would have increased the forest soil respiration. Since the ecosystem is only a small sink, it is likely that during these rapid warming periods, the net NEE resulted in a loss of carbon to the atmosphere. In 2008, where the early part only of the growing season was wetter and colder than 2007, the result was a lower NEE uptake and small release. However, the end of the growing season in 2008 was drier and warmer compared to 2007 and this more than compensated for the slower start with a resulting greater carbon uptake. June and July had the largest uptake in 2007 of -1.1 μmol $m^{-2}s^{-1}$ and for 2008, August had the largest ecosystem respiration with 2.4 μmol $m^{-2}s^{-1}$.

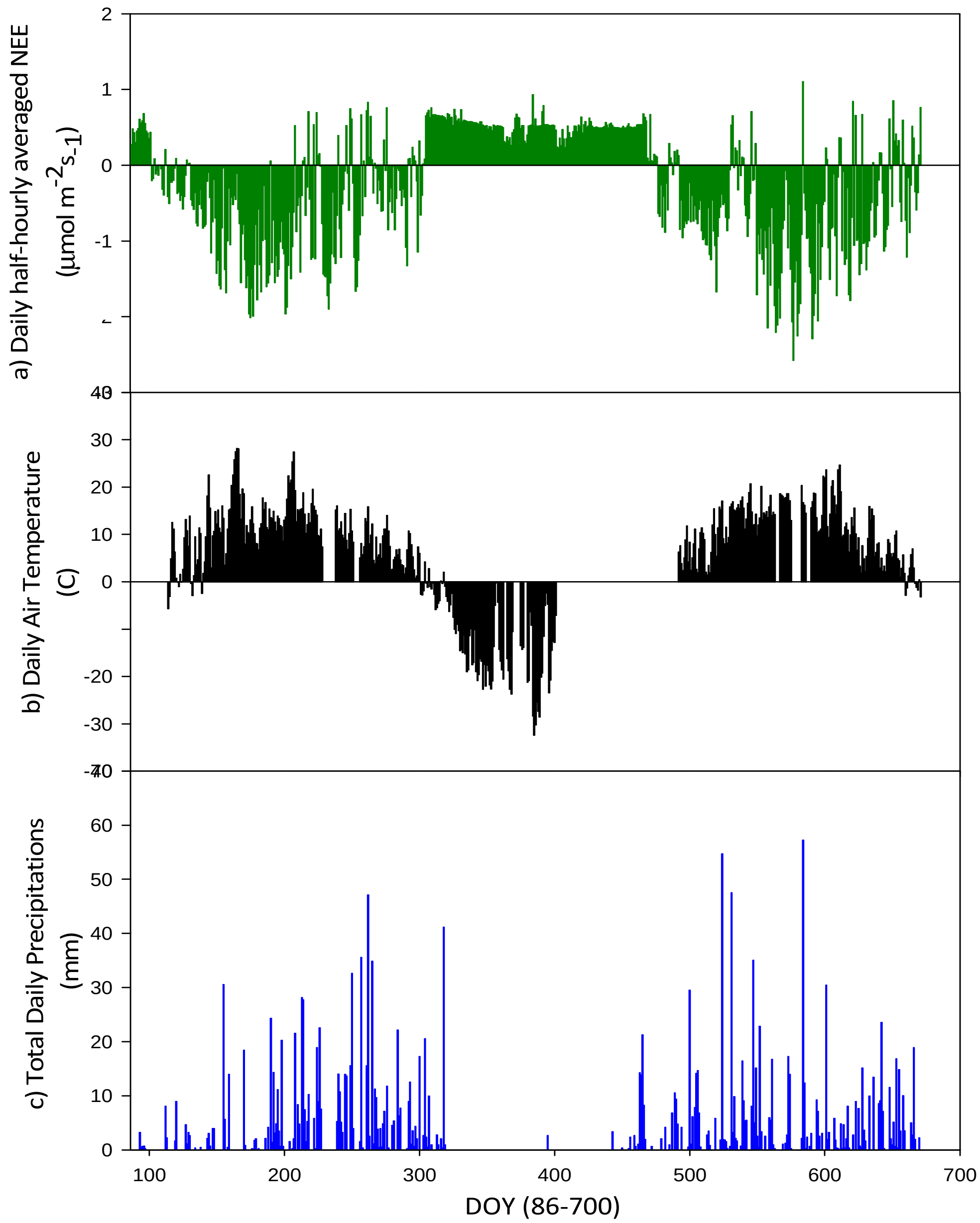

Figure 3.10 (a) Daily averages of NEE for 2007-2008 (□mol $m^{-2}s^{-1}$), (b) daily average air temperature (°C) and (c) daily sum of precipitations (mm). For both years, the growing season extended from April to October (DOY 102-304 and 104-305).

Ecosystem respiration (ER) increased in magnitude between May and October with increasing air and soil temperatures. ER was greater in the 2008 growing season than in 2007. GEP was highest in July for 2007 with 2.5 μmol $m^{-2}s^{-1}$ and in August for 2008 with 3.5 μmol $m^{-2}s^{-1}$ (Table 3.9). From July to September, both ER and GEP were greater in 2008 than in 2007 for the reasons expressed earlier. NEE was positive for both years through the winter months due to respiratory losses with an average of 0.5 μmol $m^{-2}s^{-1}$ in both 2007 and 2008 (Table 3.8). NEE for the month of June 2007 (-0.25 μmol $m^{-2}s^{-1}$) was less than a third of the 2008 value (-0.73 μmol $m^{-2}s^{-1}$), but we also noted an increase in ER starting in June 2008; 1.8 μmol $m^{-2}s^{-1}$ compared to 1.3 μmol $m^{-2}s^{-1}$ in 2007.

Table 3.8 Summary of seasonal and annual average ecosystem respiration (ER), gross ecosystem production (GEP) and net ecosystem exchange (NEE) by year. Growing season is defined for 2007 as DOY 102-304 and in 2008 as DOY 104-305. A negative sign means a net uptake.

	2007 (DOY 87-365)			**2008 (DOY 1-306)**		
	μmol m-2s-1					
Period	**ER**	**GEP**	**NEE**	**ER**	**GEP**	**NEE**
Spring	0.9	1.2	-0.3	0.8	1.0	-0.2
Summer	1.5	2.3	-0.8	2.2	3.1	-0.9
Fall	0.8	0.6	0.2	1.1	1.4	-0.3
Winter	0.5	0.0	0.5	0.5	0.0	0.5
Growing Season	1.2	1.8	-0.6	1.5	2.2	-0.6
All Data	1.0	1.3	-0.3	1.2	1.4	-0.2

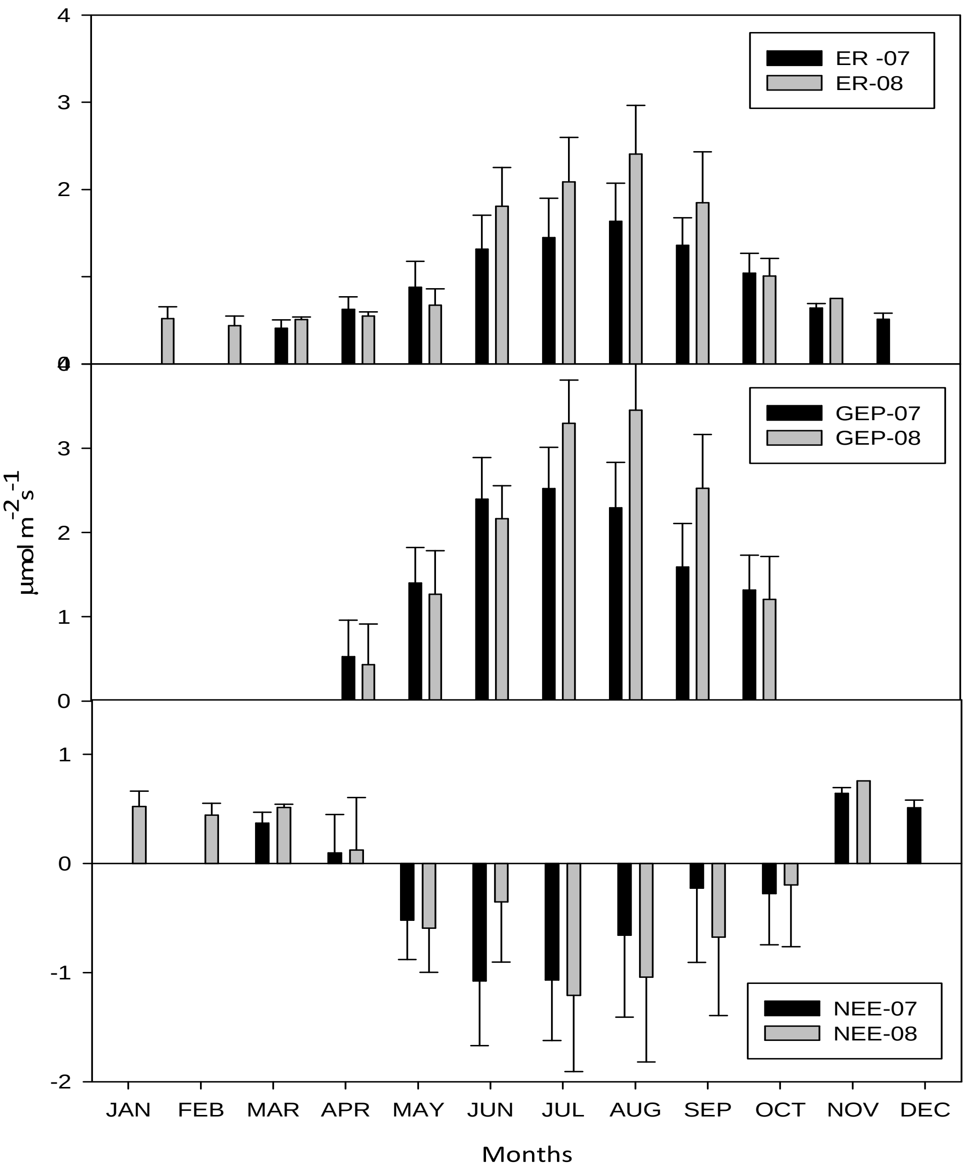

Figure 3.11 Ecosystem respiration (ER), gross ecosystem production (GEP) and net ecosystem exchange (NEE) for the years 2007 and 2008 in □mol $m^{-2}s^{-1}$.

Table 3.9 Monthly average of ER, GEP and NEE (☐mol $m^{-2}s^{-1}$) for both years of the study.

	2007			2008		
	µmol $m^{-2}s^{-1}$					
	ER	GEP	NEE	ER	GEP	NEE
APRIL	0.7	0.8	-0.1	0.6	0.7	-0.2
MAY	0.9	1.4	-0.5	0.7	1.3	-0.6
JUNE	1.3	2.4	-1.1	1.8	2.2	-0.4
JULY	1.5	2.5	-1.1	2.1	3.3	-1.2
AUG	1.6	2.3	-0.7	2.4	3.5	-1.0
SEPT	1.4	1.6	-0.2	1.8	2.5	-0.7
OCT	1.0	1.3	-0.3	1.0	1.2	-0.2

Cumulative NEE was virtually the same for both growing seasons, varying from a sink of 115.6 g C $m^{-2}d^{-1}$ in 2007 to -122.5 g C in 2008 (Figure 3.12). However, due to different meteorological conditions, there were notable differences between ER and GEP. More abundant precipitation in 2008 at the beginning of the growing season and warmer temperature have contributed to a higher ER and GEP. In 2007, ER was 257.3 µmol $m^{-2}s^{-1}$ and GEP was 368.6 µmol $m^{-2}s^{-1}$ while values in 2008 were 321.0 µmol $m^{-2}s^{-1}$ and 439.1 µmol $m^{-2}s^{-1}$ higher respectively. -

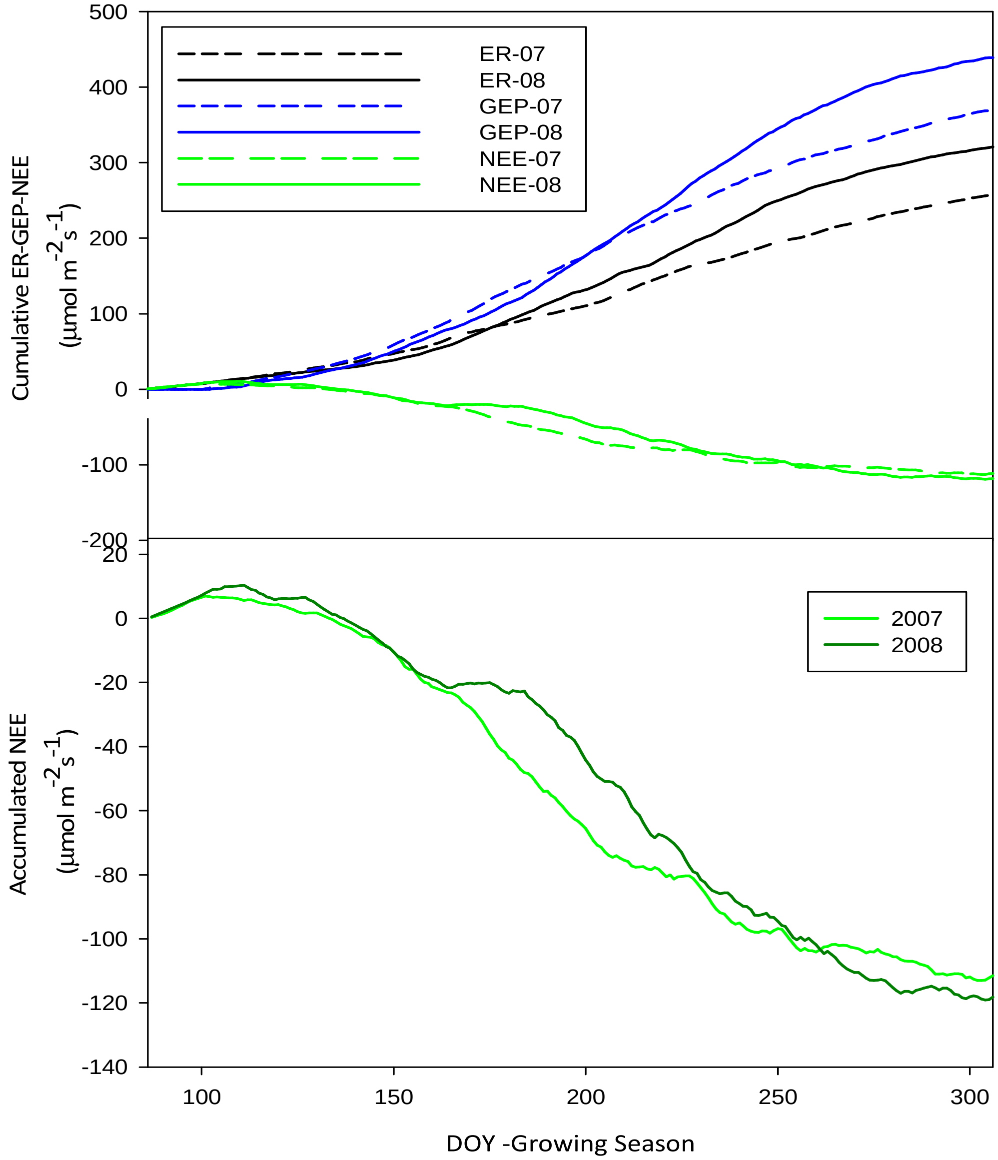

Figure 3.12 Cumulative ER, GEP, NEE for both years of the study period (□mol $m^{-2}s^{-1}$).

3.4 DISCUSSION

3.4.1 Biophysical Properties

The processes that control the uptake and release of carbon within a boreal ecosystem are driven by environmental parameters such as climate, topography, vegetation (composition and amount) and soil moisture. Nonetheless, other parameters such as the rate of organic mater decomposition, forest fire intensity, litter accumulation and soil texture (chemical properties, drainage) (Vierek *et al*., 1983, Van Cleve *et al*., 1983, Wein et MacLean, 1984) can also be considered in order to better compare and locate the EM1 forest within other research. Some of those parameters were obtained from Banville (2009) research conducted around the EM1 forest tower.

The BOREAS study which led to the Canadian Carbon Network (Margolis *et al*., 2006) has provided a rich legacy that now allows for intersite comparisons across Canadian boreal ecosystems. In black spruce dominated boreal forests, those comparisons indicate a variation in the C flux rate reported. One parameter contributing to the C variation within such boreal ecosystems would be the age structure that is often driven by the frequency of forest fires and exploitation (Kurz and Apps, 1999, Litvak *et al*., 2003; Banville *et al*., 2009). Forests re-growing from a fire disturbance will act as strong carbon sinks while mature forests will accumulate less C or be carbon neutral on an annual basis.

The EM1 site is younger than the northern old black spruce (NOBS), southern old black spruce (SOBS) and easthern old black spruce (EOBS) sites, but older than the chronosequence stands of Litvak *et al*. (2003) (Table 3.10). Nonetheless, the tree height at EM1 forest (9.0 m) is within the range (7.2 to 13.8 m; Litvak *et al*., 2003) of other Canadian black spruce forests at least older than 36 years (Litvak *et al*., 2003). It is therefore no surprise to note that the DBH of EM1 (10.0 cm) also lies within the range of other BSF (7.1 to 12.7 cm), including a younger site (36 years) near Thompson River, Manitoba. However, the Eastmain forest is much more open and exhibits a lower LAI value (1.7) than other boreal forests. Indeed, the average obtained here was closer to the younger site in Manitoba (36 years) and is lower than the 3.7 value obtained by Bergeron *et al.* (2007) at the Chibougamau boreal forest. Overall, it does lie within the range of Boreal black spruce forests. Boreas data provide an average of at 1.3 (with a range of 0.4-2.3). Table 3.2 provides forest density data.

Because the EM1 forest has an open canopy, it also possesses a rich understory. Vegetation species found within the understory survey of EM1 are very much like the understory of other studied boreal forests. Besides *kalmia angustifolia* and *rhododendron groenlandicum*, the EM1 site was rich in feather mosses, lichen and sphagnum, which were also reported at the NOBS, SOBS and EOBS sites. Only some species such as *betula grandulaso*, *salix spp*., *rosa spp*., *alnus rogosa* were either found in trace or absent.

Table 3.10 Site characteristics of the Northern (NOBS), Southern (SOBS), Eastern (EOBS) old black spruce sites, the younger sites (50 km West of Thompson River, Manitoba) from Litvak *et al*. (2003)

Location	**Manitoba (NOBS)**	**Saskatchewan (SOBS)**	**Quebec (EOBS)**	**Thompson River (50 km West)**			**Quebec EM-1**
Reference	**Gower *et al.* (2007)**	**Gower *et al.* (2007)**	**Bernier (FCRN)**	**Litvak *et al.* (2003)**			**Present study**
Lat. / Long	55.880°N / 98.481°W	53.987°N/ 105.118°W	49.692°N/ 74.342°W	55.880°N / 98.481°W			52.104°N/ 76.196°W
Age	160	130	95	11	19	36	84
Height (m)	9.1	7.2	13.8	0	2.2	3.7	9.0
DBH (cm)	8.5	7.1	12.7	0	0.7	7.1	10.0
LAI	4.8	3.8	3.7	0	0.95	1.5	1.7
Dominant vegetation type	Black Spruce	Black Spruce (Jack Pine, Tamarack)	Black Spruce (Jack Pine, Tamarack)	Black Spruce			Black Spruce (Jack Pine)
Understory	Betula grandulaso, Rhododendron groenlandicum, Vaccinium spp., Salix spp., Rosa spp. feather mosses, sphagnum	Kalmia angustifolia, Rhododendron groenlandicum, Rosa spp. feather mosses, sphagnum	Alnus rogosa, Kalmia angustifolia, Rhododendron groenlandicum, feather mosses, lichen, sphagnum	Rhododendron groenlandicum, Vaccinium spp., Salix spp., Rosa spp. feather mosses, sphagnum			Kalmia angustifolia, Rhododendron groenlandicum, feather mosses, lichen, sphagnum

Biophysical properties such as age structure, height, DBH, LAI and vegetation of the EM1 site compare well to other canadian black spruce site. The site variation is most likely due to age structure and climatic conditions.

3.4.2 Carbon Stock

Because they are believed to hold about 50% of the global C in forest, boreal ecosystems are considered an important terrestrial carbon sink (Kasischke, 2000). Indeed, their role in the Canadian and global GHG cycle has long been recognized (Dixon *et al*., 1994, D'Arrigo *et al*., 1987). Banville (2009) reported that the total soil C ranged from 7.58 to 13.64 kg C m^{-2} in mature forests in EM1 and were within the range of values reported by Bhatti et al. (2002) (6.2 to 27.4 kg C m^{-2}). However, their values were higher than the 4.3 kg C m^{-2} estimated by Yu *et al*. (2002) for comparable vegetation types in western Canada boreal forest soils. Differences in C stock may be due to variations in humidity and precipitation regimes between eastern and western boreal regions as the former are under the influence of a humid maritime climate (Banville, 2009).

3.4.3 Net Ecosystem Exchange

In addition to biophysical properties and carbon stock in soils, carbon fluxes need to be considered in any site comparison. The cumulative NEE determined for EM1 for the two growing season of the current study (-116 and -123 g C m^{-2} yr^{-1}) are lower to those reported by Welp *et al*. (2007) (-152 to -172 g C m^{-2} yr^{-1}). The EM1 forest was a greater sink than SOBS (-27 to -80 g C m^{-2} yr^{-1}; Gower *et al*., 2007; Krishnan *et al*., 2008), which is also almost 50 years older.

Table 3.11 Net ecosystem exchange (NEE) in g C m^{-2} yr^{-1} of a Northern (NOBS), Southern (SOBS), an Eastern (EOBS) old black spruce sites, a Northern Canadian site and the present study site, i.e. Eastmain-1

Location	**Manitoba (NOBS)**	**Saskatchewan (SOBS)**	**Northern Canada**	**Quebec EM-1**
Reference	**Gower *et al*. (2007) Dunn *et al*. (2007)**	**Gower *et al*. (2007) Krishnan *et al*. (2008)**	**Welp *et al*. (2007)***	**Present study**
Year	1995-2004	2000-2006	2002	2007-2008
Range (g C $m^{-2}yr^{-1}$)	-58 to 84	-27 to -80	-152 to -172	- 116 to -123

*Growing season only (2002, 2003, 2004)

The EM1 forest is similar in terms of biophysical and carbon exchange dynamics to other black spruce forest reported in the literature. The EM1 forest is therefore found to represent a typical example of Canadian boreal black spruce forest. This was the first objective of the current research. With this established, we can now use the EM1 forest as a comparison point for studying the effect of flooding on the C emissions of a reservoir.

3.5 CONCLUSION

Boreal forests play an important role in the global carbon exchange. Using a combination of continuous carbon exchange measurements through eddy covariance, and supporting meteorological and observational data for the period of March 2007 to October 2008, the effects of environmental factors and the bio-physical characteristics of the forest on net ecosystem exchange were assessed.

Biophysical characteristics of the Eastmain-1 forest were considered in order to compare this environment with other similar areas in northern Quebec. We found that the forest is dominated by mature black spruce, i.e. 84 ± 3 years, 8.9 m height with a DBH ranging from 5.0 to 25.7 cm and an average tree density of 0.5 tree per meter square. The highest tree density was found to the East of the tower, which is also the driest, while the lowest density was found to the South of the tower. Both the areas to the North and West exhibit a moister soil. Based on the ground assessment, we found that the forest floor was dominated by *Pleurozium Schreberi*, *Sphagnum spp*., *Lichen spp*., *Rhododendron groenlandicum* and *Vaccinium myrtilloides*. The average leaf area index value of 1.34, based on the TRAC measurement, was in the range of the BOREAS study for black spruce (0.4-2.3) and corresponded with visual observations of the open-nature of the canopy.

Net Ecosystem Exchange (NEE) was determined using an eddy covariance system. Seasonal NEE and ER were the highest in the summer of 2007 and 2008 with an average of -0.8 g C $m^{-2}d^{-1}$ and -0.9 g C $m^{-2}d^{-1}$ (NEE) and 1.5 g C $m^{-2}d^{-1}$ and 2.3 g C $m^{-2}d^{-1}$ (ER) respectively. For both years, we found that the CO_2 storage flux (F_s) represents about 10% of the net ecosystem exchange for the study period.

Precipitation was more abundant in the early Spring 2007, leading to an increase in soil moisture. As mentionned in Welp *et al.* (2007), soil moisture appears to have a strong control on ecosystem respiration (ER), thus warm and wet conditions contribute to increase ER at the forest and lower NEE. Nonetheless, the present study has demonstrated that the accumulated NEE at the site was virtually the same for both growing seasons, varying from a sink of -115.6 g C $m^{-2}d^{-1}$ in 2007 and to -122.5 g C $m^{-2}d^{-1}$ in 2008 (Figure 3.12).

Similarly to results found by Bergeron *et al.* (2007), the Eastmain forest was mainly a source of CO_2 to the atmosphere outside of the growing season, from November to April.

When looking at the cumulative carbon balance, one noticed that there were only 6.9 g C $m^{-2}d^{-1}$ difference between both years of the study over this boreal black spruce forest. This lack of major difference between both carbon balance confirms that the Eastmain-1 black spruce has reached a stage of stability and has not been affected by any major environment parameters of other disturbances (fire, extreme weather events, insects, etc.).

Acknowledgements

This research was funded by a grant to Drs. Nigel T. Roulet and Ian B. Strachan from the Canadian Foundation for Climate and Atmospheric Sciences (CFCAS). We would like to thank Dr. Alain Tremblay (Hydro-Quebec) for logistical support. We are also thankful to SEBJ, Dr. Jim Fyles and Dr. Benoit Cote for providing some of the forest biophysical measurement equipment. Finally, we are thankful to Helene Higgins, Youngil Kim, Lesley Winterhalt, Marie-Claude Bonneville, Onil Bergeron and numerous Jamesiens workers for their essential collaboration in the field and in the laboratory.

PREFACE CHAPTER 4

In Chapter 3, we compared the pre-flooded analog site (Boreal black spruce forest) to other northern black spruce forests in terms of biophysical and eco-physiological properties. The site was found to be a representative boreal black spruce forest. In the next chapter, using the eddy covariance technique we determine how the flooded ecosystem has responded following impoundment. We first use a source area model to split the continuous data between fluxes originating over the reservoir and those over the island. We compare the island terrestrial fluxes obtained with carbon chamber measurements to two footprints lying on the island during the same period. We then explore the diurnal and seasonal patterns of the reservoir emissions and finally contrast the NEE from the pre-flooded environment (Chapter 3) to the NEE obtained over the flooded environment and evaluate the net reservoir effect.

CHAPTER 4: Determination of direction and magnitude of net CO_2 fluxes for the post-flooded environment (Objective 2)

ABSTRACT

The net ecosystem exchange of CO_2 was measured over a flooded boreal black spruce forest using a 13 m eddy covariance flux tower installed on an island in the reservoir. Fluxes were screened for directionality and separated into those originating from the reservoir and from the island. Carbon chambers were used to evaluate CO_2 fluxes on the island and values obtained were compared to the NEE from the tower when the footprint was on the island. Reservoir fluxes were explored during 2007 and 2008 and two seasonal peaks of emissions were revealed; a stronger one in mid May corresponding to the ice break up and a second, smaller one in the early fall (mid August to September) associated with the reservoir water turnover. Fluxes from the period December 2007 to November 2008 were divided into six distinct periods to facilitate analysis: ice covered (DOY 335-142), ice break up (143-152), ice free (153-228), fall turnover (229-274), post-turnover (275-323) and winter transition (324-335)). Gap filling of the reservoir NEE was explored for the ice free and post turnover period looking at different environmental factors and wind speed resulted in the best relationship. Daily average NEE was accumulated for reservoir and forest gap-filled tower data sets. The net reservoir effect was determined to be 289.2 ± 144.6 g C m^{-2} yr^{-1} for the period December 1st, 2007 to November 30th, 2008.

4.1 INTRODUCTION

Energy demand is currently at its highest level in human history and is still suspected to increase in the next decades (US DOE, 2008). Yet, the public demand for greener electricity production is becoming stronger. At the same time, 2008 and 2009 were marked by a strong economic downturn. As a result, North American governments revealed an interest to seek green forms of energy production as part of a potential economic rescue plan. Since the 1950's, the Province of Quebec has been very dependent upon its many rivers to generate power. Like any other source of power generation, hydroelectricity cannot be considered harmless to the environment. Some of the negative effects that have been identified and studied globally include the displacement of aboriginal populations and burial sites (Fearnside, 2005), disruption of traditional hunting practices (Rosenberg *et al.*, 1995), fractioning of migration routes for large mammals (Cosson *et al.*, 1999; Vie, 1999; Mahoney and Schaefer, 2002) and methyl mercury release and bioaccumulation (Verdon *et al.*, 1991; Tremblay & Lucotte, 1997). Despite the aforementioned problems, hydroelectricity is generally believed to be an environmentally-safe way to generate power.

To date, few studies have been conducted to assess carbon (C) fluxes over a large body of water. It has been established that the creation of reservoirs does affect the biosphere-atmosphere exchange on a local scale (Delmas, 2003) through the release of biogenic gases such as methane (CH_4) and carbon dioxide (CO_2). Changes in GHG exchange resulting from the creation of a reservoir are primarily induced from the suppression of the net primary production (NPP) of the vegetation following flooding, but also from the heterotrophic respiration (HR) coming from the large stock of carbon stored in the flooded vegetation and soils. In turn, the atmosphere responds to the changes in the exchange of energy and water vapour from the surface. Although few measurements exist, younger reservoirs are believed to produce higher emissions than older reservoirs presumably due to fresher organic matter and nutrients present in the water column. However, it is believed that fluxes stabilize to a level comparable to natural boreal lakes as decomposition decreases over time (Tremblay *et al.*, 2005). Nonetheless, the extent of these impacts is still largely unknown. Therefore, there is great interest in examining if changes, such as those induced by the flooding of a forest, could significantly affect the atmospheric concentrations of GHG.

More recently however, it has been suggested that artificial hydroelectric reservoirs could constitute an anthropogenic source of GHG. This was confirmed when the first flux measurements on boreal reservoirs (Kelly *et al.,* 1994; Duchemin *et al.,* 1995) 10-years of age or older found emissions on an average of 0.4 ± 0.5 g CO_2-C m^{-2} d^{-1} and 6.6 ± 8.0 mg CH_4-C m^{-2} d^{-1} (Tremblay *et al.*, 2005). The World Commission on Dams report (Fearnside *et al.,* 1995) even went so far as to suggest that GHG emissions from tropical reservoirs may even be higher than those of a conventional oil-fired thermal generation plant. While such studies have shown that emissions from tropical hydroelectric reservoirs can be higher than 2 g CO_2-C m^{-2} d^{-1} (Tremblay *et al.*, 2005), the few studies focusing on reservoirs in the northern latitudes have indicated that daily losses in these systems rarely exceed 0.5 g CO_2-C m^{-2} d^{-1} (Tremblay *et al.*, 2005).

To date, most of this research has been conducted on older reservoirs with limited sampling. With more reservoirs being created to meet increasing electricity demand, it is imperative to assess the CO_2 fluxes from the entirety of a reservoir and include the early years after impoundment. In order to obtain a better picture of the temporal variability in reservoir emissions, continuous flux measurements are also essential.

The overall goal of this study is: (1) to determine the direction and magnitude of net CO_2 fluxes from a recently flooded boreal ecosystem using the eddy covariance technique; and (2) to determine the net CO_2-carbon exchange that results from the creation of a hydroelectric reservoir within a boreal forest.

4.2 MATERIALS AND METHODS

4.2.1 Site description

For comparison purposes, net ecosystem exchange (NEE) was measured on two different ecosystems: a pre-flooded and a post-flooded site. Chapter 3 described the forest site, hereafter referred to as the pre-flooded site (52°06'16" N, 076°11'48" W). At this site, a 23-m tall scaffold tower served as the primary instrument platform for eddy covariance instrument. In summary, it was found that this black spruce forest is dominated by mature black spruce, approximately 84 ± 3 years in age, 8.9 m in height with a DBH ranging from 5.0 to 80.5 cm and an average tree density of 0.5 tree per meter square. The forest floor is dominated by *Sphagnum spp*., *Lichen spp*., *Rhododendron groenlandicum* and *Vaccinium myrtilloides* and the average leaf area index is 1.45.

To represent the post-flooded conditions, a 13 m scaffold tower was installed on an island in the reservoir (52° 07' 29'N, 75° 55' 47"W) (Figure 4.1). The reservoir characteristics are described in Table 4.1. The island was located 5.2 km from the shore of the reservoir and several 100 m to several kilometres from any nearby islands in all directions. Prior to flooding, the island would have represented an upland forested area. The proportion of cover types flooded for the entire reservoir is 65% black spruce forest, 14% wetlands and 21% lakes and rivers.

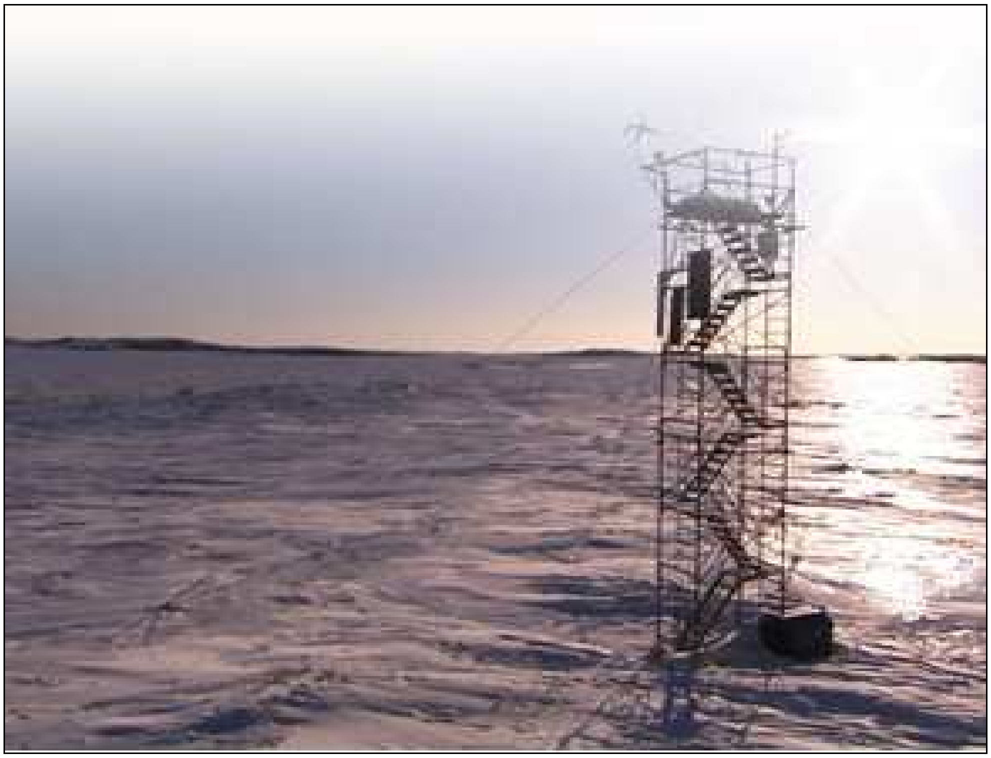

Figure 4.1 Eddy covariance tower at the flooded site (52°07’29”N, 75°55’47”W,). View from the East during winter. Photo credit: Hydro-Quebec, 2007.

Table 4.1 Characteristics of the Eastmain-1 reservoir. Information from Hydro-Quebec EIA and UQAM personal communication (2008).

Reservoir	Surface water temperature (summer)	16.9	°C
	Volume	6.9	km^3
	Active storage	4.2	km^3
	Maximum operating level (meter above sea level)	283	Masl
	Minimum operating level	274	Masl
	Drawdown	9	M
	Mean reservoir depth	28	M
	Thermocline depth	12.4	M

During the preparation of the island tower site, most of the trees on the South and South east part of the island were mechanically cut to avoid both mechanical turbulence and contamination from vegetative CO_2 uptake. The remaining ground vegetation on the eastern part of the island is dominated by dense ericaceous shrubs (*Rhododendron groenlandicum, Kalmia polifolia*, *Chameadaphnea calyculata*, *and Vaccinium occyccos*) and reindeer lichen. Chemical control of the remaining vegetation was forbidden to prevent any water contamination. The island is accessible by helicopter or by boat during the ice-free period and by snowmobile during the winter season.

4.2.2 Acquisition of Carbon Chamber Data

On the vegetated part of the island, NEE-PAR data were collected from three types of micro-sites (lowland, midland, upland), which were selected in early June to the East of the flux tower. Within each micro-site, three collars of 24 cm diameter were installed. Measurements, which followed a modified protocol from Caroll and Crill (1997), were made using a 50 cm^3 clear Plexiglas wall chamber placed over the pre-installed soil collars on eleven occasions between June and August 2008 and taken between 9h00am and 4h00pm, during periods of maximum photosynthetically active radiation (PAR), i.e. cloud free. CO_2 concentration, PAR inside and outside chamber, air and soil temperatures and soil water content were measured using respectively, an EGM4 portable system infrared gas analyzer (PP-systems, Wales, UK) powered by an internal 12V battery, a quantum sensor (Model PAR-1, PP Systems, Wales), a thermistor (Campbell Scientific, Logan, Utah) and time domain reflectometry (TDR 100, Spectrum Technologies, Inc.). During measurements, the carbon chamber was installed on the collar and water-sealed to prevent any air exchange. A fan in the chamber circulated air to maintain a constant temperature. The chamber was left on the collar for 210 seconds per set of measurements, for a total of five sets of measurements: a clear measurement (representing 78% PAR due to the transparency of the chamber), and four different shroud-covered chamber measurements (50%, 30%, 17% and 0% PAR (dark respiration). Between each measurement, the chamber was removed to allow the system to return to ambient conditions. All plants were enclosed within the chamber during measurements.

The micrometeorological sign convention was used to define positive vertical fluxes as a net release to the atmosphere and negative values to indicate a net uptake by the surface. Net ecosystem exchange (NEE) is ecosystem respiration (ER) minus gross ecosystem production (GEP) (a function of incident PAR). The relationship between NEE and PAR is typically modelled as a rectangular hyperbola as (Frolking *et al.*, 1998):

$$\mathrm{NEE} = \frac{\alpha * \mathrm{PPFD} * \mathrm{Pmax}}{\left(\left(\mathrm{Pmax} + (\alpha * \mathrm{PPFD})\right) + \mathrm{ER}\right)} \qquad (1)$$

where α is the quantum yield or the initial slope of the rectangular hyperbola, P_{max} is the maximum gross productivity and ER is the dark respiration (the y-axis intercept).

4.2.3 Eddy covariance system and supporting measurements

The eddy covariance technique (Baldocchi, 2003) was used to determine the turbulent flux of CO_2 (Fc) between the reservoir surface and the atmosphere as:

$$\mathrm{Fc} = \overline{w'\rho_C'} \qquad (2)$$

The eddy covariance system deployed at this research location includes a sonic anemometer (CSAT-3, Campbell Scientific, Logan, Utah), a fine-wire thermocouple and an open-path infrared gas analyser (IRGA; LI-7500, LI-COR, Lincoln, NA). All parameters were recorded using a fast response data logger (CR5000, Campbell Scientific, Logan, Utah) at 10 Hz, with 30-minute flux averages computed on the go and high frequency data retained. Eddy covariance measurements were started on August 20th 2006 at both island and forest sites.

A standard suite of meteorological variables was measured at each site including precipitation (TE525M tipping bucket gauge, Texas Electronics, Dallas, TX), wind speed and direction (05103-10, RM Young, Traverse City, MI), temperature and relative humidity (HMP45A, Vasala, Finland). Net radiation for the flooded site was measured with a net radiometer (CNR1, Kipp & Zonen, Delft, Netherlands) and a quantum sensor was used to measure PAR. These instruments were installed on a floating raft and powered by a 12V marine battery changed by solar panel. Data were respectively recorded on a CR10X and CR510 data logger.

The storage flux (F_s) of CO_2 within the layer between the reservoir surface and the height of the sonic anemometer was accounted for by integrating the concentration difference between successive time intervals (Δt = 30 minutes) over this layer (Mongerstern *et al*., 2004) as:

$$\mathbf{F_c = h_m \rho_a \frac{\Delta S_c}{\Delta t}} \quad (3)$$

where h_m is the measurement height (13m) and ρ_a is the mean dry air density in the layer. ΔSc, the mean CO_2 mole mixing ratio, was calculated as the difference between the following and preceding half-hour periods. Equation (4) was used with the turbulent eddy flux measured from the EC tower (*Fc*), to calculate the half-hourly net ecosystem exchange (NEE) as:

$$\mathbf{NEE = Fc + Fs} \quad (4)$$

The FSAM analytical flux footprint model (Schmid, 2002) was used to estimate the island tower upwind source area. The model requires five readily-available input parameters: sensor height (13m) and roughness length (z_o = 0.1 m), were constant; the standard deviation of the cross-wind velocity (σ_v); friction velocity (u*) and the Obukhov length were calculated from the eddy covariance data for each valid 30-minute period.

4.2.4 Automated and Manual Quality Control

Initial cleaning of the flux data was done using an in-house, automated Matlab (v.7.0 Mathworks, Natick, MA) script to ensure the quality and continuity of the dataset. Fluxes were calculated using high-frequency data from the covariance of the vertical wind velocity and the CO_2 concentration and then averaged over a 30-minute time step

(Bergeron *et al.*, 2007). Flux data were rejected for instrumental causes, such as power failure, tower maintenance, or for unfavourable weather events such as dew, rain, or heavy ice. Three-axis rotations were applied to set the 30-minute mean transverse (*v*) and vertical (*w*) components equal to zero (Tanner and Thurtell, 1969). High frequency flux data were screened and rejected based on the presence of spikes (Vickers and Mahrt, 1997) and flux data were corrected for density effects (Webb *et al.*, 1980). A visual inspection of the data plots was done to ensure that all remaining data were within appropriate ranges of values and that no instrument malfunction affected any variables. Then, the difference between the block average and the linear detrended fluxes were verified to respect the established acceptable range, of respectively >1 and <0.5. Finally, with the assumption that the CO_2 emissions from the surface of the reservoir are non-biological or photochemical in origin, we set the flux threshold to zero in order to reject winter and nighttime uptake of CO_2. No u* threshold or monthly standard deviation corrections were applied to the reservoir flux data.

4.3 RESULTS & DISCUSSION

4.3.1 Seasonal temperature

At this latitude, the climate is characterized as being cold, wet and sub-arctic continental. Seasons range from mild, short summers (10°C to 15°C from mid-June to late August) to long, harsh winters, usually beginning around October 31th and lasting for 190 days (± 14 days). The mean annual temperature is -0.7°C. Average temperature generally stays close to –18.5°C in winter from December 21st to March 21st with temperature occasionally dropping below –30°C, especially in February. The first winter freeze generally starts around DOY 307. Large lakes are usually frozen from mid-November and the ice breaks up in mid-May.

4.3.2 Wind Characteristics

For the purpose of this study, wind direction was a key element in accepting or rejecting NEE fluxes and wind speed is believed to be the main mechanism facilitating CO_2 exchange between the reservoir and the lower atmosphere. Upwind directions between 233.5° and 23.5° were considered to be free from the influence of the island, therefore representing exclusively the reservoir. For both years of the study, 48% of the wind data met this directional criterion. Seasonal windroses with wind direction and wind speed divided into five bins (1-2, 2-3, 3-4, 5-7 and >7 ms^{-1}) were plotted using WindRose Pro (v.2.3.11, Enviroware srl.). From the seasonal wind roses (Figure 4.2), it is clear that the average wind speed remains strong throughout the entire year at this post-flooded site. The absence of large trees on the island and the large open body of water around can easily explain the annual wind average being equal or higher than 7 ms^{-1}. Southerly winds dominate during the spring and winter in 2007. In the summer of 2007, the dominant winds were between the West and North-West and in fall were from the West and South-West. In 2008, the average wind direction during the spring and winter was from the South, but not as dominantly as in 2007. Wind direction was between the South-West and South-East in the spring and the West and South in the winter. In summer 2008, it is very similar to the fall of 2007, with winds between the West and South-West. Finally, in fall 2008 winds were mainly coming from the South-West and the South. Overall, prevailing winds are South and Southwest, being dominantly southwesterly in the summer and winter.

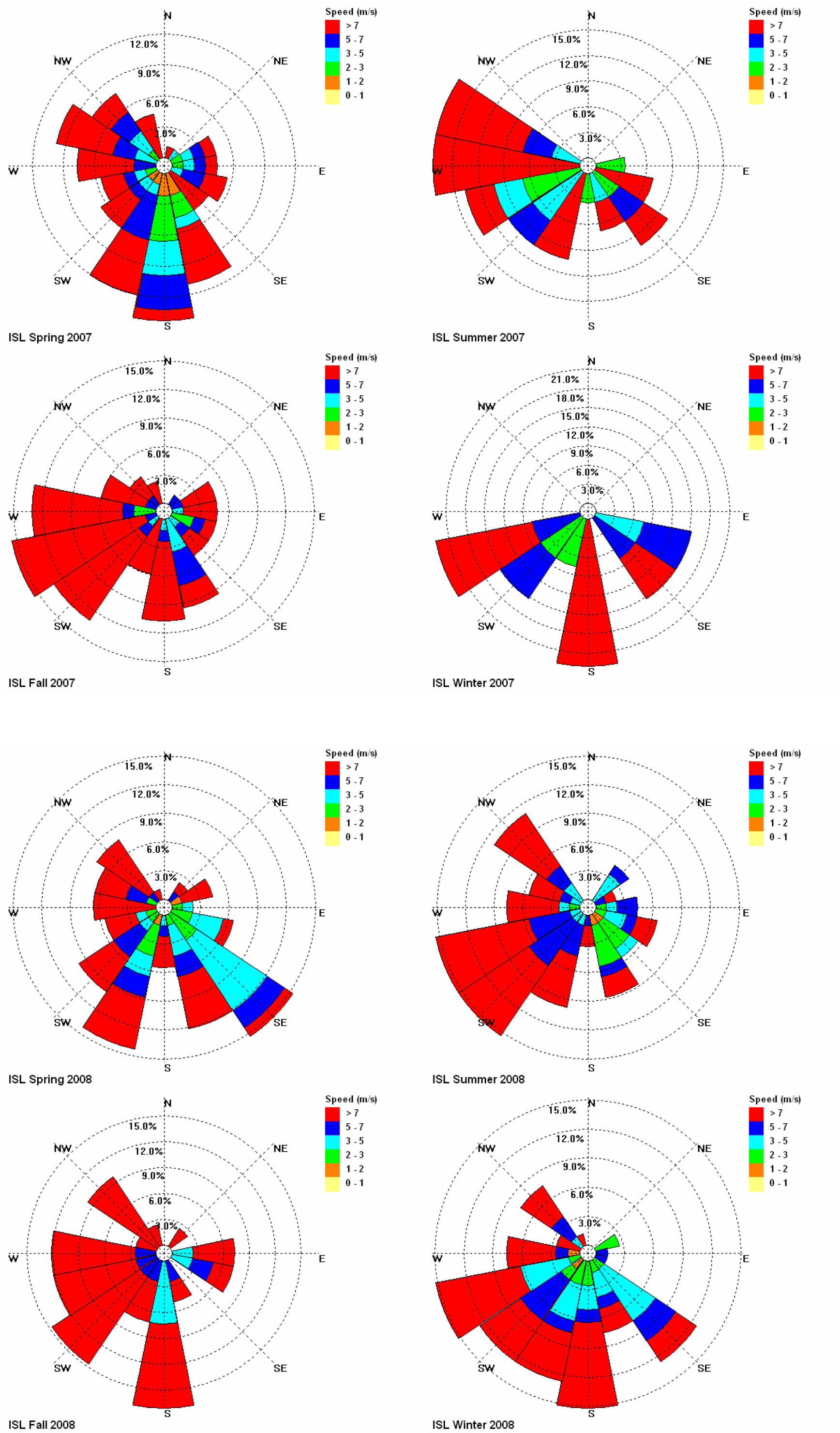

Figure 4.2 Top Figure: 2007 Seasonal wind rose at the flooded site. Wind speed was divided into 5 bins; 1-2, 2-3, 3-4, 5-7 and >7 ms-1. Bottom figure: 2008.

4.3.3 Reservoir Net Ecosystem Exchange (NEE)

4.3.3.1 Storage Flux

It was found that storage flux was mainly positive in the evening, after sunset indicating an accumulation of CO_2, while the flux was negative in early morning (Figure 4.3). As the sun rises, surface heating leads to better mixing and a flushing of the stored CO_2 as shown by the strong release of CO_2 in the early morning (especially in July) during this period. The magnitude of the storage flux in June and July were similar; the storage flux was near zero during daytime which is appropriate for the windy daytime environment of the reservoir.

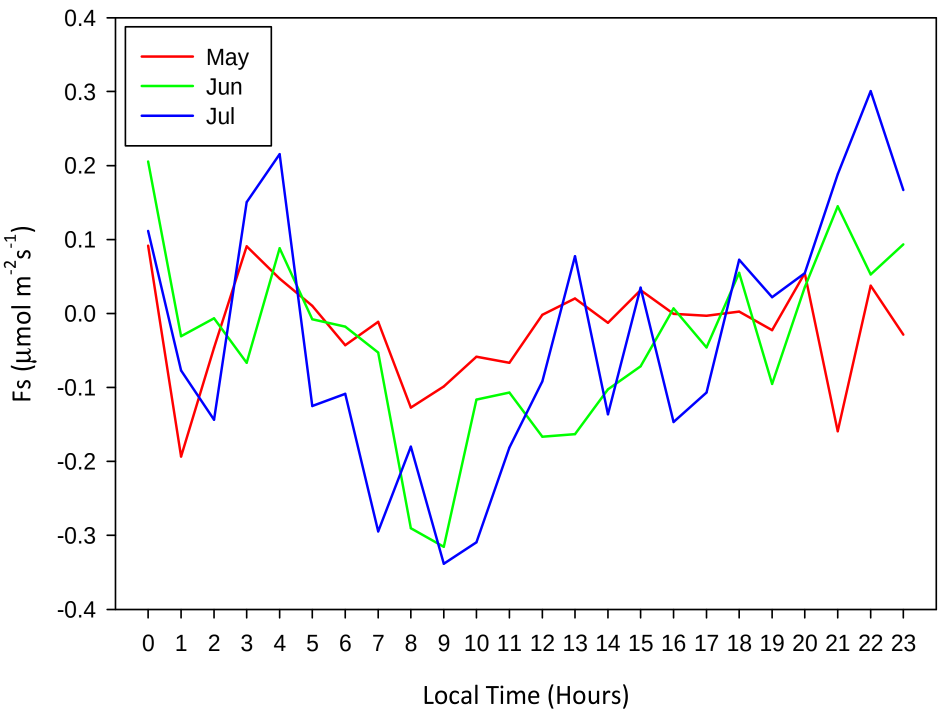

Figure 4.3 Storage (□mol $m^{-2}s^{-1}$) over the reservoir for the months of May, June and July 2008.

4.3.3.2 Directionality of NEE and Flux Footprint

Due to the very location of the tower on the island, depending on wind direction, the measured fluxes were coming from two different ecosystems: one being the remaining shrub-like vegetation of the island and the second being the reservoir itself. 30-minute average fluxes were divided into daytime and nighttime and binned in 30° intervals of wind direction (Figure 4.4). During nightime, the flux is positive from all wind directions indicating the expected ecosystem respiration from both land and water. During daytime, some wind directions indicated evidence of uptake. Therefore we needed to determine a range of direction to use as a criterion for rejecting data that could be influenced by the terrestrial ecosystem. First, the confidence interval error bars around flux data associated with the reservoir orientation were smaller than those around fluxes originating from 50° to 130° (Figure 4.4). The range of directions between 50° and 130° clearly shows a larger release during nighttime periods further indicating the influence of terrestrial sources. Based on only this information we could have determined the reservoir range to be from 130° through 50°. However, the reservoir does not behave like a static body of water (e.g. a lake), but rather faces important water level fluctuations, which can expose more or less of the land depending on the water level. Thus, based on field observations of the island contours at low water level and using a compass we decided to conservatively restrict the reservoir orientation to 233.5° to 23.5°. Although this is a conservative range, we are sure that it is excluding all terrestrial sections that might be exposed, especially the far end of the island that could from time to time contribute to bias the fluxes coming from the reservoir.

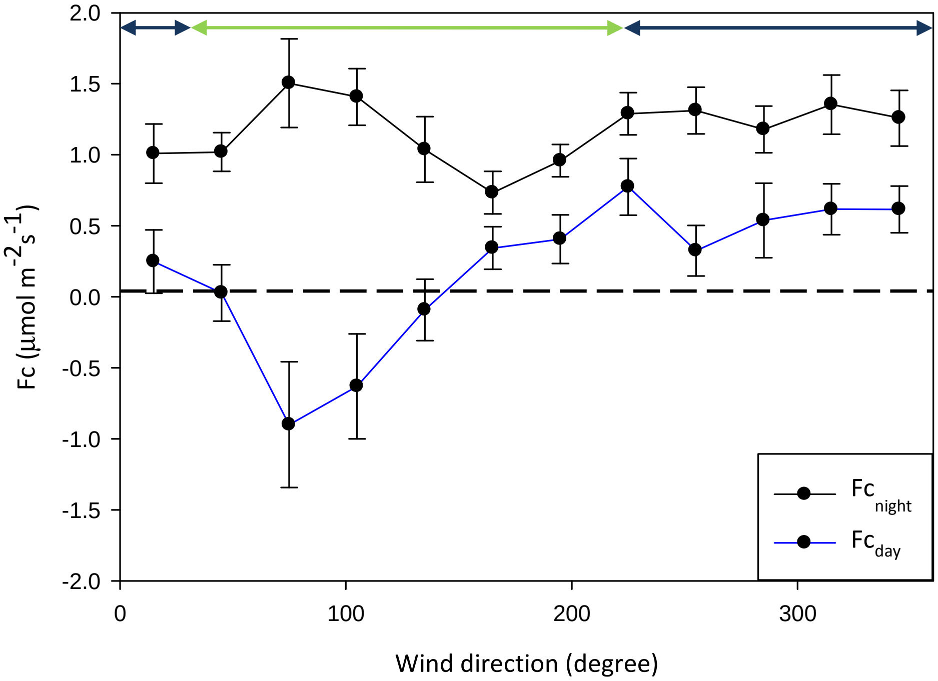

Figure 4.4 Diurnal NEE fluxes (□mol m^{-2} s^{-1}) for various wind directions (°) at the island tower for the summer months (June 21^{st}- to September 21^{st}) of 2008. The blue arrow represents the reservoir and the green arrow represents the island.

The modelled 80^{th} percentile source areas were determined for the ice-free periods between 10h00am and 3h00pm. The best performance of the model was obtained for the month of July (Figure 4.5), with 14 days falling into the acceptable range of the footprint model parameter requirements. The length and width of each footprint was fairly consistent, with an average of 370 m and 60 m, respectively. A range of footprints is depicted with several completely over water, some partially influenced by terrestrial sources and two footprints (July 9^{th} and 23^{rd}) lying entirely on the island (Figure 4.5). Again, a note of caution is required when using these footprints. As mentioned above, the island contours were obtained on a specific day in mid-July 2007 which had a corresponding reservoir water level. Because the reservoir possessed an average drawdown of ± 1 meter per month during the summer 2007 and 2008 (HQ, *personal communication, 2009*) the contour of the island changed and when the water level was lower, considerable land was exposed to the south-west of the eddy covariance tower. But by keeping a conservative window of acceptable wind direction (233.5° to 23.5°) over the reservoir and seeing that the upwind start of the footprint is many meters away from the island, we have increased confidence in the data (Figure 4.5). Nonetheless, this would remain an area to explore in further study.

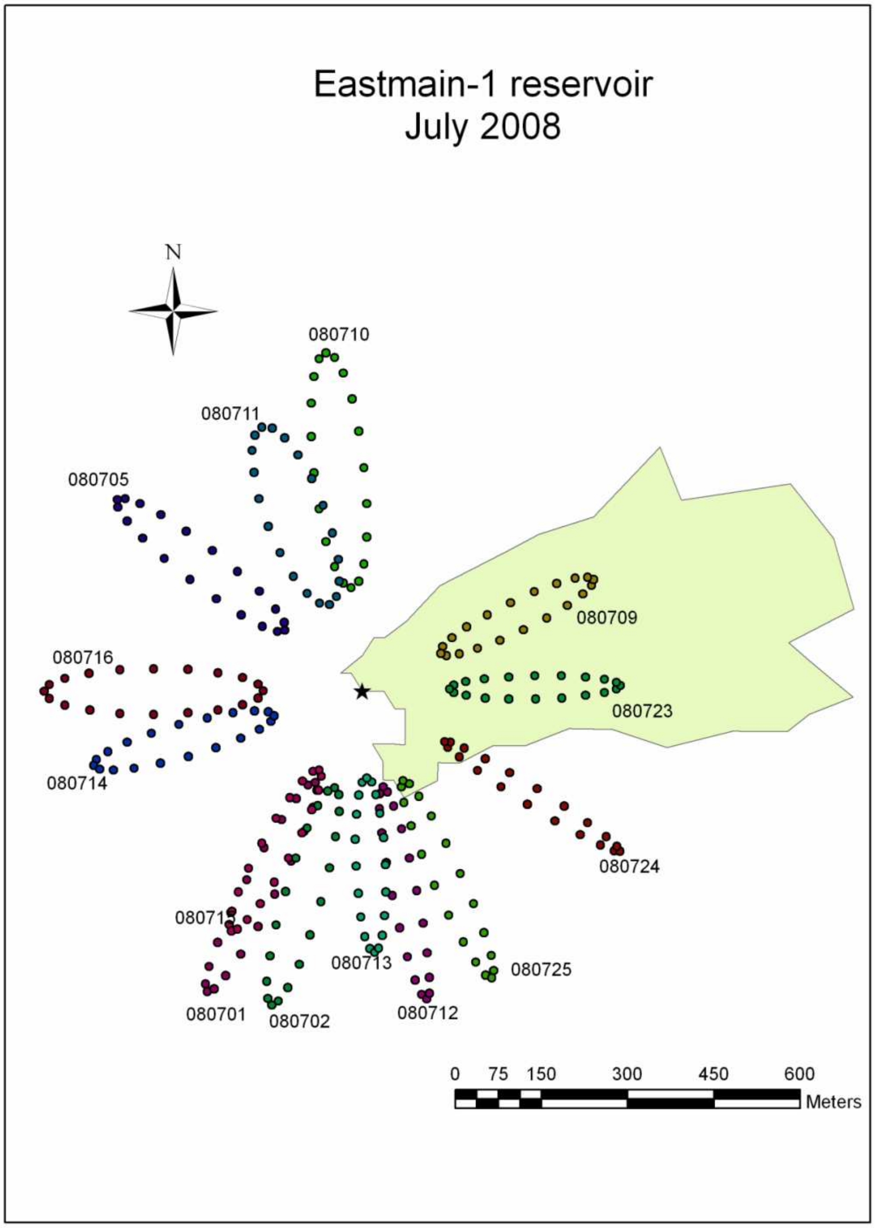

Figure 4.5 Modelled upwind source area for selected days during the months of July 2008.

4.3.3.3 Island NEE

The purpose of carbon chamber measurements on the island was: to determine fluxes coming from the vegetated island respecting the spatial variability of the vegetative community and the soil moisture gradient; and to collect some useful environmental parameters of the soil and vegetation which could eventually be used for future modelling efforts in estimating the overall reservoir carbon budget including all remaining islands.

On the island, environmental parameters of three micro-sites (lowland, midland and upland) were first compared one to another. The lowland micro-site had the least plant diversity and was dominated mainly by *Sphagnum spp*. It was the wettest of all three micro-sites. The midland micro-site was dominated by *Vaccinium myrtilloides* and small *Rhododendron groenlandicum* and the upland micro-site was dominated by large *Rhododendron groenlandicum*.

Light curves responses were produced for each of the three micro-sites, parameters were determined and then compared against studies from similar environments (Frolking *et al*., 1998; Pelletier, 2005). The high P_{max} value obtained at the upland micro-site (Table 4.2) confirms that the vegetation is similar to the understory of a natural boreal forest. Indeed, the upland micro-site composed mainly of tall (25-30 cm) shrubs and *Vaccinium groenlandicum* provided a light curve response (Figure 4.6) that is much different than the lowland and midland micro-site, which vegetation are both more similar to a bog.

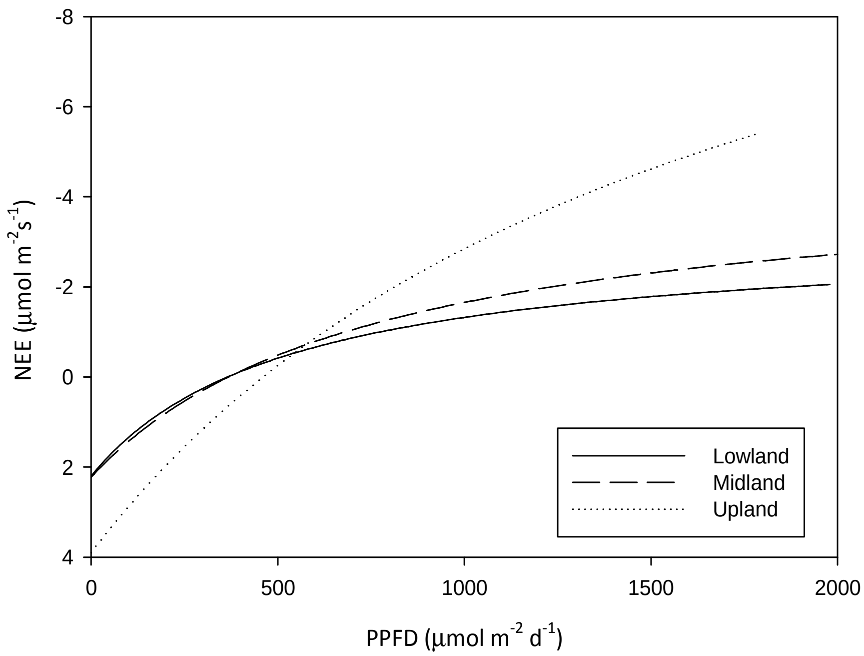

Figure 4.6 Rectangular hyperbola curve for the three micro-sites between the DOY 176-227 (June 24th and August 14th).

In general, this terrestrial island ecosystem behaves similar to a rich fen in Hudson Bay (Frolking *et al*., 1998) with both all three sites having an initial slope of the rectangular hyperbola (α) of 0.01. However, the maximum gross photosynthesis (P_{max}) of the island vegetation (8.8 μmol $m^{-2}s^{-1}$) is closer to the sphagnum (9.2 μmol $m^{-2}s^{-1}$) reported by Pelletier (2005). Respiration compares well to the mixed peatland (Frolking *et al*, 1998). The average island NEE (6.7 μmol $m^{-2}s^{-1}$) is close to both the NEE of the mixed peatland (6.1 μmol $m^{-2}s^{-1}$, Frolking *et al*., 1998) and the NEE of the sphagnum measured at LG2 (6.2 μmol $m^{-2}s^{-1}$ Pelletier, 2005). This analysis suggests that for the tree-free portions of the island, the remaining vegetation is behaving similar to an undisturbed environment.

Table 4.2 Comparison between rectangular hyperbola parameters from original field measurements and existing literature data. The parameters were obtained from the summer average NEE-PPFD curves of each transect on the post-flooded site. * Note: Pelletier has used the reverse sign convention for NEE.

Site	Site	α	Pmax	R	NEE (μmol $m^{-2}s^{-1}$)	r^2	Vegetation
Present study (2008)	Lowland	0.010	5.4	-2.2	4.6	0.67	*Sphagnum spp*
	Midland	0.009	6.8	-2.2	5.3	0.73	*Vaccinium myrt.* *Rhododendron.gr.*
	Upland	0.011	17.9	-3.9	10.5	0.80	*Rhododendron. gr.*
	Island (AVG)	0.010	8.8	-2.8	6.7	0.67	*Sphagnum spp.,* *Vaccinium myrt.,* *Rhododendron gr.*
Frolking *et al.* (1998)	Boreas	0.024	10.5	-2.4	6.07	0.64	Mixed peatland
		0.010	4.0	-1.7	1.64	0.68	Rich fen (Hudson Bay)
Pelletier* (2005)	LG1	-0.038	21.8	-15.1	1.39	0.69	*Sphagnum* spp. & shrubs
	LG2	-0.035	9.2	-9.2	6.17	0.83	Lichen hummock & shrubs
	LG3	-0.034	15.9	-10.2	2.45	0.70	*Sphagnum* spp. Hummock

In comparing chamber measurements for all three micro-sites to the tower footprints lying on the island on July 9th and July 23rd we found that the average flux obtained from carbon chamber measurements on July 19th, 20th and 22nd was -1.51 ± 0.77 μmol $m^{-2}s^{-1}$ (±CI) while the tower flux on July 9th was -5.20 ± 1.56 μmol $m^{-2}s^{-1}$ and -2.10 ± 2.15 μmol $m^{-2}s^{-1}$ on the 23rd. However, the upland collars only had a flux of -2.12 ± 2.41 μmol $m^{-2}s^{-1}$ compared to -1.26 ± 0.50 μmol $m^{-2}s^{-1}$ for the lowland and midland collars together, which again confirms that the upland micro-site behaves more like a natural boreal forest understory and the lowland and midland are more similar in nature to a mixed-bog. This can be confirmed by *in situ* observations of the bog-like type of vegetation and the lowland micro-site was at constant risk of flooding due to the reservoir drawdown which clearly contributes to maintain the environment wet and moist, like a bog.

4.3.4 Reservoir Net Ecosystem Exchange Patterns

There is no diurnal difference between the patterns of CO_2 release over the reservoir through the course of a year (Figure 4.7). This means that unlike the forest site there is no photochemical effect influencing the average 30-minutes daytime fluxes. Consequently, we were expecting to obtain a similar release of CO_2 during the day as at night. Figure 4.8a shows that indeed there is no significant difference between daytime and nighttime emissions over the reservoir. We found that because there is no photosynthesis occurring at night, fluxes both on the reservoir and the island were positive. This finding also proves that the reservoir was a net emitter of CO_2 at all times (daytime, night-time) during the summer of 2008 (Figure 4.8a).

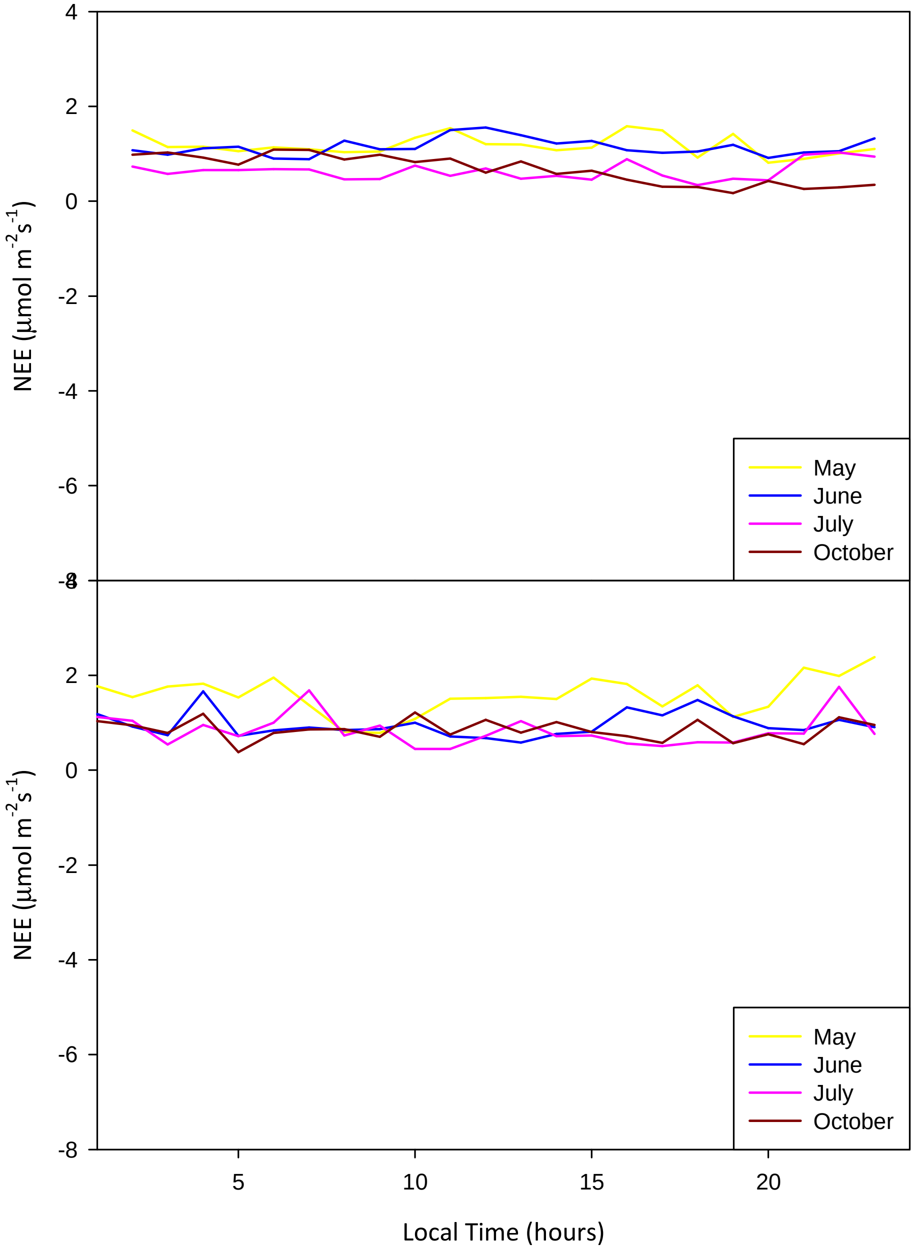

Figure 4.7 Comparison of NEE (□mol $m^{-2}s^{-1}$) at the reservoir for 2007 (top) and 2008 (bottom) for the months of May to October.

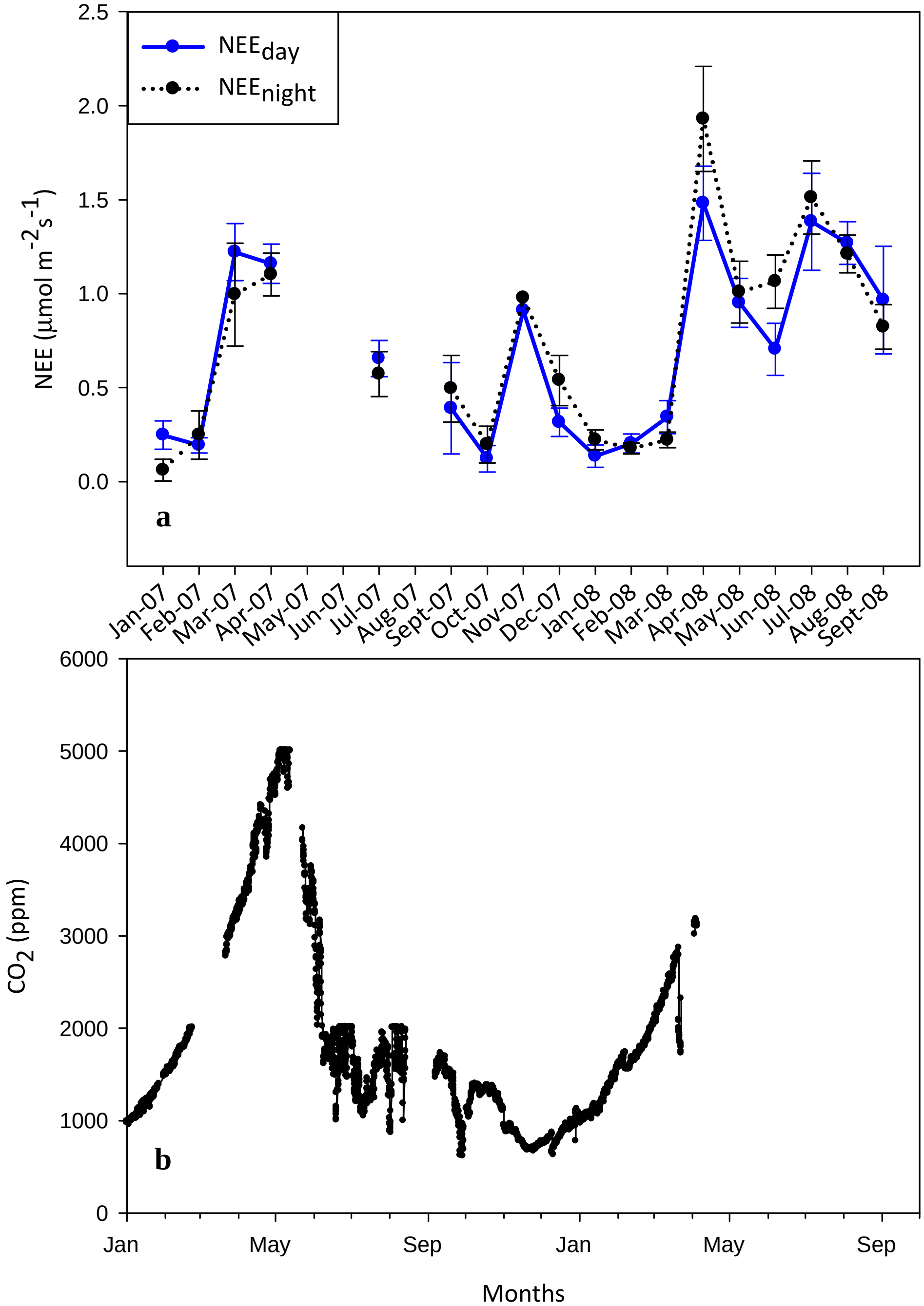

Figure 4.8 a) Monthly atmospheric NEE (□mol m^{-2}s^{-1}) recorded over the reservoir. b) Monthly CO_2 water concentration (ppm) in the water column recorded at the powerhouse. (Data used with the permission of Environnement Lte.)

Moreover during the study period, it is interesting to notice the two distinct episodes of larger CO_2 release from the reservoir (Figure 4.8a). For both years of the study, the first and larger discharge occurred at the beginning of the month of May, with daytime fluxes going from 0.22 ± 0.07 μmol $m^{-2}s^{-1}$ in April 2007 to 1.15 ± 0.14 μmol $m^{-2}s^{-1}$ in May and from 0.28 ± 0.05 μmol $m^{-2}s^{-1}$ to 1.70 ± 0.17 μmol $m^{-2}s^{-1}$ for the same periods in 2008 (Figure 4.8).

The large emissions in May follow the winter period where the reservoir is covered by ice and emissions are very small. As the ice on the reservoir breaks up in May, the CO_2 stored beneath is quickly released to the atmosphere. Rosa *et al.* (2002) state that the ice melt is an important factor to consider when measuring CO_2 emissions from a reservoir. They demonstrated that 46% of the CO_2 emissions occur during the 1st day after the ice melts, which contribute to an important release of CO_2 to the atmosphere. At Eastmain-1, this large and rapid release was observed for both years of the study.

A second peak in reservoir CO_2 emissions was observed in the early fall (Figure 4.8, between mid-August and early September), although smaller in magnitude. Natural lakes turnover, often once in the spring and again in the fall. Lake turnover is driven by air temperature. As the air temperature drops, it cools the first air-water layer. When this layer becomes colder and denser, it comes to a point where it is heavy enough to sink at the bottom of the lake, forcing the deeper layer of water to the surface. This property has been recognized to avoid a lake from completely freezing and to preserve life during the cold season. The second annual peak release of CO_2 seems to correspond very closely with the reservoir autumn turnover, which occurred prior to September 12th (Figure 4.9). The water temperature profile on June 25th 2008, between 0 and 10 meters, was largely isothermal. Then, for the entire month of July, the water temperature seemed to have stabilized to 18°C all the way between 0 and 15 meters deep. But, by the 12th of September, this equilibrium had shifted. There was no longer a water temperature variation between 15 and 18 meters as seen in July. This was caused by the natural turnover of the reservoir. Then, resulting from this mixing of water, a release of CO_2 to the atmosphere is recorded by the eddy covariance tower.

In the case of the reservoir, the spring turnover, is likely not as significant as much of the CO_2 in the water column was released upon ice break-up. By fall, CO_2 has accumulated in the stable bottom water layer which is quickly moved to the surface and released to the atmosphere following turnover.

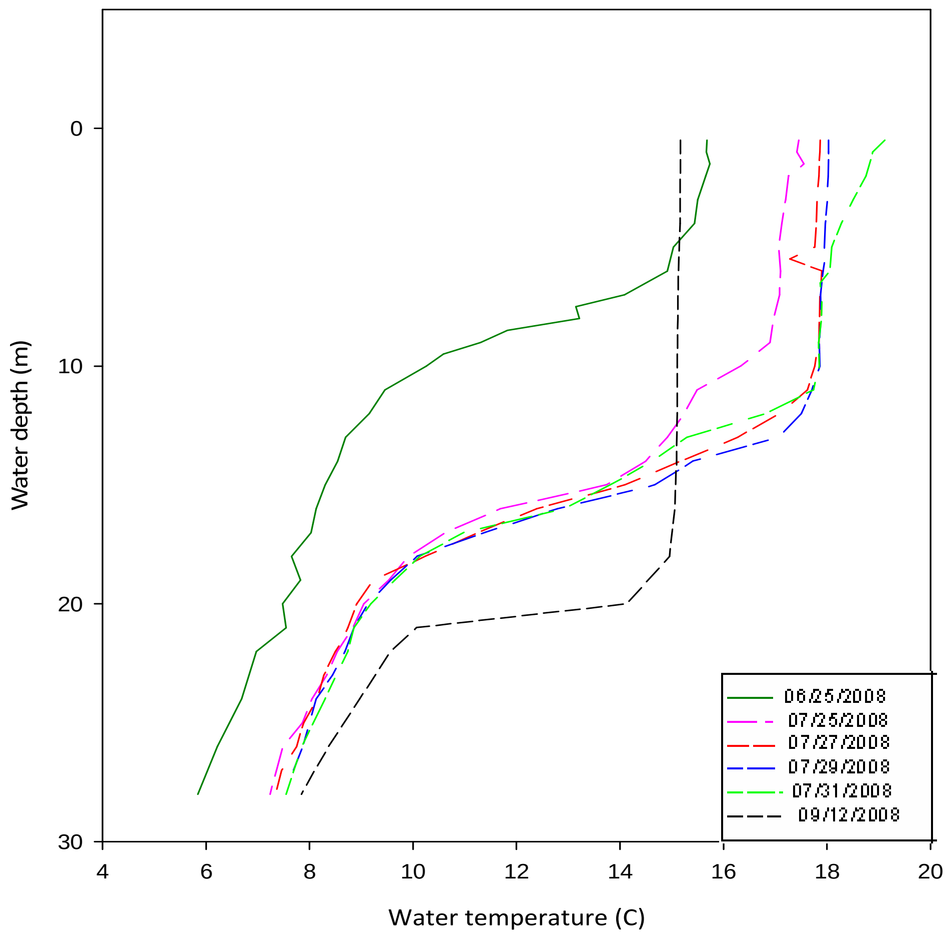

Figure 4.9 Water temperature profile in the reservoir water column near the island study site for the summer of 2008. (Data from Dr. P. DelGiorgio, UQAM).

4.3.5 Net Reservoir Effect

In order to compare the reservoir with the analog forest site, we needed to standardize the observation period. We calculated annual net exchange for the 12-month period defined as December 2007 to November 2008. This is done so that the annual period began when the reservoir was completely frozen and covered all of the variability occurring over the reservoir; ice covered, ice free and the spring and winter transitions. To better define these periods, we computed a 14-day moving average of NEE for the entire year. By examining this data for departures from the longer average emissions, we determined that the ice break up spanned the period DOY 143-152 and the reservoir turnover was DOY 229-274. Through this analysis, a rapid decrease in emissions between DOY 324 and 335 occurred which corresponds to the winter transition and ice formation on the reservoir.

This resulted in six practical periods for comparison with the forest data termed ice covered, ice break up, ice free, turnover, post-turnover and winter transition. Many options were available for selecting the data treatments prior to comparison. For both forest and reservoir datasets, we used NEE that included the calculated storage term. We used the gap-filled dataset at the forest because the techniques for gap filling terrestrial data have been rigorously evaluated (e.g. Lafleur et al., 2003).

4.3.5.1 Reservoir NEE Gap Filling

We attempted to find a usable relationship for gap filling the reservoir data. During the ice-free period, a good relationship was found between wind speed at the EC measurement height and NEE ($r^2 = 0.31$). However, this relationship did not hold during the peak emission events (ice break up, turn-over) nor during the winter frozen period. This makes sense, as the hypothesized process is that greater wind speed causes increased turbulence in the near-surface water and enables the exchange of CO_2 across the water-air boundary. In the winter, increasing wind speed does not cause increased exchange through the ice. Finally, during the transition periods, different processes (freezing; thawing) confound the relationship. During turn-over, the rate of CO_2

movement from the benthic sources is altered by the rapid turnover of the stable lower water layer.

According to Coyne and Kelly (1974), the primary source of CO_2 to the water is benthic respiration. Their study also states that the effect of increasing sediment temperatures should be to increase benthic respiration and therefore the magnitude of the CO_2 gradient. An increase in water temperature should also act to decrease the CO_2 differential because CO_2 solubility in water decreases as temperature increases. Since our data have also determined that there is no net biological or photochemical effect on the release of CO_2 out of the reservoir at the surface (Figure 4.7), we needed to explore another mechanism. We looked into mechanical processes that could contribute to the release of CO_2 from the surface (Table 4.3).

Table 4.3 Relationships between 30-minute reservoir NEE and selected environmental variables.

		Air temperature (°C)	Barometric Pressure (kPa)	Friction Velocity (u*)	Wind speed (exponential) (ms^{-1})
2007	**r^2**	0.02	0.01	0.14	**0.24**
2008	**r^2**	0.02	0.00	**0.16**	0.12

Friction velocity (u*) and wind speed, which are closely related, appeared to provide the best global fit using all the ice-free data. This is similar to the results presented by Coyne and Kelly (1974) who reported that the rate of turbulent exchange of CO_2 across the water surface should increase with wind speed, thereby decreasing the CO_2 gradient. Using 30-minute wind speed from individual periods, an exponential equation of the form

$$y = y_0 + ax^b \tag{5}$$

was chosen where y_0 represents the rate of diffusion at zero wind speed, *a* and *b* are model fit constants and *x* is wind speed. The ice free period and the post turnover period of 2008 produced the best results (r^2 of 0.31) and the resulting equation was $y = 0.3985 + 0.0028x^{2.70}$ (Figure 4.10). This relationship is similar to those used in gap filling ecosystem respiration with soil temperature. A better fit could be attained by removing the y-intercept term in equation (6) but this implies that the exchange is zero at zero wind speed which is not physically realistic.

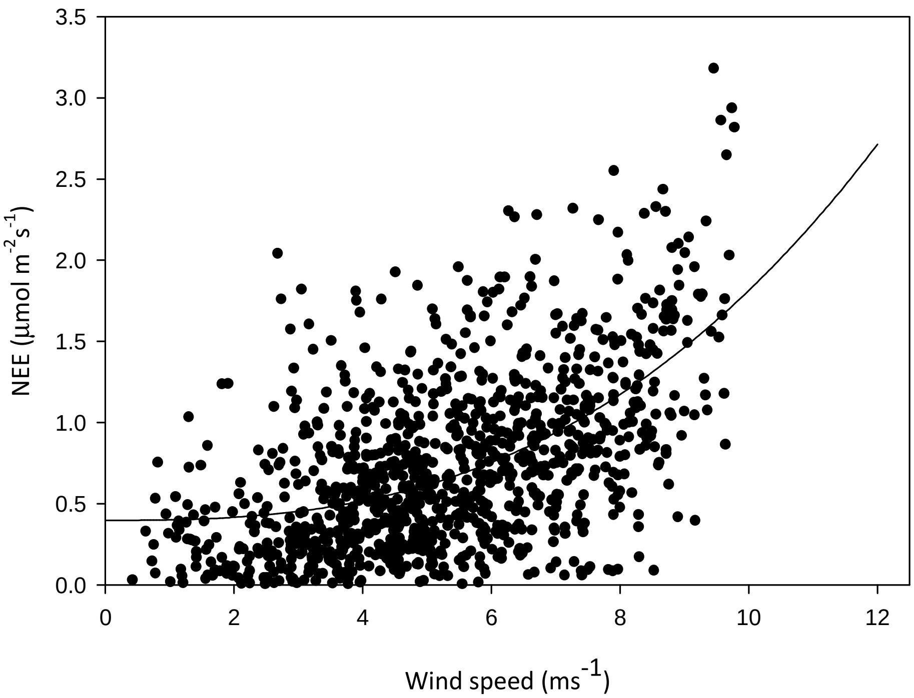

Figure 4.10 NEE wind speed relationship for the ice free (June 1st to August 15th) and post-turnover period (October 1st to November 18th).

In repeating the process for the ice-covered period, we obtained a low r^2 of 0.13, which demonstrates that wind speed cannot be the main mechanism influencing the release of CO_2 out of the reservoir during the winter time. Other environmental variables proved equally poor or worse for this period. Monson et *al*. (2006) reported that the amount of winter carbon dioxide loss in a terrestrial ecosystem is potentially susceptible to changes in the depth of the snowpack: a shallower snowpack has less insulation potential, causing colder soil temperatures and potentially lower soil respiration rates. However, contrarily to a snow pack, over a frozen aquatic environment, CO_2 is trapped under a layer of ice. As an example, the Arctic Ocean's role in determining regional CO_2 balance has been ignored to date because its continuous sea-ice-cover is considered to impede gaseous exchange with the atmosphere so efficiently that no global climate models include CO_2 exchange over sea-ice (Semiletov *et al*., 2007). However, over the Eastmain-1 reservoir, during the ice covered season we measured 0.23 ± 0.01 g C $m^{-2}d^{-1}$ (±SE). This potentially indicates underestimation in C loss from ice-covered aquatic ecosystems.

Despite the reasonably good relationship obtained for the ice-free and post-turnover period, we decided that it was not worth introducing more bias to the data by gap filling and therefore the comparison with the pre-flooded analog site would be done with non-gap-filled reservoir data.

4.3.5.2 Error Estimation for Cumulative NEE

We decided to treat the data set of the ice free and the post-turnover periods the same as the other four periods, meaning that we used the average of the half hour flux per day only when there were more than nine half hours of valid data. Days with fewer than nine half-hours were assigned the period average NEE which was obtained as an average of the entire remaining 30min data set for that period. This resulted in a complete data set from December 2007 to November 2008 which had 37% of the original data.

At the forest site, gap filled CO_2 flux data were accumulated to obtain the annual NEE values up to November 13^{th}, 2008 at which time the system experienced instrument failure. The final two weeks of November were gap filled using a NEE-air temperature relationship (r^2 = 0.65). The standard errors associated with each daily average were accumulated over the year similarly. The accumulation of error for the reservoir data set was treated differently. In order to get a more accurate representation of the cumulative error of the reservoir NEE, we used the following procedure: any day with more than nine half-hours retained its standard error; for the other days, based on Ammann et al. (2007) we added 15% of the period average NEE value to the period average standard error and assigned this to the day in question. This had the result of increasing the error bounds for those days with fewer than nine valid data points.

4.3.5.3 Reservoir vs. Forest NEE

The available reservoir NEE data was compared with the forest NEE gap filled data to summarize the reservoir effect for each period (Table 4.4). The availability of data over the reservoir throughout the year ranges from 10% (of all the data from valid directions) during the ice-covered period to 52% during the ice break-up. The small availability results from the quality control procedures (eliminate data that were affected by undesirable weather events, instrument malfunctioning, high frequency spikes).

Table 4.4 Comparison between the pre- and post-flooded site for the twelve month period December 1st, 2007 to November 30th, 2008. NEE is the average net ecosystem exchange of the reservoir for the period indicated; σ and SE are the standard deviation and the standard error of NEE, respectively. NET is the difference: reservoir NEE - forest NEE.

Period	Site	NEE (g C m-2d-1)	σ	± SE	% data	NET (g C m-2d-1)	± SE
Ice covered (DOY 335-365;1-142)	**Res**	0.23	6.25	0.01	10	0.04	0.02
	For	0.19	1.17	0.01	100		
Ice break up (DOY 143-152)	**Res**	1.78	1.47	0.09	52	2.90	0.18
	For	-1.12	1.95	0.09	100		
Ice free (DOY 153-228)	**Res**	0.84	0.66	0.02	27	1.75	0.07
	For	-0.91	2.97	0.05	100		
Fall turnover (DOY 229-274)	**Res**	1.27	0.76	0.03	35	2.03	0.10
	For	-0.76	3.56	0.08	100		
Post turnover (DOY 275-323)	**Res**	0.86	0.58	0.03	18	0.65	0.06
	For	0.21	1.59	0.03	100		
Winter transition (DOY 324-335)	**Res**	0.47	0.34	0.02	36	0.04	0.04
	For	0.43	0.30	0.01	100		

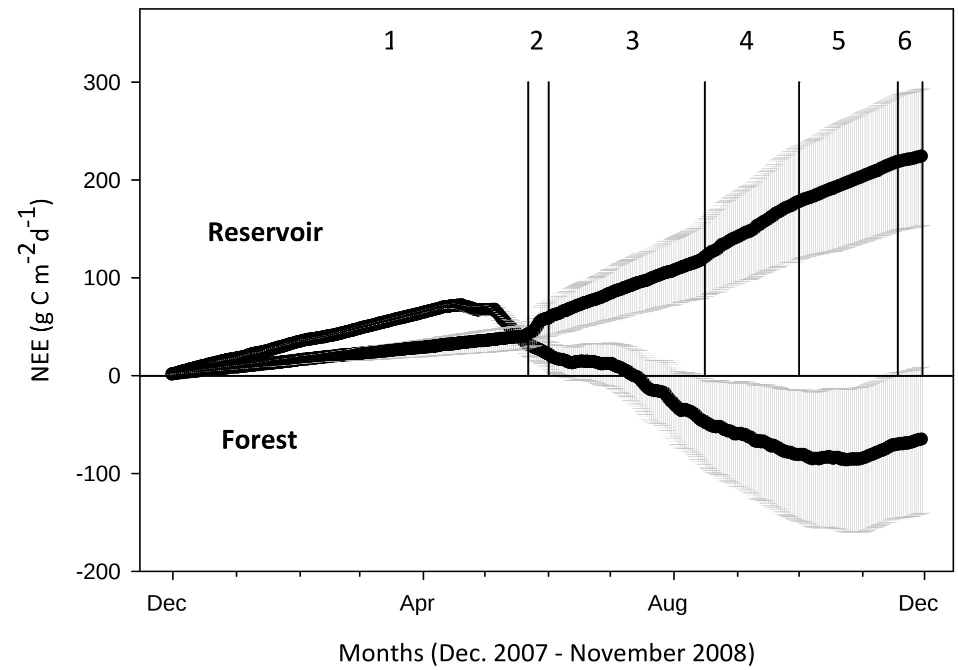

Figure 4.11 Cumulative forest and reservoir NEE (g C m^{-2} yr^{-1}) based on the six identified periods between December 1st, 2007 to November 31st 2008. Period 1: Ice covered, 2: Ice break up, 3: Ice free, 4: Turnover, 5: Post turnover and 6: winter transition.

On an annual basis the reservoir is a constant emitter. The forest and reservoir had similar C emissions during the winter transition and the ice-covered periods (0.47 ± 0.02 and 0.43 g C $m^{-2}d^{-1}$ for the reservoir and forest, respectively). Similar emissions between both sites are also noted during the ice-covered period with the reservoir emitting 0.23 ± 0.01 g C $m^{-2}d^{-1}$ and the forest 0.19 ± 0.01 g C $m^{-2}d^{-1}$. During the ice break up period, there is a large quantity of CO_2 being released on the order of 1.78 ± 0.09 g C $m^{-2}d^{-1}$ in a short time span (9 days). By the time of the ice break-up, the forest switchover to net carbon uptake has occurred and the difference between the two increases. During the ice-free and post-turnover periods the reservoir had relatively constant emissions with 0.84 ± 0.02 g C $m^{-2}d^{-1}$ and 0.86 ± 0.03 g C $m^{-2}d^{-1}$, respectively. The forest was a sink of C during the ice-free period with -0.91 ± 0.05 g C $m^{-2}d^{-1}$, but switched to a C source during the period that corresponds with the reservoir post-turnover with an emission of 0.21 ±

0.03 g C $m^{-2}d^{-1}$. The ice breakup was on the order of 1.78 ± 0.09 g C $m^{-2}d^{-1}$ and was 1.27 ± 0.03 g C $m^{-2}d^{-1}$ during the turnover.

The net reservoir effect ($NET_{reservoir\ effect} = NEE_{reservoir} – NEE_{forest}$) is estimated to be 289.2 ± 144.6 g C $m^{-2}yr^{-1}$ for the twelve month period December 1st, 2007 to November 30th, 2008. One could argue that the limitation of this research is that the value for net reservoir effect is based on a single year of data. However, two years of data at the forest have revealed that interannual variability in the growing season is small with -115.6 g C $m^{-2}yr^{-1}$ for 2007 and -122.5 g C $m^{-2}yr^{-1}$ in 2008. It is likely that a similar small variability in winter emissions will be found. Although we report data for only the year of 2008 over the reservoir, we do not expect the processes driving carbon release from the reservoir to change from this point in time forward. As the reservoir ages, the amount of readily-available organic matter diminishes and the gross C emissions will stabilize or decrease. Therefore, the estimate of net reservoir emissions represents an upper limit going forward.

4.4 DISCUSSION

4.4.1 Flux Comparison

With the present study we found that the net ecosystem exchange of the EM1 reservoir was estimated to be 223.2 ± 69.9 g C m^{-2} yr^{-1}. When compared to previous research in similar situations, the EM1 reservoir is found to behave similarly to other young flooded environments. For instance, the EM1 reservoir falls in the range of the ELARP reservoir 199 (110-368) g C m^{-2} yr^{-1} (Kelly et al., 2007) and FLUDEX 149-299 g C m^{-2} yr^{-1} (Bodaly et al., 2004) each not being older than 5 years. On the other hand, fluxes of natural boreal lakes and reservoir older than 25 years range from 8 to 88 g C m^{-2} yr^{-1}. The analysis and comparison of the existing studies of fluxes over reservoirs and lakes reveals that reservoirs are greater emitters of CO_2 to the atmosphere in their early stages (Table 4.5). There are some exceptions such as the 12-19 years old Robert Bourassa reservoir which had mean measured emissions of 149 g C m^{-2} yr^{-1} but note that the range reported there is also large (from 16 to 1195 g C m^{-2} yr^{-1}).

Moreover, almost all measurements presented in table 4.5 were obtained with measurements techniques involving the directly measurement on the water surface itself (e.g. carbon chambers) and unlike this present study, none used the eddy covariance technique. However, despite the differences in the technique of measurement, on the whole, results obtained over the EM1 reservoir appear to be within the range of other studies realized over young reservoirs.

Table 4.5 Summary of the average CO_2 emissions of northern hydroelectric reservoirs. :

Diffusive Fluxes; B: Bubbling or Ebullition; NA: Data not available

Location	Reservoir	Area (km^2)	Depth (m)	Age (yr)	Type of Flux	(mg CO_2 /m^2d)	(g C/ m^2yr)	References
		Canada						
Quebec	Laforge-1	1000	6.2	1-5	D & B	2300 (200-8500)	229 (20-846)	Duchemin *et al.,* 1995; Duchemin, 2000
	Robert Bourassa	2500	NA	12-19	D & B	1500 (160-12 000)	149 (16-1195)	Kelly *et al.,* 1994; Duchemin *et al.,* 1995; Duchemin, 2000
	Eastmain-Opinaca	1000	NA	12-13	D	3450 (2200-4300)	343 (219-428)	Kelly et *et al.,* 1994; Duchemin *et al.,* 1995; Duchemin, 2000
	Cabonga	400	NA	68-70	D & B	1400 (320-4800)	139 (32-478)	Duchemin *et al.,* 1995; Duchemin, 2000
	Boreal lakes (3)	8	4.7		D	333 ± 224	33±22	Soumis *et al.,* 2007
		1.6	1.6					
		17.5	3.6					
	Temperate lakes (3)	60.2	8.6		D	691 ± 1385	69±138	
		38.1	9.7					
		1764	15.5					
	Boreal rivers	NA	NA		D	802 ± 157	80±16	
	Boreal reservoir (LA1 & LaGrande) (whole)	1000 & 2835	6.2 & 22	29 (1978) & 11 (1996)	D	779 ± 282	78±28	
	Boreal reservoir (coves)					632 ± 139	69±138	
	Boreal reservoir (thalweg)					877 ± 321	88±32	
	LG2	2835	22	28 (1978)	D	80-1800	8-179	Roehm *et al.,* 2006
	LG3	NA	NA	NA	D	400-1500	40-149	
	D24	NA	3	28 (1978)	D	15 471	1540	Duchemin *et al.,* 2006
British Columbia	Reveistoke	120	NA	8	D	2200 (1560-3000)	219 (155-299)	Schellhase *et al.,* 1997
	Kinsbasket	430	NA	19	D	530 (460-600)	53 (46-60)	
	Arrow	520	NA	22	D	1300 (570-1770)	129 (57-176)	
	Whatshan	15	NA	40	D	670 (540-790)	67 (54-79)	
Ontario	ELARP	0.2	NA	4 (1993)	D & B	2000 (1100-3700)	199 (110-368)	Kelly *et al.,* 1997
	FLUDEX	0.5-0.7 ha	1-2	5 (1999)	NA	1500-3000	149-299	Bodaly *et al.,* 2004;

4.4.2 Study Limitation

The very assumption of this research encompasses some limitations that may have affected the outcome of this research. Logistic constraints dictated that we assume that the pre-flooded forest analogue site was representative of the currently flooded forest around the reservoir tower. In Chapter 3, it was demonstrated that the EM1 forest was similar to other Canadian boreal forests and could therefore serve as a baseline for comparison with the flooded forest. Ideally, in order to state without a doubt that the pre-flooded and the flooded forest were alike, forest eco-physiological characteristics and net ecosystem exchange at the flooded site would have been assessed. While this was impossible to realize when the present study began, a convergence of evidence at the flooded sites makes it possible to confirm that the choosen pre-flooded site is representative and similar to the now flooded forest.

First, the remaining vegetation on the island was surveyed. It was found, before being partially cut for the purpose of this study, that black spruce was the dominant tree around the reservoir tower. The understory, which was assessed during carbon chamber measurements, was similar to that found at the EM1 forest with species such as *kalmia angustifolia*, *rhododendron groenlandicum*, feather mosses, lichen and sphagnum spp.

During this study, we obtained from the reservoir tower instances where the modelled flux footprint lay entirely on the island. Two examples are July 9th and July 23rd. The flux tower measured a flux of -5.4 g C m^{-2} d^{-1} on July 9 and -2.2 g C m^{-2} d^{-1} on July 23. During the same period, the analogue forest was an average sink of -2.7 g C m^{-2} d^{-1} . Obviously, there has been modification to the remaining vegetation, especially with manual tree cutting, but the footprint was large enough to include the remaining treed vegetated part of the island, which would normally have been rejected from our reservoir fluxes analysis. Although this agument is only based on two footprints, it still provides an indication that the NEE between the two locations was similar prior to impoundment.

Since this comparison value influences the computation of the net reservoir effect, an expansion of the comparions can be done.

In this calculation, the net reservoir effect is the difference between the NEE from the reservoir and the NEE from the forest and using the analogue forest this is found to be 289.2 ± 144.6 g C $m^{-2}yr^{-1}$. If we replace the NEE forest with that reported for both young forests and older mature black forest stands, then a range in potential values can be determined. Thus the net reservoir effect becomes the difference between the fluxes of a young reservoir and an old mature old black spruce forest being near carbon neutral (Gower *et al*., 2007; Krishnan *et al*., 2008) or a young boreal forest (Litvak *et al*., 2003) which annually stores more carbon. Indeed, Litvak *et al*. (2003) clearly stated that stand age is critical to understanding the carbon balance of boreal forests on a regional basis. They demonstrated that most of the net biomass accumulation appears to take place from 20 to 70 years after a fire, with the highest rates of accumulation in a brief 30-year period while stands younger than 20 years appear to lack sufficient leaf area for rapid carbon accumulation and stands older than 70 years appear to be in near zero carbon balance with the atmosphere.

Thus, using the values from Gower *et al*. (2007) and Krishnan *et al*. (2008) 130-160 years-old SOBS site fluxes, we present here an attempt to give a range of net reservoir effect depending on the age structure of the flooded boreal forest.

1. <u>Net reservoir effect in a mature flooded forest (Present study):</u>

$NET_{\text{reservoir effect}}$ (g C $m^{-2}yr^{-1}$) = $NEE_{\text{reservoir}}$ – $NEE_{\text{forest-MATURE}}$
$NET_{\text{reservoir effect}}$ (g C $m^{-2}yr^{-1}$) = 223 g C $m^{-2}yr^{-1}$ – (-65 g C $m^{-2}yr^{-1}$) = **289 g C $\mathbf{m^{-2}yr^{-1}}$**.

2. <u>Net reservoir effect in an old flooded forest (Gower *et al* . (2007) Krishnan *et al*. (2008)):</u>

NET $_{\text{reservoir effect}}$ (g C m^{-2}*yr^{-1}*) = NEE $_{\text{reservoir}}$ – NEE $_{\text{forest-OLD MATURE}}$

NET $_{\text{reservoir effect}}$ (g C m^{-2}yr^{-1}) = 223 g C m^{-2}yr^{-1} – (-27 g C m^{-2}yr^{-1}) = **250 ± g C m^{-2}yr^{-1}.**

We now have a general representation of a net reservoir effect depending on the age of the flooded forest. In an older, mature forest, the net effect is 250 g C m^{-2} yr^{-1}. Our forest, being 80 years old is similar to this case with a net effect of 289 g C m^{-2} yr^{-1}. The difference between the two is 39 g C m^{-2} yr^{-1}. One can thus extrapolate that in the first years of flooding, the net reservoir effect created by flooding a young canadian boreal forest would be much higher. Thus, based on these calculations, we can assume that the net effect of reservoir impoundment on C exchange would be the measured 289 with a range of ± 39 g C m^{-2} yr^{-1} based on representative literature examples.

Even though the above calculations act as a representation of reservoir impoundment on different boreal age stand, we know for a fact that the flooded forest was certainly not a young forest since there was no evident sign of recent forest fire on the island and on around this site on the reservoir. If the forest present before flooding was an older mature black spruce forest which acts as a weaker carbon sink, then the reservoir net effect would even be less than what the present study has computed.

4.5 CONCLUSION

This study has shown the effect of flooding a forest ecosystem in terms of net C exchange during an early year of impoundment. Reservoir creation has lead to an increase in carbon fluxes to the atmosphere in agreement with Weissenberger *et al*. (2009). In the first years following flooding of the reservoir, organic carbon release from flooded soils exceeds CO_2 emissions, implying the downstream export of large quantities of eroded soil organic carbon. After this initial period, CO_2 emissions are fuelled by organic carbon originating from terrestrial organic matter present in the water column, explaining why older reservoirs still can emit carbon long after impoundment (Weissenberger *et al*., 2009). Using the eddy covariance technique, it was demonstrated that the direction and magnitude of net CO_2 fluxes from a recently created hydroelectric reservoir was positive (to the atmopshere) and remained relatively constant throughout the year, not being influenced by biological or photochemical parameters.

The higher May 2008 NEE flux corresponded to the period of ice breakup on the reservoir. When taken separately, vegetation patterns and carbon fluxes from three-micro sites measured on the island revealed that the midland and lowland micro-sites on the island are behaving like a mixed bog and that the upland micro-site is more representative of the boreal forest understory. Based on two footprints entirely on the island, fluxes seemed to represent the forested part of the island due to the observed greater uptake, but in both cases island fluxes were negative as a result of photosynthetic activity.

We found that because there is no photosynthesis occurring at night, fluxes originating from both the reservoir and the island were positive. On the reservoir, this study has demonstrated that there are no photochemical effects influencing the average 30-minute daytime fluxes, thus we obtained a similar release of CO_2 during the day as at night. The reservoir was a net emitter of CO_2 at all times (daytime, night-time) during the summer of 2008 (Figure 4.8a). Furthermore, two peaks of emission were also identified, one at the ice break up in May and a second during the fall reservoir turnover.

Taking the potential age structure of the pre-existing forest into account, the net reservoir effect was determined to be 289 g C m^{-2} yr^{-1} with a range of 250 to 328 g C m^{-2} yr^{-1}. This obtained value of 289 g C m^{-2} yr^{-1} (2908.69 mg CO_2 m^{-2} d^{-1}) also agrees with Tremblay *et al*. (2002) study which value was 4400 ± 4000 mg CO_2 m^{-2} d^{-1}.

Acknowledgements

This research was funded by a grant to Drs. Nigel T. Roulet and Ian B. Strachan from the Canadian Foundation for Climate and Atmospheric Sciences (CFCAS). We would like to thank Dr. Alain Tremblay (Hydro-Quebec) for logistical support throughout this project. We thank SEBJ and Mike Dalva for technical support and Drs. Tim Moore and Michele Garneau for valuable advice. Finally, we thank Marie-Claude Bonneville, Onil Bergeron, Eric Christensen, Helene Higgins, Lesley Winterhalt and numerous Jamesiens workers for their essential collaboration in the field and in the analyses.

CHAPTER 5: Conclusions and Future Studies

5.1 Context

Despite a general knowledge that reservoir creation releases GHG, no serious study had attempted to quantify these emissions in a boreal environment through a comparison of the carbon exchange within pre- and post-flooded environments. On November 5th, 2005, in Eastmain, Northern James Bay, a 604 km^2 reservoir was created and reached its maximal impoundment capacity by May 29th, 2006. A multidisciplinary research project was established which aimed to quantify CH_4 and CO_2 emissions from the pre- and post-flooded environments using aquatic, terrestrial and atmospheric analysis. For the first time, the problem was addressed by treating the creation of a hydroelectric reservoir from a land cover change perspective. The overarching research question addressed by the entire project was: "*What is the net carbon exchange that results from the creation of a hydroelectric reservoir within the northern boreal forest region*?" Through continuous carbon flux data obtained from micrometeorological techniques, this research thesis aimed to answer the following question: "*What is the magnitude and direction of carbon exchange that results from a boreal forest being flooded for hydroelectric purposes*"?

The specific research questions and objectives were to:

1. Determine and compare the eco-physiological characteristics of the boreal black spruce forest pre-flooded analogue site with similar areas in northern Quebec;

2. Determine the direction and magnitude of net CO_2 fluxes for the pre- and post-flooded environments;

3. Identify the key environmental drivers of CO_2 over the flooded site.

5.2 Conclusions

The analog pre-flooded forest site was mainly composed of black spruce (*Picea mariana*) with the floor cover dominated by *Sphagnum spp*., *Lichen spp*., *Rhododendron groenlandicum* and *Vaccinium myrtilloides*. The average tree density was 0.5 tree per meter square, and the average tree height and age were respectively, 8.9 ± 2.8 meters and 84 ± 3 years. The forest was determined to be a net sink of carbon from May to October in each of the two study years. The average NEE and ER for the summers of 2007 and 2008 were -0.8 g C $m^{-2}d^{-1}$ and -0.9 g C $m^{-2}d^{-1}$ for NEE, respectively and 1.5 g C $m^{-2}d^{-1}$ and 2.2 g C $m^{-2}d^{-1}$ for ER. respectively. The cumulative NEE at the site was similar for both growing seasons, varying from a sink of -115.6 g C $m^{-2}d^{-1}$ in 2007 to -122.5 g C $m^{-2}d^{-1}$ in 2008. The overall composition and ecophysiological behaviour was similar to other boreal black spruce forests reported in the literature.

The tower flux data from the reservoir tower showed that fluxes originating both from the reservoir and the island were positive. The daytime reservoir fluxes were also positive indicating that there seemed to be no photochemical effects influencing the average 30-minutes daytime fluxes. The reservoir was a net emitter of CO_2 at all times (daytime, night-time) during the summer of 2008. To simplify the annual flux analysis, the reservoir emissions were divided into six distinct periods: ice covered, ice break up, ice free, turnover, post-turnover and winter transition. Each of those period expressed emissions greater than zero. Moreover, two peaks of emission were identified, one at the ice break up in May (DOY 143-152) with 1.78 ± 0.09 g C $m^{-2}d^{-1}$ and a second during the reservoir turnover (DOY 229-274) with 1.27 ± 0.03 g C $m^{-2}d^{-1}$. In combining the pre-flooded and reservoir data sets, this first estimate of the net reservoir effect was determined to be 289.2 ± 144.6 g C $m^{-2}yr^{-1}$ for the twelve month period December 2007 to November 2008. Analysis of subsequent years will illustrate whether this difference is subject to variability.

5.3 Future studies

Further studies are essential to improve our knowledge and understanding of the dynamic of a newly impounded reservoir. In light of this study, it would be interesting to determine the island contour points at various levels of the reservoir drawdown to discover how the water level variation might affect the resulting carbon fluxes as measured by the island flux tower. In order to obtain an overall net reservoir effect, it would be relevant to take into consideration the remaining vegetated island on the reservoir, which this study has demonstrated are still taking up carbon. Finally, analysis of further years would be necessary to determine the direction of emissions of this young flooded forest over time, but also to verify the observed seasonal patterns such as the large emissions of carbon occuring after the ice break up. Nonetheless, this study has demonstrated that the Eastmain-1 reservoir is a constant emitter of carbon and a first estimate of its net effect has been evaluated for the year of December 2007 to November 2008.

Literature Cited

Aber J.D. and Melillo J.M., Second Edition, (2001) *Terrestrial Ecosystems*, Harcourt Academic Press, 556pp., London.

Aberg J., Bergstrom A.-K., Algesten G., Soderback K., Jansson M., (2004) A comparison of the carbon balances of a natural lake and a hydroelectric reservoir in northern Sweden. *Water Research. 38*, 531–538.

Amiro B.D., Barr A.G., Black T.A., Iwashita H., Kljun N., McCaughey J.H., Morgenstern K., Murayama S., Nesic Z., Orchansky A.L., Saigusa N., (2006) Carbon, energy and water fluxes at mature and disturbed forest sites, Saskatchewan, Canada. *Agricultural and Forest Meteorology*, *136*, 237-251.

Ammann C., Flechard C.R., Leifeld J., Neftel A., Fuher J., (2007) The carbon budget of newly established temperate grassland depends on management intensity. *Agriculture Ecosystems and Environment*, *121*, 5-20.

D'Arrigo, R., G.C., Jacoby, I.Y. Fung., (1987) Boreal forests and atmosphere-biosphere exchange of carbon dioxide. *Nature*, *329*, 321-323.

Arvola L., Kortelainen P., Bergstrom I., Kankaala P., Ojala A., Pajunen H., Kaki T., Makela S., Rantakari M., (2002) *Understanding the Global System, the Finnish Perspective*. 232pp., Finnish Global Change Research Programme FIGARE, Finland.

Aubinet, M., Grelle A., Ibrom A., Rannik U., Moncrieff J., Foken T., Kowalski A.S., Martin P.H., Berbigier P., Bernhofer C., Clement R., Elbers J., Granier A., Grunwald T., Moregenstern K., Pilegaard K., Rebmann C., Snijders W., Valentini R., Vesala T., (2000) Estimates of the annual net carbon and water exchange of forests: the EUROFLUX methodology. *Adv. Ecol. Res., 30*, 113-175.

Baldocchi D.D., (2003) Assessing the eddy covariance technique for evaluating carbon dioxide exchange rates of ecosystems: past, present and future. *Global Change Biology, 9*, 479-492.

Bhatti, J.S. and M.J. Apps., (2000) Carbon and nitrogen storage in upland boreal forests. *A systems analysis of the global boreal forest*. Directed by Lal. R., J.M. Kimbell and B.A Stewart p. 126-143. New York: Cambridge University Press.

Bhatti, J.S., M.J. Apps., H. Jiang., (2002) Influence of nurients, disturbances and site conditions on carbon stocks along a boreal forest transect in central Canada. *Plant and Soil*, *242*, 1-14.

Black TA, Gaumont-Guay D, Jassal RS, Amiro BD, Jarvis PG, Gower ST, Kelliher FM, Dunn A, Wofsy SC., (2005) Measurement of CO_2 exchange between boreal forest and the atmosphere. Griffiths H, Jarvis PJ, editors. *The carbon balance of forest biomes*. Taylor and Francis Group. 151-186 pp., New York.

Bergeron O., Margolis H.A., Black T.A., Coursolle C., Dunn A.L., Barrs A.G., Wofsy S.C., (2007) Comparison of carbon dioxide fluxes over three boreal Black Spruce forests in Canada. *Global Change Biology*, *13*, 89-107.

Bergeron O., Margolis H.A., Coursolle C., Giasson M-A., (2008) How does forest harvest influence carbon dioxide fluxes of black spruce ecosystems in eastern North America?" *Agricultural and Forest Meteorology*, *148,* (4), 537-548.

Blanken Peter D., Rouse W.R., Culf A.D., Spence C., Boudreau L.D., Jasper J.N., Kochtubaja B., Schertzer W.M., Marsh P., Verseghy D., (2000) Eddy covariance measurements of evaporation from Great Slave Lake, Northwest Territories, Canada. *Water Resources Research*, *6*, (4), 1069-1077.

Blanken P.D., Rouse W.R., Schertzer W.M., (2002) Enhancement of Evaporation from a Large Northern Lake by the Entrainment of Warm. Dry Air. *Journal of Hydrometeorology*, *4*, 680-693.

Bodaly R.A., Beaty K.G., Hendzel L.H., Majewski A.R., Paterson M.J., Rolfhus K.R., Penn A.F., St-Louis V., Hall B.D., Matthews C.J.D., Cherewyk K.A., Mailman M., Hurley J.P., Schiff S.L., Venkiteswaran J.J., (2004) Peer Reviewed: Experiencing with Hydroelectric reservoirs. *Environ. Sci. Technol*., *38,* (18), 346A-354A, DOI: 10.1021/es040614u.

Bonan, G.B., and H.H. Shugart., (1989) Environmental factors and ecological processes in boreal forests. *Annual Review of Ecology and Systematics, 20*, 1-28.

Bond-Lamberty B., Wang C., Gower S.T., (2002) Aboveground and belowground biomass and sapwood area allometric equations for six boreal tree species of northern Manitoba. *Can. J. For. Res., 32*, 1441–1450, DOI: 10.1139/X02-063.

Bond-Lamberty, B., Peckham S.D., Ahl D.E., Gower S.T., (2007) Fire as the dominant driver of central Canadian boreal forest carbon balance. *Nature, 450*, 89-92.

Broecker W.S., Ledwell J.R., Takahasji T., Weiss R., Merlivat L., Memery L., Peng T.H., Jahne B., Munnich K.O., (1986) Isotopic versus micrometeorological ocean CO_2 fluxes: A serious conflict. *Journal of Geophys. Res.*, *91*, (C9), 10517-10527.

Brooks P.D., McKnight D.M., Bencala K.E., (1999) The relationship between soil heterotrophic activity, soil dissolved organic carbon (DOC) leachate, and catchment scale DOC export in headwater catchments. *Water Resour Res*, *35*, 1895-1902.

Canuel R., Duchemin E., Lucotte M., (1997) Handbook on greenhouse gases sampling and analytical techniques. International Workshop on Greenhouse Gases, Brazil.

Carroll P. and Crill P.M., (1997) Carbon balance of a temperate poor fen. *Global Biogeochemical Cycles*, *11*, 349–356.

Chen M.J. and Cihlar J., (1995) Plant canopy gap size analysis theory for improving optical measurements of leaf area index. *Appl. Opt.*, *34*, 6211-6222.

Chen M.J., Rich P.M., Gower S.T., Norman J.M., Plummer S., (1997) Leaf area index of boreal forests: Theory, techniques, and measurements. *Journal of Geophysical Research*, *12*, (D24), 29, 429-443.

Chen J.M., Govind A., Sonnentag O., Zhang Y., Barr A., Amiro B., (2006) Leaf area index measurements at Fluxnet-Canada forests sites. *Agricultural and Forest Meteorology*, *140*, (1-4), 257-268.

O'Connell K.E.B., Gower S.T., Norman J.M., (2003) Net Ecosystem Production of Two Contrasting Boreal Black Spruce Forest Communities. *Ecosystems*, *6*, (3), 248-260 DOI:10.1007/s10021-002-0202-9.

Cosson, J.F., Ringuet S., Claessens O., de Massary J.C., Dalecky A., Villier J.F., Granjon L., Pons J.M., (1999) Ecological changes in recent land-bridge islands in French Guiana, with emphasis on vertebrate communities. *Biological Conservation*, *91*, (2-3), DOI:10.1016/S0006-3207(99)00091-9.

Coyne P.I., Kelly J.J., (1974) Carbon dioxide partial pressures in Arctic surface waters. *Limnology and Oceanography*, *19*, (6), 928-938.

Crusius J. and Wanninkhof R., (2003) Gas transfer velocities measured at low wind speed over a lake. *Limnology and Oceanography, 48*, (3), 1010–1017.

Cullenward D. & Victor D.G., (2006) An Editorial Comment The dam debate and its discontents. *Climatic change, 75*, 81-86.

Davidson E.A., K. Savage K., Verchot L.V., Navarro R., (2002) Minimizing artifacts and biases in chamber-based measurements of soil respiration. *Agricultural and Forest Meteorology, 113*, 21–37.

Deacon E.L., (1977) Gas transfer to and across an air-water interface. Dynam*ic meteorology and oceanography*, *29*, (4), 363.

Del Giorgio P.A., Williams P.J., (2005) *Respiration in aquatic ecosystems*. Oxford Biology, Oxford University. 325pp., New-York.

DeLuca, T.H., Zackrisson O., Nilsson M-C., Sellstedt A., (2002) Quantifying nitrogen-fixation in feather moss carpets of boreal forests. *Nature, 419*, 917-920.

Dixon R., Brown S., Houghton R., Solomon A., Trexler M., and Wisniewski J., (1994) Carbon pools and flux of global forest ecosystems, *Science*, *263*, 185–190.

Dos Santos M.A., Rosa L.P., Sikar B., Sikar E., dos Santos E.O., (2006) Gross Greenhouse gas fluxes from hydro-power reservoir compared to thermo-power plants. *Energy Policy*, *34*, (4), 481-488.

Duchemin E., Lucotte M., Canuel R., Chamberland A., (1995) Production of greenhouse gases CH_4 and CO_2 by hydroelectric reservoirs of the boreal region. *Global Biogeochemical cycles*, *9*, (4), 529-540.

Duchemin E., Canuel R., Ferland P., Lucotte M., (1999) Etude de la production de gaz a effet de serre par les reservoirs hydroelectriques d'Hydro-Quebec et des lacs naturels (volet 2). Rapport Scientifique, Hydro-Quebec, Dir. Princ. Planification Strategique.

Duchemin E., Lucotte M., Canuel R., (1999) Comparison of the static chamber and thin boundary layer equation methods for measuring greenhouse gas emissions from large water bodies. *Environ Sci Tech*, *33*, 350-357.

Duchemin E, Marc L., Canuel R., Soumis N., (2006) First assessment of methane and carbon dioxide emissions from shallow and deep zones of boreal reservoirs upon ice break-up. *Lakes & Reservoirs: Research and Management*, *11*, 9-19.

Duchemin E., Lucotte M., St-Louis V., Canuel R., (2002) Hydroelectric reservoirs as an anthropogenic source of greenhouse gases. *World Resource Review*, *14*, (3), 334-353.

Eaton A.K., Rouse R.W., Lafleur P.M., Marsh P., Blanken P.D., (2004) Surface Energy Balance of the Western and Central Canadian Subartic: Variations in the Energy Balance among Five Major Terrain Types. *Journal of Climate*, *14*, 3692-3703.

Energy Information Administration (2008) Official Energy Statistics from the US Government. [Online] Available on: <http://www.eia.doe.gov/basics/energybasics101.html > Retrieved on August 3rd, 2009.

Environment Canada. (May 2004) [Online] Natural Resources Canada. Available on: <http://atlas.nrcan.gc.ca/site/english/learningresources/theme_modules/borealforest/index.html> Retrieved on March 18th, 2008.

Environment Canada. (January 2008) [Online] Natural Resources Canada. Available on: <http://www.ccrs.nrcan.gc.ca/optic/coarse/beps/trac_e.php> Retrieved on June 18th, 2008.

Environment Canada, Weather Office, [Online], Available on: <http://www.climate.weatheroffice.ec.gc.ca/climateData/hourlydata_f.html?timeframe=1&Prov=XX&StationID=8676&Year=2007&Month=10&Day=24> Consulted on February 23rd, 2009.

Eugster,W.,Kling, G., Jonas, T.,McPhaden, J.P.,Wüest,A., McIntyre, S., Chapin III, F.S., (2003) CO_2 exchange between air and water in an Arctic Alaskan and a midlatitude Swiss lake: importance of convective mixing. *J. Geophys. Res.*, *108,* (D12), 4362, DOI:10.1029/2002JD002653.

Falge E., Baldocchi D.D., Olson R., Anthoni P., Aubinet M., Bernhofer C., Burba G., Ceulemans R., Clement R., Dolman H., Granier A., Gross P., Grunwald T., Hollinger D., Jensen N.O., Katul G., Kerenen P., Kowalski A., Ta Lai C., Law B.E., Meyers T., Moncrieff J., Moors E., Munger J.W., Pilegaard K., Rannik U., Rebmann C., Suyker A., Tenhunen J., Tu K., Verma S., Vesala T., Wilson K., Wofsy S., (2001) Gap filling strategies for defensible annual sums of net ecosystem exchange. *Agricultural and Forest Meteorology*, *107*, (1), 43-69.

Fearnside P.M., (1997) Greenhouse-gas emissions from Amazonian hydroelectric reservoirs: the example of Brazil's Tucurui Dam as compared to fossil fuel alternatives. *Environmental Conservation*, *24*, (1), 64-75.

Fearnside P., (2005) Brazil's Samuel Dam: Lessons for Hydroelectric Development Policy and the Environment in Amazonia. *Environmental Management*, *35*, (1), 1–19, DOI: 10.1007/s00267-004-0100-3.

Fluxnet-Canada Measurements Protocol. Fluxnet-Canada Network Management Office, Faculté de Foresterie et de Géomatique, August 2003.

Frolking S.E., Bubier J.L., Moore T.R., Ball T., Bellisario M., Bhardwaj A., Caroll P., Crill P.M., Lafleur P., McCaughey J.H., Roulet N.T., Suyker A.E., Verrna B., Waddington M., Whiting G.J., (1998) Relationship between ecosystem productivity and photosynthetically active radiation for northern peatlands. *Global Biogeochemical Cycles*, *12*, (1), 115-126.

Gaumont-Guay D., Black TA., Griffis TJ., Barr AG., Morgenstern K., Jassal RS., Nesic Z., (2006) Influence of temperature and drought on seasonal and interannual variations of soil, bole and ecosystem respiration in a boreal aspen stand, *Agricultural and Forest Meteorology, 140*, 203–219.

Goulden M.L., Daube B.C., Fan S.M., Sutton D.J., Bazzaz F.A., Munger F.W., Wofsy S.C., (1997) Physiological response of a black spruce forest to weather. *J. Geophys. Res., 102*, 28987-28996.

Goulden M.L. and Crill P.M., (1997) Automated measurements of CO_2 exchange at the moss surface of a black spruce forest. *Tree Physiology*, *17*, 537-542.

Goulden M.L., Wofsy S.C., Harden J.W., (1998) Sensitivity of boreal forest carbon balance to soil thaw. *Science*, *279*, 214-217.

Gower S.T., J.G. Vogel, J.M. Norman, C.J. Kucharik, S.J. Steele, T.K. Stow., (1997) Carbon distribution and aboveground net primary production in aspen, jack pine and black spruce stands in Saskatchewan and Manitoba, Canada. *Journal of Geophysical Research*, *102* (24D), 29029-29041.

Gower S.T., Kucharik C.J., Norman J.M., (1999) Direct and indirect estimation of leaf area index, f(APAR), and net primary production of terrestrial ecosystems. *Remote Sensing of Environment*, *70*, (1), 29-51.

Grigal DF., Kernik LK., (1984) Generality of black spruce estimation equations. *Can. J. For. Res., 14*, 468-470.

Guerin Frederic, Abril G., Serca D., Delon C., Richard S., Delmas R., Tremblay A., Varfalvy L., (2007) Gas transfer velocities of CO_2 and CH_4 in a tropical reservoir and its river downstream. *Journal of Marine Systems, 66*, 161-172.

Hatfield J.L. and Baker J.M., (2005) *Micrometeorology in Agricultural Systems*. American Society of Agronomy, Inc., 584pp., Madison, WI, USA.

Helie J-F., Hillaire-Marcel C., (2005) Diffusive CO_2 Flux at the Air-Water Interface of the Robert-Bourassa Hydroelectric Reservoir in Northern Quebec: Isotopic Approach (13C). Environmental Science, Springer Berlin Heidelberg, 355-382pp.

Huttunen J.T., Alm J., Liikanen A., Juutinen S., Larmola T., Hammar T., Silvola J., Martikainen P.J., (2003) Fluxes of methane, carbon dioxide and nitrous oxide in boreal lakes and potential anthropogenic effects on the aquatic greenhouse gas emissions. *Chemosphere, 52*, 609-621.

Hydro-Quebec Production. (December 2004) [Online] Environmental Impact Assessment. Available on: <http://www.hydroquebec.com/rupert/en/pdf/vol_01_en_web.pdfCh8>. Retrieved on March 13th, 2008.

Hydro-Québec. (2009) [Online] Available on: <http://www.hydroquebec.com/4d_includes/surveiller/PcFR2009-102.htm> Retrieved on August 3rd, 2009.

Jaccard Mark, (2006) *Sustainable Fossil Fuels*, Cambridge Press, 381pp.

Janssens I.A., Kowalski AS., Ceulemans R., (2001) Forest floor CO_2 fluxes estimated by eddy covariance and chamber-based model. *Agricultural and Forest Meteorology 106*, 61–69.

Jarvis P.G., Massheder J.M., Hale S.E., Moncrieff J.B., Rayment M., Scott S.L., (1997) Seasonal variation of carbon dioxide, water vapour, and energy exchanges of a boreal Black Spruce forest. *J. Geophys. Res., 102,* (D24), 28953-28966.

Jarvis P, Linder S., (2000) Constraints to growth of boreal forests. *Nature*, *405*, 904-905.

Kasischke, E.S. and B.J. Stocks., (2000) Modeling of fire and ecosystem processes and the effects of climate change on carbon cycling in boreal forests. Chap in *Fire, Climate Change and Carbon Cycling in the Boreal Forest*, Ecological Studies Series, Springer, p. 347-355, Verlag, New York.

Keeling C.D., Chin J.F.S., Whorf T.P., (1996) Increased activity of northern vegetation inferred from atmospheric CO_2 measurements. *Nature, 382*, 146-149.

Kelly C.A., Rudd J.W.M., St-Louis V.L., Moore T., (1994) Turning attention to reservoir surfaces, a neglected area in greenhouse studies. *Eos*., *75*, 332-333.

Kirschbaum MUF., (2006) The temperature dependance of organic-matter decomposition – still a topic of debate. *Soil Biol Biochem 38*: 2510-2518.

Kljun N., Black T.A., Griffis T.J., Barr A.G., Gaumont-Guay D., Morgenstern K., McCaughey J.H., Nesic Z., (2006) Response of Net Ecosystem Productivity of three boreal forest stands to drought. *Ecosystems*, *9*, 1128-1144.

Krishnan P., Black T.A., Barr A.G., Grant N.J., Guay D.G., Nesic Z., (2006) Factors Controlling the Interannual Variability in the Carbon Balance of a Southern Boreal Black Spruce Forest. *Agricultural and forest meteorology*, *107*, (1), 43-69.

Kyoto Protocol's Clean Development Mechanism passes 100 millionth certified emission reduction milestone. [Online] Available at: <http://unfccc.int/files/press/releases/application/pdf/20071218_100_mio_cer_press_release_final.pdf>
Retrieved on January 25th, 2008.

Lafleur P.M., Roulet N.T., Admiral S.W., (2001) Annual cycle of CO_2 exchange at a bog peatland. *Journal of Geophysical Research*, *106*, (D3), 3071-3081.

Lafleur P.M., Roulet N.T., Bubier J.L., Frolking S., Moore T., (2003) Interannual variability in the peatland-atmosphere carbon dioxide exchange at an ombrotrophic bog. *Global Biogeochemical Cycles*, *17*, (2), 1-13.

Lambert M., Fréchette J-L., (2002) Campagne d'échantillonnage sur les émissions de gaz a effet de serre des réservoirs et des lacs environnants, rapport de terrain 2001. Direction Environnement, Hydro-Quebec, Montreal.

Lambert MC, Ung CH, Raulier F., (2005) Canadian national tree aboveground biomass equations, *Can. J. For. Res, 35*, 1996–2018.

Larzilliere Michel, Roy D., Chretien P., Ringuette T., Varfalvy L., (2005) Greenhouse Gas Emissions — Fluxes and Processes : Development and Use of an Experimental near Infrared Open Path Diode Laser Prototype for Continuous Measurement of CO_2 and CH_4 Fluxes from Boreal Hydro Reservoirs and Lakes. Environmental Science, Earth and Environmental Sciences, 732pp., Springer Berlin Heidelberg.

Leblanc S.G., Chen J.M., Kwongs M., (2002) Tracing Radiation and Architecture of Canopies, Trac Manual Version 2.1.3. Natural Resources Canada.

Lindroth A., Grelle A., Moren A.S., (1998) Long-term measurements of boreal forest carbon balance reveals large temperature sensitivity. *Glob. Change Biol*., *4*, 443-450.

Liss P.S., Slater P.G., (1974) Flux of gases across an air-water interface. *Nature*, *247*, 181-184.

Litvak M., S. Miller, S.C. Wofsy, M. Goulder, (2003) Effect of stand age on whole ecosystem CO2 exchange in the Canadian boreal forest. *Journal of Geophysical research*, *108*. No D3, XXXX DOI:10.1/1029/2001JD000854

Livingston G.P., Hutchinson G.L., (1995) Enclosure-based measurement of trace gas exchange: applications and sources or error. In: Matson, P.A. Harris, R.C., (eds.), *Biogenic Trace Gases: Measuring Emissions from Soil and Water*. Blackwell Scientific Publications, Oxford, pp. 14-51.

Louis V.L., Hall B.D., Matthews C.J.D., Cherewyk K.A., Mailman M., Hurley J.P., Schiff S.L., Venkieswaran J.J., (2004) Experimenting with Hydroelectric Reservoirs. *Environmental Science and Technology*, *38*, (18), 374-352A.

Lucas R., Cronin N., Lee A., Moghaddam M., Witte C., Tickle P., (2006) Empirical relationships between AIRSAR backscatter and LIDAR- derived forest biomass, Queensland, Australia. *Remote Sensing of Environment*, *100*, (3), 407-425, DOI:10.1016/j.rse.2005.10.019.

Mahoney, S.P., Schaefer J., (2002) Hydroelectric development and the disruption of migration in caribou. *Biological Conservation*, *107*, (2), 147-153.

Margolis, H.A., Flanagan, L.B., and Amiro, B.D., 2006. The Fluxnet-Canada Research Network: Influence of climate and disturbance on carbon cycling in forests and peatlands. *Agricultural and Forest Meteorology 140*: 1-5.

Markkanen T., Rannik U., Keronen P., Suni T., Vesala T., (2001) Eddy covariance fluxes over a boreal Scots pine forest. *Bor. Environ. Res*., *6*, 65-78.

Matthews Cory J.D., Joyce E.M., St-Louis V.L., Schiff S.L., Venkiteswaran J.J., Hall B.D., Bodaly R.A., Beaty K.G., (2005) Carbon Dioxde and Methane Production in Small Reservoir Flooding Upland Boreal Forest. *Ecosystems, 8*, 267-285.

McCaughey J.H., Pejam M.R., Arain M.A., Cameron D.A., (2006) Carbon dioxide and energy fluxes from a boreal mixedwood forest ecosystem in Ontario, Canada. *Agricultural and Forest Meteorology, 140*, 79-96.

McMillan A.M.S., Winston G.C., Goulden M.L., (2008) Age-dependent response of boreal forest to temperature and rainfall variability. *Global Change Biology*., *14*, (8), 1904-1926, DOI: 10.1111/j.1365-2486.2008.01614.x.

Ministere des Resources Naturelles et de la Faune (2008) [Online] Available on: <www.mrnf.gouv.qc.ca/aires/index.jsp>
Retrieved on June 12th, 2008.

Monson R., Lipson D., Burns S.P., Turnipseed A.A., Delany A.C., Williams M.W., Schmidt S.K., (2006) Winter forest soil respiration controlled by climate and microbial community composition. *Nature, 439*, (9), DOI:10.1038/nature04555.

Moren, A-S., Lindroth A., CO_2 exchange at the floor of a boreal forest, (2000), *Agricultural and Forest Meteorology, 101*, 1–14.

Munger W., Barford C., Wofsy S., (2000) Atmospheric exchanges. In Foster, D., and Aber J. (eds.), *Forest landscape Dynamics in New England* (in preparation).

Natural Resources Canada (2006) Canada's Energy Outlook: The reference case 2006. Analysis and Division Modeling, Ontario, Canada. ISBN 0-662-43440-4. [Online] Available on: <http://www.nrcan-rncan.gc.ca/com/resoress/publications/peo/peo2006-eng.pdf> Retrieved on October 2008.

Newton PF., Amponsah IG., (2007) Comparative evaluation of five height–diameter models developed for black spruce and jack pine stand-types in terms of goodness-of-fit, lack-of-fit and predictive ability. *Forest Ecology and Management, 247*, 149–166.

Ochsner T. E., Sauer T.J., Horton R., (2007) Soil Heat Storage Measurements in Energy Balance Studies. *American Society of Agronomy*, *99*, 311-319, DOI: 10.2134/agronj2005.0103S

Oke, T., (1987) *Boundary Layer Climates, 2nd edition.* Co-published by Routledge, London and John Wiley & Sons, 435pp., New York.

Piao, S. Ciais P., Friedlingstein P., Peylin P., Reichstein M., Luyssaert S., Margolis H., Fang J., Barr A., Chen A., Grelle A., Hollinger D.Y., Laurila T., Lindroth A., Richardson A.D., Vesala T., (2008) Net carbon dioxide losses of northern ecosystems in response to autumn warming. *Nature*, *451*, 49-53.

Prairie Y.T., Bird D.F., Cole J.J., (2002) The summer metabolic balance in the epilimnion of southeastern Quebec lakes. *Limnology and Oceanography*, *47,* (1), 316-321.

Rayment M.B., Jarvis P.G., (2000) Temporal and spatial variation of soil CO_2 flux in a Canadian boreal forest. *Soil Biology & Biochemistry, 32*, 35-45.

Ressources Naturelles et Faune (2008) [Online] Available on: <www.mddep.gouv.qc.ca/biodiversite/aires_protegees/articles/0805-01.htm> Retrieved on June 12th, 2008.

Roehm C., Tremblay A., (2006) Role of turbines in the carbon dioxide emissions from two boreal reservoirs, Quebec, Canada. *Journal of Geophysical Research*, *111*, (D24), D24101.1-D24101.9, DOI:10.1029/2006JD007292.

Rosa L.P., Santos M.A., (2000) Certainty and uncertainty in the science of greenhouse gas emissions from power dams a report on the state of the art for the World Commission on Dams, WCD, March 2000, Final Report.

Rosa L.P., dos Santos M.A., Matvienko B., Sikar E., (2002) Hydroelectric reservoirs and global warming. *RIO 02 - World Climate & Energy Event,* January 6-11.

Rosenberg D.M., Bodaly R.A., Usher P.J., (1995) Environmental and social impacts of large scale hydroelectric development: who is listening? *Global Environmental Change, 5*, (2), 127-148, DOI: 10.1016/0959-3780(95)0018-J.

Savage K.E., Davidson E.A., (2003) REVIEW ARTICLE: FIELD TECHNIQUES A comparison of manual and automated systems for soilCO2 flux measurements: trade-offs between spatial and temporal resolution, *Journal of Experimental Botany*, *54*, (384), 891-899, DOI: 10.1093/jxb/erg121.

Schlesinger W.H., (1997) *Biogeochemistry: an Analysis of Global Change* (2nd. Ed.), Academic Press, 588pp., San Diego, CA.

Schulze E.-D., (1999) Productivity of forests in the Eurosiberian boreal region and their potential to act as a carbon sink—a synthesis, *Global Change Biol*., *5*, 703–722.

Semiletov I.P., Pipko I.I., Repina I., Shakhova N.E., (2007) Carbonate chemistry dynamics and carbon dioxide fluxes across the atmosphere-ice-water interfaces in the Arctic Ocean: Pacific sector of the Arctic. *Journal of Marine Systems*, *66*, 204-226.

Soumis N., Lucotte M., Larose C., Veillette F., Canuel R., (2007) Photomineralization in a boreal hydroelectric reservoir: a comparison with natural aquatic ecosystems. *Earth and Environmental Science*, *86*, 123-135.

Stenberg P., (1996) Correcting LAI-2000 estimates for clumping of needles in shoots of conifers. *Agricultural and Forest Meteorology*, *79*, 1-8.

St-Louis V. L., Kelly C.A., Duchemin E., Rudd J.W.M., Rosenberg D.M., (2000) Reservoir Surfaces as Sources of Greenhouse Gases to the Atmosphere: A Global Estimate. *Bioscience*, *50*, (9), 767-775.

Strachan I.B., McCaughey J.H., (1996) Spatial and vertical leaf area index of a deciduous forest resolved using the LAI-2000 Plant Canopy Analyzer. *Forest Science*, *42,* 176-181.

Strachan I.B., (1993) Energy partitioning and canopy structure in deciduous and mixed forests, Chalk River, Ontario. Queen’s University, Ontario, 158pp.

Strachan I.B., Stewart D.W., Pattey E., (2005) Determination of leaf area index in agricultural systems. In: *Micrometeorology in Agricultural Systems*. American Society of Agronomy, Inc., 584pp., Madison, WI, USA.

Suni T, Berninger F, Vesala T *et al.* (2000) Air temperature triggers the recovery of evergreen boreal forest photosynthesis in spring. *Global Change Biology*, *9*, 1410-1426.

Swanson R.V., Flanagan L.B., (2001) Environmental regulation of carbon dioxide exchange at the forest floor in a boreal black spruce ecosystem, *Agricultural and Forest Meteorology, 108*, 165–181.

Tanner C.B., Thurtell G.W., (1969) Anemoclinometer measurements of Reynolds stress and heat transport in the atmospheric surface layers. US Army Electronics Command and Technical Report No. ECOM-66-G22F. University of Wisconsin, Madison, WI, 10 pp.

Ter-Mikaelian MT., Korzukhin MD., (1997) Biomass equations for sixty-five North American tree species, *Forest Ecology and Management, 97*, 1-24.

Tremblay A., Lucotte M., (1997) Accumulation of total mercury and methyl mercury in insect larvae of hydroelectric reservoirs. *Can. J. Fish. Aquat. Sci*., *54*, 832-841.

Tremblay Alain, Varfalvy L., Roehm C., Garneau M., (2005) *The issue of GHG from hydroelectric reservoirs: from boreal to tropical regions*. Springer, 732pp.

Tremblay A., Lambert M., Gagnon L., (2004) *Do hydroelectric reservoirs emit greenhouse gases?* Environmental management. Springer New York, 0364-152X (Print) 1432-1009 (Online). DOI10.1007/s00267-003-9158-6.

Topp G.C., Sattlecker S., (1983) A rapid measurement of horizontal and vertical components of saturated hydraulic conductivity. *Can Agric. Eng., 25*, 193-197.

United States. Department of Energy. (2009) [Online] Available on: <http://www.whitehouse.gov/issues/energy_and_environment/> Retrieved on August 3rd, 2009.

United States Dept. of Energy, Energy Information Administration, (2008). Report #:DOE/EIA-0484, [Online] Available on: <http://www.eia.doe.gov/oiaf/ieo/world.html> Retrieved on February 26th, 2009.

Van Cleve K.L., O.R. Schlentner, L.A. Viereck, C.T. Dyrness., (1983) Productivity and nutrient cycling in taiga ecosystems. *Canadian Journal of Forest Research*, *13*, 747-766.

Verdon R., Brouard D., Demers C., Lalumiere R., Laperle M., Schetagne R., (1991) Mercury evolution (1978-1988) in fishes of the La Grande hydroelectric complex, Quebec, Canada. *Water, Air & Soil Pollution*, *56*, (56), 405-417, DOI 10.1007/BF00342287.

Vickers, D., Mahrt, L., (1997) Quality control and flux sampling problems for tower and aircraft data. *J Atmos Ocean Tech, 14*, 512-526.

Vie J.C., (1999) Wildlife rescues—the case of the Petit Saut hydroelectric dam in French Guiana. *Oryx*, *33*, (2), 115-126.

Viereck, L.A., C.T. Dyrness, K. Van Cleve, M.J. Foote., (1983) Vegetation, soils and forest productivity in selected forest types in interior Alaska. *Canadian Journal of Forest Research*, *13*, p. 703-720.

Waddington J.M., Roulet N.T., (2000) Carbon balance of a boreal patterned peatland. *Global Change Biology*, *6*, (1), 87-97.

Webb E.K., Pearman G.I., Leuning R., (1980) Correction of flux measurements for density effects due to heat and water vapour transfer. *Quarterly Journal of the Royal Meteorological Society*, *106*, 85-100.

Wein R.W., D. A. MacLean., (1984) The role of fire in northern circumpolar ecosystems. *Forest Science*, *30*, no. 3, 615-616.

Weissenberger S., Lucotte M., Stephane H., Soumis N., Duchemin E., Canuel R., (2009) Modeling the carbon dynamics of the La Grande hydroelectric complex in northern Quebec, *Ecological Modelling* (In Press).

Whitehead D., Gower S.T., (2001) Photosynthesis and light-use efficiency by plants in a Canadian boreal forest ecosystem, *Tree Physiology, 21*, 925–929.

Williams T.G., Flanagan L.B., (1996) Effect of changes in water content on photosynthesis, transpiration and discrimination against 13C02 and C180160 in *Pleurozium* and *Sphagnum,Oecologia*, *108,* 38-46.

Williams T.G., Flanagan LB., (1998) Measuring and modelling environmental influences on photosynthetic gas exchange in Sphagnum and Pleurozium. Pl*ant, Cell and Environment*, *21*, 555–564.

Whittington H.W., Robson I.A., (1994) Hydroelectric power in emissions-constrained electricity generation. *Engineering Science and Education Journal, 3*, (4), 185-191.

Wofsy S., (2001) Gap filling strategies for long term energy flux data sets. *Agricultural and Forest Meteorology*, *107*, 71-77.

Woods Hole Research Center (2007) [Online] Available on:
<http://www.whrc.org/borealnamerica/our_work/field_meas.htm>
Retrieved on March 22nd, 2008.

World Biome (1995) [Online] Available on:
<http://www.worldbiome.com/biomes_map.htm>
Retrieved on March 2008.

Yu Z., M. Apps, Bhatti J., (2002) Implications of floristic and environmental variation for carbon cycle dynamics in boreal forest ecosystems of central Canada. *Journal of Vegetation Sciences*, *13*, p 327-40.

Yuste, J.C., Nagy M., Janssens I.A., Carrara A., Ceulemans R., (2005) Soil respiration in a mixed temperate forest and its contribution to total ecosystem respiration. *Tree Physiology, 25*, 609–619.